Title
Provenance, Offset Equivalent and Palinspastic Reconstruction of the Miocene Cajon Valley Formation, Southern California

Author
Stang, Dallon

Publication Date
2013

Peer reviewed|Thesis/dissertation

UNIVERSITY OF CALIFORNIA

Los Angeles

Provenance, Offset Equivalent and Palinspastic Reconstruction of the Miocene Cajon Valley Formation, Southern California

A thesis submitted in partial satisfaction of the

requirements for the degree of Master of Science in Geology

By

Dallon Michael Stang

2013

ABSTRACT OF THE THESIS

Provenance, Offset Equivalent and Palinspastic Reconstruction of the Miocene Cajon Valley Formation, Southern California

By

Dallon Michael Stang

Master of Science in Geology

University of California, Los Angeles, 2013

Professor Raymond V. Ingersoll, Chair

Petrographic, conglomerate and detrital-zircon analyses of formations in southern California can determine consanguineous petrofacies and lithofacies that help constrain paleotectonic and paleogeographic reconstructions of the southwestern United States. Arkosic sandstone of the lower Middle Miocene Cajon Valley formation is exposed on the southwest edge of the Mojave block and juxtaposed against Mesozoic and Paleozoic rocks by the San Andreas fault (SAf). Early work in Cajon Valley referred to the formation as Punchbowl, due to its similar appearance to the Punchbowl Formation at Devil's Punchbowl (northwest along the SAf). However, paleontological work placed Cajon Valley strata in the Hemingfordian-Barstovian (18-14 Ma), as opposed to the Clarendonian-Hemphillian (13-9 Ma) Punchbowl Formation. Since the Cajon Valley formation was deposited prior to being truncated by the San Andreas fault, the 2400m-thick, laterally extensive subaerial deposits likely were deposited across what is now the fault

trace. Restoring 310 km of dextral slip on the SAf system should indicate the location of offset equivalent sandstone. Restoration of slip on the SAf system places Cajon Valley adjacent to the Caliente and La Panza Ranges, east of San Luis Obispo. Although analysis of detrital zircon from Cenozoic sandstone throughout southern California has been crucial in establishing paleodrainage areas, detrital zircon from the Cajon Valley and equivalent formations had not been analyzed prior to this study.

Paleocurrents measured throughout the Cajon Valley formation indicate a source to the NE, in the Mojave Desert. Sandstone samples analyzed in thin section using the Gazzi-Dickinson method of point-counting are homogeneously arkosic, with slight compositional variability, making differentiation of the Cajon Valley formation and potential offset equivalents problematic. However, Branch Canyon Sandstone and Santa Margarita Formation samples are compositionally the best match for the Cajon Valley formation.

Detrital-zircon ages were determined from the Cajon Valley formation and related strata. These data are slightly more variable than sandstone composition, with distinct age peaks at 85-90 Ma, 150 Ma and 250 Ma. These ages correlate with batholiths in the SW Mojave Desert. Of the nine samples from six formations collected as potential offset equivalents, Branch Canyon and Santa Margarita samples are most similar to Cajon Valley samples, in terms of both detrital-zircon ages and sandstone composition.

Based on 310km of post-Miocene offset on the San Andreas fault system, the Cajon Valley formation restores adjacent to shallow-marine sandstone of the Santa Margarita Formation and Branch Canyon Sandstone Member of the Monterey Formation in the Caliente and La Panza ranges. Cajon Valley sandstone is interpreted to represent a Miocene fluvial system on a coastal plain, flowing toward a delta on a narrow continental shelf.

The thesis of Dallon Stang is approved.

Edward Rhodes

Axel Schmitt

Raymond V. Ingersoll, Committee Chair

University of California, Los Angeles

2013

TABLE OF CONTENTS

Chapter	Page
ABSTRACT OF THE THESIS	ii
APPROVAL PAGE	iv
LIST OF FIGURES	viii
LIST OF TABLES	viii
LIST OF APPENDICES	viii
ACKNOWLEDGEMENTS	ix
INTRODUCTION	1
REGIONAL SETTING, LITHOLOGY AND STRATIGRAPHY	1
Previous Work	1
Basement Lithology	2
Precambrian Gneiss	3
Cretaceous Granodiorite	3
Stratigraphy	3
Paleocene San Francisquito Formation	3
Lower Miocene Vaqueros Formation	3
Middle Miocene "Punchbowl Formation" in Cajon Valley	4
Crowder Formation	7
Harold Formation and Shoemaker Gravel	7
POTENTIAL OFFSET EQUIVALENTS AND RELATED ROCKS	7
Caliente and La Panza Ranges	7

Branch Canyon Sandstone 7

Santa Margarita Formation 8

Simmler Formation 8

Caliente Formation 9

Monterey Formation 9

Devil's Punchbowl 9

PALEOCURRENTS 10

Paleocurrent Indicators 10

Methods 10

Results 11

SANDSTONE PETROLOGY 11

Methods 11

Collection and Preparation 11

Petrography 12

Analysis 12

Results 12

Cajon Valley formation 12

Punchbowl Formation 13

Potential offset equivalents 13

DETRITAL-ZIRCON ANALYSIS 14

Methods 14

Collection and Preparation 14

Analysis 15

Results 15

PROVENANCE AND PALEOGEOGRAPHIC IMPLICATIONS 17

Potential Plutonic Sources 17

Depositional Environments 19

CONCLUSIONS 19

FIGURE CAPTIONS 22

FIGURES 25

TABLES 36

APPENDICES 40

REFERENCES CITED 71

LIST OF FIGURES

Figure 1: Generalized tectonic map showing sample locations. 25

Figure 2: Across-fault stratigraphic correlation (Woodburne, 1975) 26

Figure 3: Well-rounded arkosic sandstone hogback in Cajon Valley 27

Figure 4: Paleocurrent map and rose diagram for Cajon Valley 28

Figure 5: Pre-Miocene palinspastic reconstruction of Jacobson et al. (2011) 29

Figure 6: Southern California paleodrainage reconstruction of Ingersoll et al. (2013) 30

Figure 7: Sandstone point count QFL ternary diagram 31

Figure 8: Sandstone point count QFkFp ternary diagram 32

Figure 9: Sandstone point count LvLmLs ternary diagram 33

Figure 10: Detrital zircon probability density plots 34

Figure 11: Lower Miocene depositional interpretation of Cajon Valley 35

LIST OF TABLES

Table 1: Sample details and GPS coordinates 36

Table 2: Petrographic point count categories 37

Table 3: Raw petrographic point count data 38

Table 4: Recalculated parameters defined 39

Table 5: Calculated compositional percentages 39

LIST OF APPENDICES

Appendix A: Cajon Valley formation imbricated clast measurements 40

Appendix B: Detrital-zircon LA MC-ICPMS data 45

ACKNOWLEDGEMENTS

First and foremost, I thank Ray Ingersoll for inspiring me to study sedimentology and tectonics as an undergraduate, and for his guidance and patience in advising me as a graduate student. I thank my committee members Ray Ingersoll, Ed Rhodes and Axel Schmitt for providing thoughtful insights regarding my thesis manuscript. Funding for detrital-zircon ages was provided by The Academic Senate of the University of California, Los Angeles. Detrital-zircon provenance discussions with Carl Jacobson were very helpful in depositional system interpretation. I thank Jade-Star Lackey and Jonathan Harris at Pomona College for allowing me use of their lab facilities, and Kevin Coffey for guidance in mineral separation at UCLA. I also thank Chelsi White and other University of Arizona researchers for their help in dating zircons, and Kevin Coffey and Johanna Hoyt for assistance in the field. Lastly, I thank my mother Andrea for her love and support, and my father Peter, without whom I would not have gotten to this point. I dedicate this thesis in his memory.

INTRODUCTION

Cajon Canyon separates the San Gabriel and San Bernardino mountain ranges to the west and east, respectively, on the southern edge of the Mojave Desert of southern California (Fig. 1); Cajon Valley trends NW-SE on the northeast side of the easternmost San Gabriel Mountains. The Miocene Cajon Valley formation, originally named Punchbowl formation (Noble, 1954), is juxtaposed against Cretaceous Pelona Schist, Precambrian gneiss and Cretaceous granodiorite by the currently active San Andreas fault and the inactive Cajon Valley fault (Dibblee, 2003a, b).

This study aims to determine the provenance and depositional paleogeography of the lower Middle Miocene Cajon Valley formation, employing detrital-zircon, petrographic and conglomerate-imbrication analyses. By reversing well-constrained slip on the San Andreas fault system, we are able to find offset equivalent sandstone and conglomerate contemporaneous with those of the Cajon Valley formation. Successful matching of offset equivalents will better constrain the paleotectonic, paleogeographic and paleodrainage history of southern California.

REGIONAL SETTING, LITHOLOGY AND STRATIGRAPHY

Previous Work

Nonmarine sedimentary strata in Cajon Valley were first described as being upper Miocene, based on vertebrate paleontology, and correlative to the Punchbowl Formation at its type locality of Devil's Punchbowl, on the SW side of the San Andreas fault (Noble, 1954; Fig. 1). If correctly correlated, then this would imply that offset on the San Andreas fault was only ~30 km for these sedimentary strata. The Punchbowl Formation was subsequently assigned a Pliocene age (Tedford and Downs, 1965), but given the similar appearance between the two "correlated" areas and the poorly understood San Andreas fault system at the time, Noble's interpretation of the Cajon beds was not challenged until the 1970s.

In a general stratigraphic and paleontologic study of the Cajon Valley area, Woodburne and Golz (1972) determined the sedimentary strata in Cajon Valley to be of Hemingfordian-Barstovian age (18-14 Ma), as opposed to the Clarendonian-Hemphillian (13-9 Ma) age for the Punchbowl Formation. They divided the Cajon Valley formation into seven members, with an overall upward fining trend and slight variations in color; all members consist predominantly of conglomeratic arkosic sandstone.

In a comprehensive study of Cenozoic stratigraphy in the Transverse Ranges, Woodburne (1975) correlated potentially offset rock units cut by the San Andreas fault system. Sedimentary strata in Cajon Valley were inferred to correlate with similar strata in Cuyama Valley and the Caliente Range to the northwest (Fig. 2). These correlations can be tested employing detrital-zircon and petrographic analyses.

An exhaustive study of the late Cenozoic tectonic history of the Cajon Pass area by Weldon (1986) shed light on potential causes for sedimentation in Cajon Valley, although this work emphasized evolution of the modern San Andreas fault and not its Miocene history.

Paleomagnetic studies in Cajon Valley indicate a 30±8° clockwise vertical-axis rotation in the basal Cajon Valley formation, but not in the overlying (or contemporaneous, discussed below) Crowder Formation or Plio-Pleistocene units (Liu et al., 1988). This rotation is attributed to movement on the Squaw Peak fault in the NE of the valley (Fig. 1), interpreted to have been a thrust fault in the mid to Late Miocene, rather than regional rotation associated with the Mojave block (Weldon, 1986; Liu et al., 1988). These measurements, however, were taken only near the Squaw Peak fault, and therefore, are interpreted as unrepresentative of the entire basin; as a result, vertical-axis rotations did not affect paleocurrent indicators (discussed below).

Basement Lithology

Precambrian Gneiss

Highly foliated Precambrian gneissic rocks, which are in contact with the Cajon Valley formation along the Cajon Valley fault along the southwest side of the valley (Fig. 1), are intruded by Cretaceous granodiorite (Dibblee, 2003b).

Cretaceous Granodiorite

Exposed Cretaceous granodiorite nonconformably underlies the Vaqueros and Cajon Valley formations in Cajon Valley (Dibblee 2003a, b). Contacts between the granodiorite and Cajon Valley formation across the Cajon Valley fault are irregular and geometrically complex in the southwest corner of the valley.

Stratigraphy

Paleocene San Francisquito Formation

A Paleocene episode of marine deposition is recorded by limited exposures of the San Francisquito Formation. Woodburne and Golz (1972) described and Dibblee (2003a) mapped the 300m-thick San Francisquito Formation as nonconformably overlying Cretaceous granodiorite and being unconformably overlain by the "Punchbowl" or Cajon Valley formation in the southeastern part of the basin. Within 3 km to the northwest, however, lies the Oligocene-Lower Miocene Vaqueros Formation with the same unconformable contacts. The San Francisquito and Vaqueros formations are not in contact, and the same stratigraphic position for both suggests that they may be the same formation, with slight lateral variations in lithology. However, no paleontological evidence has been cited to test this hypothesis (Woodburne and Golz, 1972).

Lower Miocene Vaqueros Formation

The 160m-thick Lower Miocene Vaqueros Formation, which is primarily clastic, but contains carbonate, has a molluscan assemblage indicating Early Miocene shallow-marine

paleoenvironments (Woodburne and Golz, 1972). The Vaqueros Formation is exposed in the SW part of Cajon Valley, underlying the Cajon Valley formation (Dibblee, 2003b).

Middle Miocene "Punchbowl Formation" in Cajon Valley

The "Punchbowl Formation", as it was originally named in Cajon Valley, is characterized by over 2400m of yellow to maroon, well indurated arkosic conglomerate and conglomeratic sandstone, early Middle Miocene in age (Noble 1954; Woodburne and Golz, 1972). Fine-grained beds and lithologic diversity increase up section. Mapping, and stratigraphic and paleontologic studies have been completed (e.g., Noble 1954; Woodburne and Golz, 1972), but detailed lithology or provenance studies had not been completed prior to the present study. The following lithologic descriptions of each member in the Cajon Valley formation ("Punchbowl formation") are modified from Woodburne and Golz (1972). The likely braided-stream depositional environments and basin architecture resulted in complex outcrop relationships for the members.

Tp^1. Tp^1 of the "Punchbowl formation" in Cajon Valley is characterized by pale gray-to-white, arkosic conglomerate and conglomeratic sandstone. Melanocratic clasts of fine-grained metamorphic rocks are locally abundant. Tp^1 is vertically and possibly also laterally gradational. Tp^1 is 215-305 m thick and rests unconformably on the Vaqueros Formation or nonconformably on Cretaceous granodiorite; its upper contact is gradational with Tp^2.

Tp^2. Similar to Tp^1, arkosic conglomerate and conglomeratic sandstone predominate in the Hemingfordian Tp^2; however, Tp^2 has an upward increase of interbedded, fine-grained sandstone. Tp^2 is pale buff overall, ranging in thickness from 426 m in the south to 550 m northwest of Cajon Valley. Strata are well indurated, resulting in most of the topographic features in the valley (Fig. 3). Tp^2 abuts granodioritic gneiss across the Cajon Valley fault.

Tp^3. Tp^3 has lithology similar to Tp^2, only its fine-grained beds are less resistant. Tp^3 nonconformably overlies Cretaceous granodiorite, and is gradationally overlain by Tp^4 and Tp^5. Tp^3 is 150-550 m thick, reaching its maximum in the northwest. Rhinoceros and ground-squirrel fossils indicate that Tp^3 is upper Hemingfordian (Woodburne and Golz, 1972).

Tp^4. Exposure of Tp^4 is limited to the southern part of Cajon Valley. Characteristic coarse-grained sediment is biotite-rich, with gray-buff, arkosic conglomerate and conglomeratic sandstone predominating. Tp^4 reaches a maximum thickness of 213 m. Coarse clasts are equal parts granodiorite and volcanics, with little to none of the fine-grained metamorphic clasts in Tp^1. Within Tp^4 are abundant latite to quartz latite metavolcanics. Limited exposure of Tp^4 suggests that it is possibly the coarse-grained, lateral equivalent of Tp^5 (discussed below). No fossils have been reported from Tp^4, but stratigraphic relations indicate a probable Late Miocene age.

Tp^5. Tp^5 is characterized by heterogeneous beds and highly variable thickness, being 565 m in the southeast and 915 m in the northwest. Conglomerate and conglomeratic sandstone are interbedded with yellow, coarse-to-medium-grained sandstone. Near the middle of the section are black mudstone, plant-bearing lignite and freshwater limestone with gastropod, ostracode, charophyte and algal-mound fossils; fossil Miocene horses are also found in Tp^5 (Woodburne and Golz, 1972).

Tp^{5a}. Tp^{5a}, which is laterally gradational with Tp^5, is composed predominantly of red-brown conglomerate and conglomeratic sandstone, with cobbles and pebbles being angular granodioritic gneiss, marble, quartzite and fine-grained schist. Tp^{5a} is 885 m thick and wedge shaped, and interfingers with white arkosic conglomeratic sandstone to the east.

Tp^6. Tp^6 is characterized by white to pale-yellow conglomerate and conglomeratic sandstone with abundant dark-green and maroon porphyritic-tuff and latite clasts, interbedded with fine-grained sandstone, mudstone and siltstone. Coarse-grained beds are more abundant than finer ones. Tp^6 is 275 m thick, but is unconformably overlain by the Crowder Formation, so its original thickness is unknown. Tp^6, which is found in the central and northwest parts of Cajon Valley, contains few fossils, but is probably Upper Miocene (Woodburne and Golz, 1972).

Weldon et al. (1993) claimed that Tp^6 has a western provenance across the modern San Andreas fault, based on the absence of paleocurrent indicators, a marked decrease in the pink arkosic component that is prevalent in Tp$^{1-5}$, and the presence of red-sandstone clasts. If Tp^6 were derived from across the SAf, then the southwest-dipping paleoslope responsible for Tp$^{1-5}$ would have been inverted; a potential cause for this inversion could have been dip-slip motion on the proto-San Andreas, prior to its current transform motion (Weldon, 1986). Weldon et al. (1993) suggested that motion on the San Andreas fault was only about 1 cm/yr. during the Miocene, whereas it has increased to 3.5 cm/yr. since 5-4 Ma. Weldon et al. (1993) lacked petrographic evidence that the red-sandstone clasts were from the Vasquez Formation (e.g., Hendrix and Ingersoll, 1987), which they interpreted as a possible westerly source rock. However, the red beds present within Tp$^{3-5}$ (Woodburne and Golz, 1972) could be possible sources for red sandstone clasts in the overlying unit; multiple unconformities and variable thicknesses within the Cajon Valley formation suggest that in-situ erosion and redeposition of clasts might have been significant, thus negating the need for external sources for the red-sandstone clasts. Sample locations for Cajon Valley formation sandstone in this study are listed in Table 1 and shown on Fig. 1.

Crowder Formation

The Crowder Formation (1000 m thick) is characterized by fluviatile conglomerate and conglomeratic sandstone that unconformably overlie the Cajon Valley formation and grade upward into the Harold Formation (Woodburne and Golz, 1972; Dibblee 2003a,b). Clasts in the Crowder Formation reflect a San Gabriel Mountains provenance (Woodburne and Golz, 1972). The Crowder Formation was first assigned a Hemphillian or Blancan age (9-2 Ma) (Woodburne, 1975), but the discovery of middle Miocene fossils in its basal unit indicated that it could be as old as 14 Ma (Reynolds, 1984), meaning its age overlaps the depositional age of the Cajon Valley formation. The interaction of these two formations and separate provenance is poorly constrained and should be addressed in future work.

Harold Formation and Shoemaker Gravel

Overlying the Crowder Formation are the Harold Formation and Shoemaker Gravel (Dibblee 2003a, b). Similar to parts of the Crowder Formation, they contain abundant clasts of Pelona Schist and other materials derived from the western San Gabriel Mountains and are believed to be Irvingtonian to Rancholabrean (1.5-0 Ma) (Woodburne, 1975).

POTENTIAL OFFSET EQUIVALENTS AND RELATED ROCKS

Caliente and La Panza Ranges

The Caliente Range and adjacent Cuyama Valley lie to the southwest of the San Andreas fault northwest of Cajon Valley (Fig. 1). Detailed descriptions of Eocene through Pleistocene strata can be found in Hill et al. (1958).

Branch Canyon Sandstone

Defined by Hill et al. (1958), the Branch Canyon Sandstone is exposed on the south side of Cuyama Valley and in the northeast of the Caliente Range (Fig. 1). Composed mainly of gray-to-

buff marine sandstone, the Branch Canyon Sandstone (915 m) represents the transition (both vertically and horizontally) between continental Caliente Formation and marine Monterey Formation (Hill et al., 1958). Deposition occurred throughout the Hemingfordian and Barstovian (18-14 Ma), as well constrained by abundant microfossils and three basaltic intrusions (Hill et al., 1958).

Subsequent to the original definition, Dibblee (1967) associated the Branch Canyon Sandstone proper with marine sandstone outcrops extending to the north, and mapped it as a member of the Monterey Formation. This resulted in a 60km-long exposure of Branch Canyon Sandstone, from the Caliente Range and Cuyama Valley in the southeast to the La Panza range in the northwest. Both samples analyzed in this study (DMS-12-BC1, 2) were collected near the southeasternmost outcrop in the Caliente Range (Fig. 1; Table 1).

Santa Margarita Formation

Overlying the Branch Canyon Sandstone in the SW, and Monterey Formation in the NE Caliente Range, the Santa Margarita Formation reaches a maximum thickness of 300 m (Hill et al., 1958). It is predominantly a white sandstone with two shale members, interpreted to be littoral, based on marine microfossils, and Clarendonian (12-10 Ma) based on megafossils (Hill et al., 1958). Dibblee (1967) also associated the originally defined Santa Margarita Formation in the Caliente Range with other white sandstone units to the north. One sample (DMS-12-SM1) was collected near the southeasternmost outcrop, near the Branch Canyon samples, and one (DMS-12-SM2) was collected to the northwest in the La Panza Range (Fig. 1; Table 1).

Simmler Formation

Continuous pink to dark-gray, medium-grained Miocene massive sandstone, 1000 m thick, constitutes the Simmler Formation, which crops out in the NW and SE Caliente Range, the

adjacent Cuyama Badlands, as well as the La Panza Range to the northwest (Hill et al., 1958). Its base is unexposed, but well data suggest that it overlies granitic basement in at least some areas (Weldon, 1986). The Simmler Formation coarsens to red and gray conglomerate with gneiss and granite clasts to the SE of the Caliente Range in the Cuyama Badlands (Hill et al., 1958). One sample of Simmler, DMS-12-S1, was collected in the La Panza Range (Fig. 1; Table 1)

Caliente Formation

The Caliente Formation crops out in the SE Caliente Range, near the Carrizo Plain (Fig. 1). It is composed of 900m-thick continental redbeds that are laterally gradational toward the west with the marine Branch Canyon Sandstone. The Caliente Formation varies from red to gray and has a 100m-thick basaltic member in its middle. It is Hemingfordian to Clarendonian (18-10 Ma) in age, overlapping in age with the Branch Canyon Sandstone (Hill et al., 1958; Woodburne, 1975). Two sand(stone) samples of Caliente Formation (JFH-11-21C, 23C) were collected in a previous study (discussed later) in the Caliente Range (Fig. 1; Table 1).

Monterey Formation

The Monterey Formation in the Caliente Range/Cuyama area lies conformably below the Santa Margarita Formation, and grades laterally into the Branch Canyon Formation. It is 680 m of predominantly siliceous shale and clay beds, with some 1m-thick gray sandstone beds (Hill et al., 1985). Foraminiferal assemblages indicate that the shale is Hemingfordian to Barstovian (18-14 Ma) (Hill et al., 1985). One sample, DMS-12-MTY1, of Monterey Formation was collected in the La Panza Range (Fig. 1; Table 1).

Devil's Punchbowl

The type location of the Punchbowl Formation, located in Devil's Punchbowl, 30 km to the northwest of Cajon Valley and southwest of the SAf (Fig. 1), was first described by Noble

(1954) and more precisely dated by Tedford and Downs (1965). The dominantly coarse-grained conglomeratic sandstone strata are similar in appearance to the Cajon Valley formation, which resulted in early correlation between the two formations (e.g., Noble, 1954). Woodburne and Golz (1972) clearly demonstrated an age discrepancy between the two formations. Subsequently developed constraints on offset along the San Andreas fault system (e.g., Weldon et al., 1993) have negated any possible correlation between the two "Punchbowl" formations. Detrital-zircon ages and sandstone petrology from one sample of Punchbowl proper (KTC-12-Tps1) analyzed in the present study provide additional tests of this possible correlation.

PALEOCURRENTS

Paleocurrent Indicators

Paleocurrent indicators were measured and recorded wherever exposed in the Cajon Valley formation. The three-dimensional nature of sandstone cross bedding was difficult to assess in most places due to the well rounded hogbacks that typify Cajon Valley (Fig. 3). Conglomeratic packages within the sandstone, however, contain imbricated clasts in most outcrops, despite previous workers' (e.g., Woodburne and Golz, 1972) generalization that they are not present. Previous work has alluded to SSW paleocurrent directions (e.g., Woodburne and Golz, 1972; Weldon, 1986); however, to the author's knowledge, no measurements have been published.

Formations surveyed on the SW side of the San Andreas fault are not nearly as conglomeratic as the Cajon Valley formation. Similarity of sandstone petrology and detrital-zircon ages (discussed below) on either side of the fault, however, suggests that this discrepancy is likely a result of paleoenviromental changes downstream (to the SW).

Methods

Wherever convincingly imbricated, 10 orientation measurements were made of the maximum cross-sectional planes between imbricated clasts within the same bed. Sixteen locations (Fig. 4) were measured, resulting in a total of 160 measurements (Appendix 1). Bedding strike-and-dip measurements at each location were used to correct for tectonic tilting using STEREONET8 (algorithms described in Almendinger et al., 2012). After rotating imbricated planes to remove the effects of tilting, downstream paleocurrent directions were determined, with transport toward the up-dip direction. Readings where original dips restored to <10° were removed from the data set as being unreliable, leaving 15 out of the 16 measured locations (Fig. 4).

Results

Average paleocurrent direction was dominantly toward the SSW, in accord with previous suppositions. Averaged directions at each location are shown in Fig. 4. Measurements are dominantly from the SE part of the valley, where coarsest members of the lower Cajon Valley formation are exposed. The upper Cajon Valley formation to the NW is finer-grained and more weathered, with coherent bedding in most places difficult to find. Imbrications in this area are either nonexistent or unconvincing; rarely were 10 clasts, imbricated or otherwise, found in one coherent bed.

SANDSTONE PETROLOGY

Methods

Collection and Preparation

Sand(stone) samples were collected throughout the Cajon Valley formation and in selected potential offset equivalents (Fig. 1; Table 1). Well indurated sandstone samples were cut perpendicular to bedding. Unconsolidated and poorly consolidated samples were impregnated

with epoxy. Uncovered thin sections were prepared by Ram Alkaly of R.A. Petrographic, Los Angeles, CA. Thin sections were etched with dilute hydrofluoric acid and stained with a saturated solution of sodium hexanitrocobaltate. This etching and staining combination helps to differentiate quartz, plagioclase feldspar and potassium feldspar, which are unaltered, heavily etched and stained with yellow dots, respectively (e.g. Ingersoll and Cavazza, 1991).

Petrography

Thin sections were point-counted (400-500 points/section) using the Gazzi-Dickinson method (i.e., Gazzi, 1966; Dickinson 1970; Ingersoll et al., 1984), so that each crystal coarser than silt (>0.0625 mm) is counted as that crystal, regardless of whether or not it is part of a larger detrital grain. Counting-grid spacing was greater than average grain size. Counting categories are defined in Table 2, and raw counts are shown in Table 3. All compositional determinations were made on a Nikon Eclipse E400 POL microscope fitted with a James Swift automated stage and point counter. Subcategorical details were noted on Clay Adams manual laboratory counters.

Analysis

Six sandstone samples from the Cajon Valley formation and 11 related samples (Fig.1; Table 1) were analyzed using 13 compositional categories for framework grains (Table 2). Percentages were then calculated for quartz-feldspar-lithic fragment (QFL), monocrystalline quartz-potassium feldspar-plagioclase feldspar (QmFkFp) and metamorphic-volcanic-sedimentary lithic (LmLvLs) ternary plots. The parameters used for these categories are defined in Table 4.

Results

Cajon Valley formation

Sandstone from the Cajon Valley formation is quartzofeldspathic and clusters well on all three ternaries used in this study. All six samples (Fig. 1; Table 1) have slightly higher feldspar concentration than quartz, and minimal lithic components (Fig. 7, Table 5). Fp/F, as defined in Table 4, averages 0.59, with one anomalously low 0.42 (Table 5), reflected best in Fig. 8. Lithic components are dominantly sedimentary or metamorphic (Fig. 9; Table 5); however, lithic percentages have low significance because of their low numbers (QFL%L does not exceed 9% for any sample; Table 5). The best ternary for comparing Cajon Valley sandstone with potential offset equivalents is QmFkFp (Fig. 8).

Punchbowl Formation

Five samples of the type Punchbowl Formation of Devil's Punchbowl (Fig. 1) were point-counted to test the hypothesis that the two "Punchbowl formations" are not correlative (e.g., Powell et al., 1993). Punchbowl sandstone has higher QFL%F (Fig. 7; Table 5), QmFkFp%Fp (Fig. 8; Table 5), Fp/F (Table 5) and LmLvLs%Lv (Fig. 9; Table 5) than Cajon Valley sandstone. This higher feldspar content, particularly plagioclase, and presence of volcanic lithics is indicative of a more heterogeneous provenance for the Punchbowl Formation, as compared with the Cajon Valley formation, consistent with detrital-zircon ages (described below).

Potential offset equivalents

Of the six samples representing four formations collected in the Caliente Range, sample DMS-12-MTY1, from the Monterey Formation, is least similar to Cajon Valley sandstone. It is the only quartzolithic sample (Fig. 7), with the lowest Fp/F at 0.36 (Table 5). The low plagioclase content (Fig. 8; Table 5) reflects either a more mature sediment or more granitic provenance (or both). Many sedimentary lithic fragments are probably intrabasinal (e.g., Zuffa, 1985), thus creating ambiguity in provenance interpretation.

The Simmler Formation sample (DMS-12-S1) is the most feldspathic analyzed sample (Fig. 7). Fp/F of 0.62 (Table 5), and the dominance of sedimentary and metamorphic lithic components (Fig. 9; Table 5) matches well with the Cajon Valley samples, but lower quartz content (Fig. 7; Table 5) might reflect a more dioritic or monzonitic provenance compared to the inferred granitic sources for the Cajon Valley formation.

The Santa Margarita Formation is the second-best petrographic match with the Cajon Valley formation. Both samples (DMS-12-SM1,2) cluster with Cajon Valley sandstone on QFL and QmFkFp ternaries (Fig. 7, Fig. 8). Fp/F of 0.58-0.61 and QFL%L < 5% (Fig. 7; Table 5) are also similar to Cajon Valley sandstone. On the other hand, the two formations have contrasting lithic types; Ls and Lm dominate in Cajon Valley sandstone, whereas Santa Margarita sandstone has high felsic-volcanic content (Fig. 9; Table 5). This slight contrast may have resulted from downstream input of volcanic material, expressed in the shallow-marine Santa Margarita Formation and not the continental Cajon Valley sandstone.

The overall best petrographic match for the Cajon Valley formation is Branch Canyon Sandstone (DMS-12-BC1,2). With an average Fp/F of 0.58 and QFL%L <2% (Fig. 7; Table 5), Branch Canyon Sandstone is similarly arkosic, and clusters with Cajon Valley sandstone on QFL and QmFkFp ternary diagrams (Fig. 7, Fig. 8). What makes Branch Canyon Sandstone a better match than the Santa Margarita Formation is its low volcanic lithic component (Fig. 9; Table 5); Branch Canyon lithic grains are mostly sedimentary and metamorphic, and plot near Cajon Valley samples on the LmLvLs ternary (Fig. 9).

DETRITAL-ZIRCON ANALYSIS

Methods

Collection and Preparation

Sand samples were collected for detrital-zircon analysis at the same locations as the samples of lithified sandstone for thin sections (Fig. 1). These sand samples were separated using a Ro-Tap Testing Sieve Shaker, saving sediment finer than the USA Standard Testing Sieve no. 60 (250 μm) to be further processed. The sediment was subjected to baths of dilute hydrochloric acid to remove any carbonate potentially cementing grains. Samples were then condensed to a higher density using a sluice table at Pomona College's Geology Department. Magnetic grains were removed using a Neodymium magnet. Lastly, density separations using 3.32 g/cm^3 density Methyl Iodide in UCLA's Mineral Separation Lab concentrated the densest minerals to be used for zircon age determination. Concentrated zircon samples were sent to the University of Arizona Laserchron where they were mounted in epoxy for laser-ablation multiple-collector inductively coupled plasma mass spectrometry (LA MC-ICPMS) (e.g., Gehrels et al. 2008).

Analysis

U-Th-Pb isotope ratios were measured to calculate ages of detrital-zircon samples. Mounted zircons were ablated, using backscattered electron (BSE) images of each sample as a guide for grain selection. Although dating > 100 zircons from each sample would be ideal (e.g. Gehrels et al., 2008), some samples contained few zircons, and samples with tightly clustered ages needed fewer ages to characterize the population distribution. Thus, the number of zircons dated for each sample varies from 12 to 77 (Fig. 10; Appendix 2). Zircons were ablated at their cores to determine original magmatic crystallization ages as accurately as possible.

Results

Age distribution plots for all analyzed samples are shown in Fig. 10. All Cajon Valley sandstone samples (in red on the left column) have distinct peaks at 85-90 Ma, 150 Ma and 250 Ma. Dashed gray bars have been added through all samples to highlight these ages. The

stratigraphically lowest sample (DMS-12-CV1) has a small Precambrian peak, around 1700 Ma, that other Cajon Valley samples lack. These ages are attributed to either reworking and inclusion of the underlying San Francisquito Formation (e.g. Jacobson et al., 2011), or input from rocks no longer exposed in the southern Mojave Desert.

Of the potential offset equivalent and related sandstone sampled (right column), Monterey (DMS-12-MTY1), Simmler (DMS-12-S1) and Punchbowl (KTC-12-Tps1) Formations are unlikely correlated to the Cajon Valley formation based on detrital zircons. Monterey sample DMS-12-MTY1 does not contain any of the distinct peaks present in each of the Cajon Valley sandstone samples. Simmler sample DMS-12-S1 matches well for the 85-90 Ma and 250 Ma peaks, but lacks 150 Ma zircon (Fig. 10). Punchbowl sample KTC-12-Tps1 has wider, less distinct peaks around all three ages compared to all six Cajon Valley samples, in accord with other unpublished ages for this formation (Hoyt, 2012); this result further confirms the hypothesis that the Punchbowl Formation and Cajon Valley formation are unrelated. These two formations may have been derived, in part, from similar plutonic source rocks of the Mojave Desert, but the wider array of Precambrian zircons in Punchbowl sand suggests more diverse sources.

Caliente Formation samples JFH-11-21C and JFH-11-23C have similar peaks to those of the Cajon Valley formation, but the paleogeographic locations and paleotectonic settings of these strata southwest of the San Andreas fault, as outlined by Hoyt (2012), negate their direct correlation. These samples were analyzed as a continuation of Hoyt's (2012) work, and thin sections were not available for the aforementioned petrographic analysis.

The remaining Santa Margarita and Branch Canyon samples from the Coast Ranges seem to most closely resemble Cajon Valley sandstone. Samples DMS-12-BC2 and DMS-12-SM2

exhibit all three characteristic peaks, along with an older ~1700 Ma peak, like the basal Cajon Valley formation (Fig. 10). Samples DMS-12-BC1 and DMS-12-SM1 are slightly dissimilar, with a subdued 150 Ma peak and an additional Cenozoic peak, respectively. Since both of these formations would represent downstream sedimentation (SSW of the Cajon Valley formation following restoration of San Andreas slip [see below]), addition of locally derived detrital zircons and modification of relative age peaks would be expected.

It is interesting to note that the best-fitting offset equivalent samples, DMS-12-SM2 and DMS-12-BC2, were sampled in the Caliente Range (Fig. 1), 80 km south of what would be a full 310 km offset with Cajon Valley. Longshore currents could have dispersed sand derived from the Cajon Valley drainage system along the coast; laterally extensive plutons in the Mojave Desert could have provided sediment to multiple drainage systems, which would have resulted in compositionally consistent detritus along the coast. However, the possibility exists that reported ages could be inaccurate, and the best-fit offset equivalent sandstone was not actually sampled in this study.

PROVENANCE AND PALEOGEOGRAPHIC IMPLICATIONS

Potential Plutonic Sources

The westernmost San Bernardino Mountains contain granitoids with Permian-Triassic, Late Jurassic and mid-Cretaceous ages similar to detrital-zircon ages from the Cajon Valley formation, however they were only uplifted around 5 Ma (Barth and Wooden, 2006; Barth et al., 2008). These plutonic rocks, which are remnants of large contiguous plutons stretching across the Mojave region, reflect the local source rocks for the arkosic sand derived from the NNE, as determined by imbricated conglomerate clasts. The lack of Precambrian zircons in the Cajon Valley samples and distinct SSW paleocurrents require that the source rocks were located

southwest of the Mogollon Highlands (Fig. 5, Jacobson et al., 2011). Potential source terranes are, therefore, limited to the southwestern Mojave. Cajon Valley sediment is unlikely to have been sourced from the Sierra Nevada, traveling SE along the eastern side of the batholith, as the zircon signature would be expected to have a higher concentration of Cretaceous zircon (Barth et al., 1997, 2008).

Geochronological and geochemical studies have demonstrated that subduction at the western North American margin resulted in emplacement of voluminous intrusive bodies at sporadic intervals, suggestive of episodic magmatism in both time and place (Burchfiel et al., 1981; Barth et al., 1997, 2008; Barth and Wooden, 2006). Thus, plutonic rocks of distinct ages in the southwestern Mojave Desert are reflected in the sharp peaks on the zircon probability plots of this study.

Triassic rocks in the southwestern Mojave, that offer the best match for the 250 Ma peak in all Cajon Valley and equivalent sandstone, occur in the Granite Mountains adjacent to the San Bernardino Mountains and the Little San Bernardino Mountains. Both are principally monzonite and quartz monzonite, with lesser granodiorite (Barth and Wooden, 2006).

The Late Jurassic was a period of active plutonism in the southwest U.S. Cordillera, with a belt of plutonic and volcanic rocks stretching at least 200 km through the Mojave to the central Transverse Ranges (Barth and Wooden, 2006, 2008). Barth et al. (2008) showed numerous plutons throughout the Mojave dated 149-157 Ma. Some of these plutons outcrop in the western and central San Bernardino Mountains, despite being heavily intruded during subsequent plutonism (Barth et al., 2008).

Plutonism occurred widely in the Mojave region between 105 to ca. 80 Ma (e.g. Wright et al., 1987; Miller et al., 1996; Schermer et al., 2001; Walker et al., 2002), encompassing all of the

early Late Cretaceous-aged detrital zircon dated in this study within the Cajon Valley formation. Remnants of these rocks are exposed throughout the Mojave, including the mountains NE of Victorville, upstream along paleocurrents for the Cajon Valley formation (Fig. 5).

Depositional Environments

When palinspastically reconstructed, the 10km-wide outcrop of Cajon Valley formation is placed against ~80 km of continuous shallow-marine sandstone southwest of the SAf. Because the 310 km offset of the SAf is well constrained (e.g.,Graham et al., 1989; Weldon et al., 1993), juxtaposition of continental and shallow-marine sandstone resulted from a connection of upstream and downstream components within a source-to-sink system. The Branch Canyon Sandstone and Santa Margarita Formation probably represent deltaic and shallow-marine deposits deposited by rivers transporting sediment through the Cajon Valley area (Fig. 11). This would place the Cajon Valley area coast-adjacent; this interpretation is consistent with the marine paleoenvironments of the underlying Vaqueros and San Francisquito formations in Cajon Valley (Woodburne, 1975; Weldon, 1986), and the third-order sampling scale for Caliente/La Panza samples, as opposed to the second-order Cajon Valley samples (e.g., Ingersoll et al., 1993). Deposition of Cajon Valley alluvium on top of marine deposits would represent progradation of a delta system into marine paleoenvironments.

CONCLUSIONS

Based on paleontological data and well constrained SAf offset, previous work in Cajon Valley debunked correlation of the Cajon Valley formation with the Punchbowl Formation at Devil's Punchbowl across the SAf (Woodburne and Golz, 1972; Weldon, 1986). Since the Hemingfordian-Barstovian (18-14 Ma) Cajon Valley formation was deposited prior to being truncated by the San Andreas fault, the 2400m-thick, 10km-wide nonmarine deposits likely were

also deposited across the current fault trace to the SW. Palinspastic restoration of 310 km of dextral slip on the SAf system places the Cajon Valley formation alongside what should be equivalent sandstone; this reconstruction adjoins Cajon Valley deposits next to similar-aged, shallow-marine sandstone in the Caliente and La Panza Ranges.

Sandstone samples collected from the Cajon Valley formation, potential offset equivalents and related strata are dominantly arkosic, with only minor variations in composition; consequently, differentiation of Cajon Valley formation and potential offset equivalents using largely similar sandstone compositions alone is unconvincing. QFL, QmFkFp and LmLvLs ternaries demonstrate that all samples are predominantly quartzofeldspathic with moderately higher plagioclase relative to potassium feldspar. Lithic components vary the most among samples, but low abundances of lithic fragments render their relative proportions unreliable as provenance indicators. Sandstone from the Branch Canyon Sandstone and the Santa Margarita Formation from the Caliente and La Panza Ranges are compositionally the best matches for Cajon Valley sandstone.

Nearly 800 detrital-zircon ages from Cajon Valley and related sandstone proved to be more effective than petrography for determining cross-fault correlations. Distinct age peaks at 85-90 Ma, 150 Ma and 250 Ma are apparent in all samples collected in the Cajon Valley formation, which seems to be devoid of any Precambrian zircon in all but its basal unit. Of the samples collected as potential offset equivalents, the Branch Canyon Sandstone and Santa Margarita Formation seem to be most similar to the Cajon Valley formation. The Punchbowl Formation of Devil's Punchbowl appears to have had similar-aged plutonic source rocks, but with additional diverse rocks and ages. Similarly, the Monterey, Caliente and Simmler formations, all from the

La Panza Range, exhibit zircon age distributions that differ enough from the Cajon Valley formation to invalidate them as being directly related.

The SSW paleoflow direction determined from imbricated conglomerate clasts throughout the Cajon Valley formation suggests sources to the NNE, in the Mojave Desert. The sharply defined age peaks and lack of Precambrian zircon in the Cajon Valley formation limit possible sources to local areas in the Mojave Desert. The three Mesozoic age peaks of Cajon Valley sandstone correspond to batholithic belts in the Mojave Desert (Barth et al., 2008). Uncertainties concerning the former lateral extent of these batholiths make distinguishing precise locations for source rocks impossible. Precambrian rocks in the Mogollon Highlands provide a NE limit to possible source areas for zircon deposited in the Cajon Valley formation.

The 10km-wide exposure of conglomeratic sandstone in Cajon Valley, complete with scour-and-fill structures and cross bedding, is suggestive of a braided-stream system (Woodburne and Golz, 1972). Using the well constrained 310 km of slip on the San Andreas fault system, and the SSW paleocurrent direction determined in this study, the Cajon Valley formation restores adjacent to laterally extensive, shallow-marine sandstone of the Santa Margarita Formation and Branch Canyon Sandstone in the Caliente and La Panza ranges. Both the Santa Margarita Formation and Branch Canyon Sandstone are exposed over 80 km and represent a broad, shallow-marine depositional system. Although the three distinct zircon age peaks exhibited by Cajon Valley samples are present in offset equivalents, these formations likely represent shallow-marine deposition resulting from sediment input from multiple fluvio-deltaic systems (Fig. 11). The Cajon Valley formation is interpreted to represent a Miocene braided-fluvial system on a coastal plain, flowing toward a delta on the continental shelf, now preserved as Santa Margarita and Branch Canyon sandstone in the Caliente and La Panza Ranges.

FIGURE CAPTIONS

Figure 1: Location map showing sampling sites for this study. Cajon Valley's proximity to the San Andreas fault, its age, and interpreted braided-stream depositional system suggest that offset equivalent sediments should lie 310 km to the NW, due to subsequent slip on the San Gabriel/San Andreas faults after deposition.

Figure 2: Stratigraphic correlation of basins across major strike-slip faults in California, modified from Woodburne (1975). Branch Canyon Sandstone in the Caliente Range, the Santa Margarita Formation of the La Panza Range and lower Caliente Formation in Cuyama Valley overlap temporally with the Hemingfordian-Barstovian Cajon Valley Formation in Cajon Valley. Note that the stratotype Punchbowl Formation is Clarendonian-Hemphillian in age.

Figure 3: A well-rounded hogback outcrop of Cajon Valley formation (formerly referred to as Punchbowl) conglomeratic sandstone. Coarse lenses and lenticular bedding are ubiquitous throughout the formation, indicative of fluvial deposition. The 10km width and lack of fine-grained material suggest that a sizeable braided stream flowed through the valley in Miocene time. Photo taken looking west, at location of DMS-12-CV6, Fig. 1.

Figure 4: Paleocurrents determined at 15 locations in Cajon Valley from imbricated clasts within conglomeratic packages are illustrated with directional arrows. Conglomeratic packages are concentrated in the SE of the valley, with the NW being more sand-rich and less resistant to weathering, resulting in subdued topography. In the Hemingfordian-Barstovian, this stream flow

was dominantly to the S-SW, illustrated best on the inset rose diagram. Some local variations exist, but nothing more than would be expected in a braided-stream depositional system.

Figure 5: Pre-Miocene palinspastic reconstruction of southern California (from Jacobson et al. 2011). Cajon Pass (CP) is outlined in red. Since paleocurrent indicators suggest a NE source for Cajon Valley formation, sediment was likely derived from the southern Mojave Desert. In this figure, most igneous rocks in the vicinity are 300 Ma or younger.

Figure 6: A palinspastic southern California paleodrainage reconstruction from Ingersoll et al. (2013). The reconstruction illustrates detrital-zircon ages in southern California, which have been used to determine the extent of the drainage catchment for the Sespe delta; however no ages have been published for Cajon Valley or its surrounding area (circled in red).

Figure 7: QFL ternary diagram of sandstone point count data. Samples are color-coded by formation. Q – quartz, F – feldspar, L – Lithic fragment, defined in Table 2. Each apex represents 100% composition. Data shown in Table 5.

Figure 8: QmFkFp ternary diagram of sandstone point count data. Qm – Monocrystalline quartz, Fk – potassium feldspar, Fp – plagioclase feldspar. Each apex represents 100% composition. Data shown in Table 5.

Figure 9: LmLvLs ternary diagram of sandstone point count data. Lm – metamorphic lithic, Lv – volcanic lithic, Ls – sedimentary lithic. Each apex represents 100% composition. Data shown in Table 5.

Figure 10: Probability density plots for all samples in this study. Cajon Valley samples are in the stratigraphic order in left column, with potential offset equivalent and related rocks on the right. Samples are color-coded by formation as in ternary diagrams. 400-1200 Ma ages have been removed from the horizontal axis due to a complete absence from all samples in this study. Three distinct peaks occur in all Cajon Valley samples, at 85-90 Ma, 150 Ma and 250 Ma. Of the potential offset equivalents, Branch Canyon Sandstone and Santa Margarita samples are the best matches, although some older peaks exist (discussed in text).

Figure 11: Inset of palinspastically reconstructed plutonic source rocks of the Mojave Desert as shown in Fig. 5. The map has been modified with Miocene depositional styles overlain for the Cajon Valley area and offset equivalents. Braided-stream deposition was constrained to Cajon Valley with deposition of Santa Margarita, Branch Canyon and similar sediments in shallow marine settings further downstream and across the San Andreas fault system. Deposition of deep marine Monterey Fm. Fine grained sediments and turbidite sands occurred even further SW. While all paleocurrents in Cajon Valley point to the SW (Fig. 4), there were likely other adjacent drainages along the paleoshore, depositing similar, arkosic sands. Arrows show generalized paleoflow directions for the Cajon Valley Fm. and longshore current, which would have homogenized the shallow marine sediments. Note that the drainage area for Cajon Valley does not extend into pre-Triassic plutonic rocks.

FIGURES

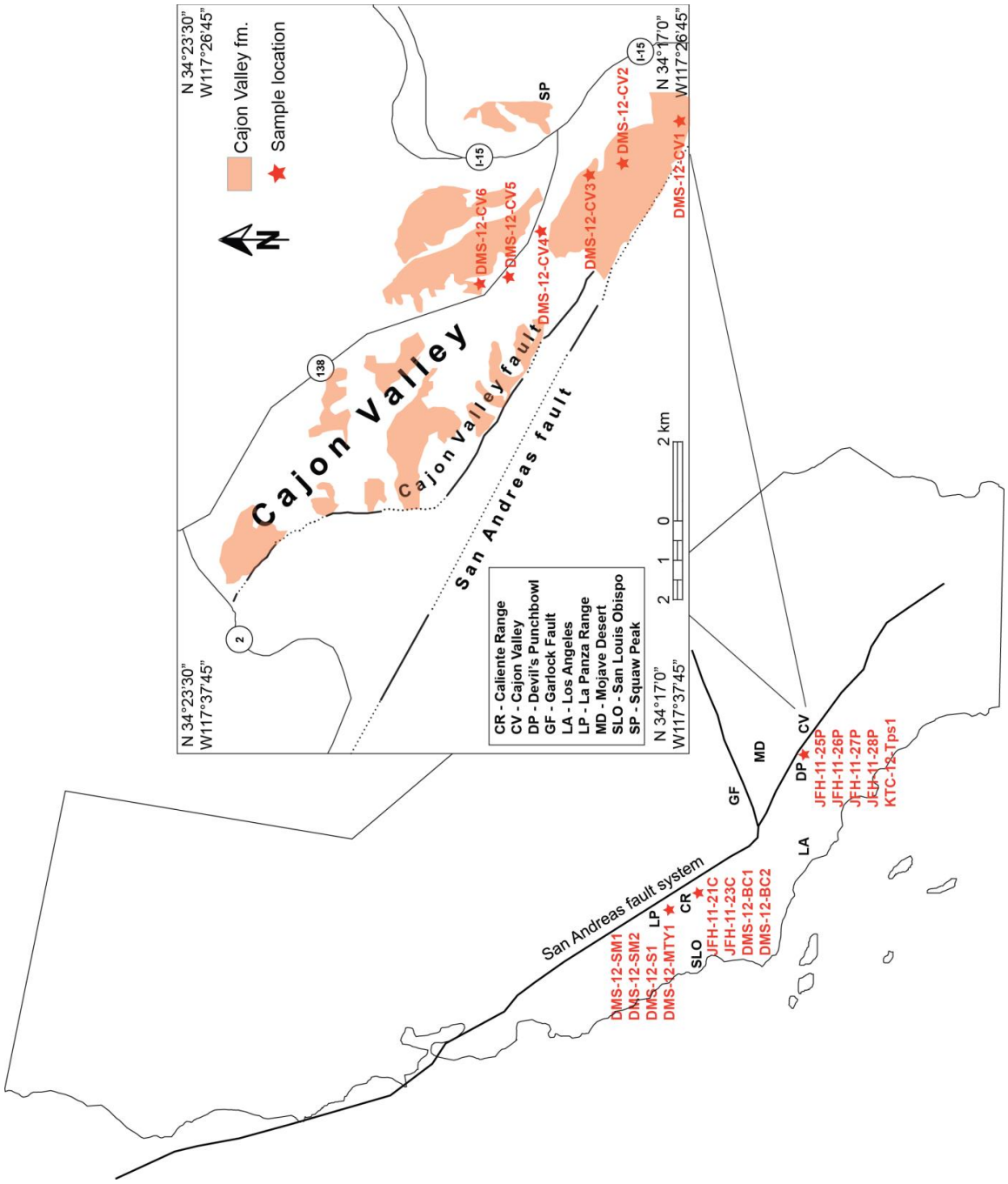

Figure 1: Generalized tectonic map showing sample locations for this study

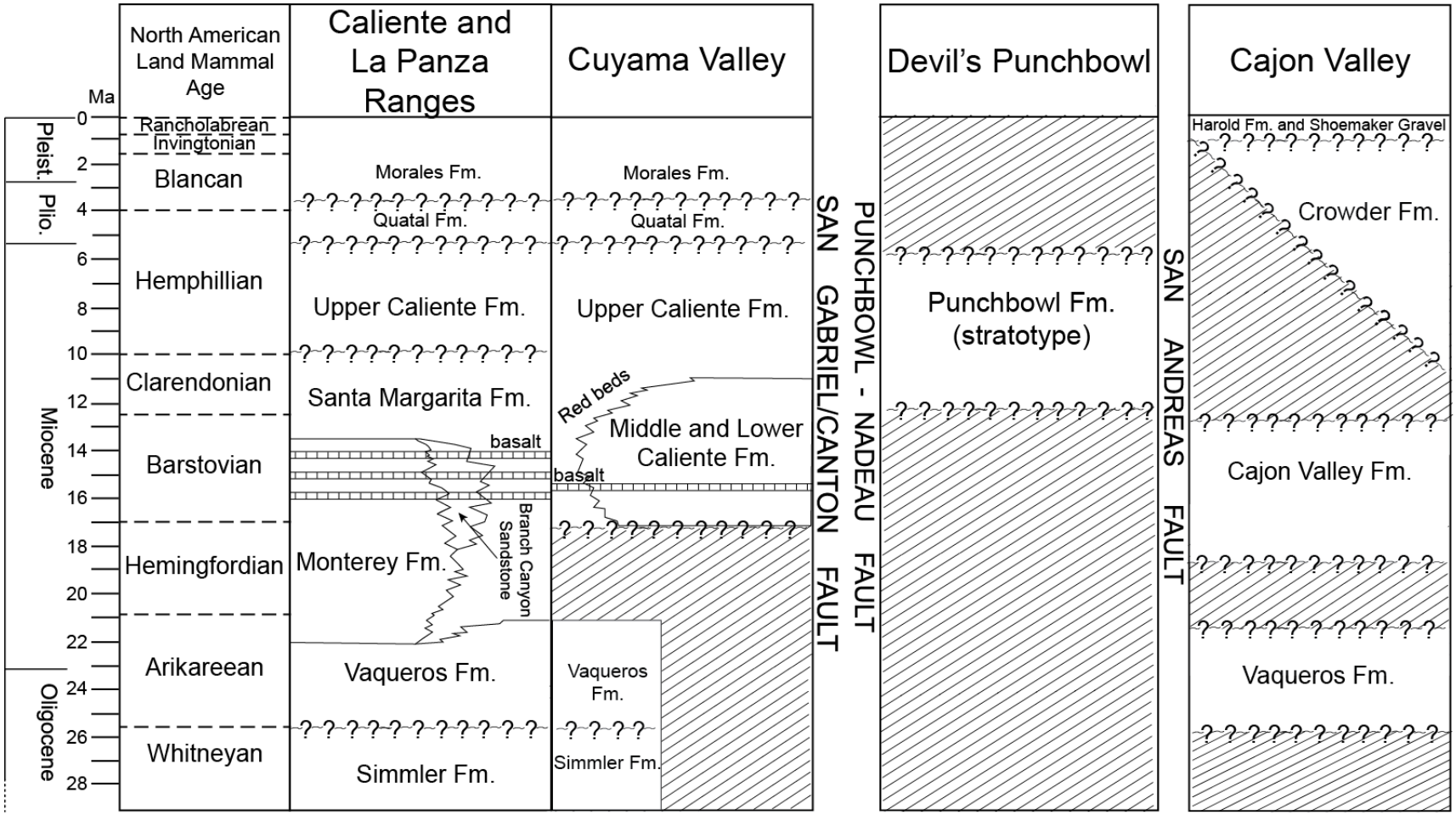

Figure 2: Across-fault stratigraphic correlation, modified after Woodburne, 1975.

Figure 3: Well-rounded arkosic sandstone hogback in Cajon Valley.
Photograph looking west at location of DMS-12-CV6 in Fig.1

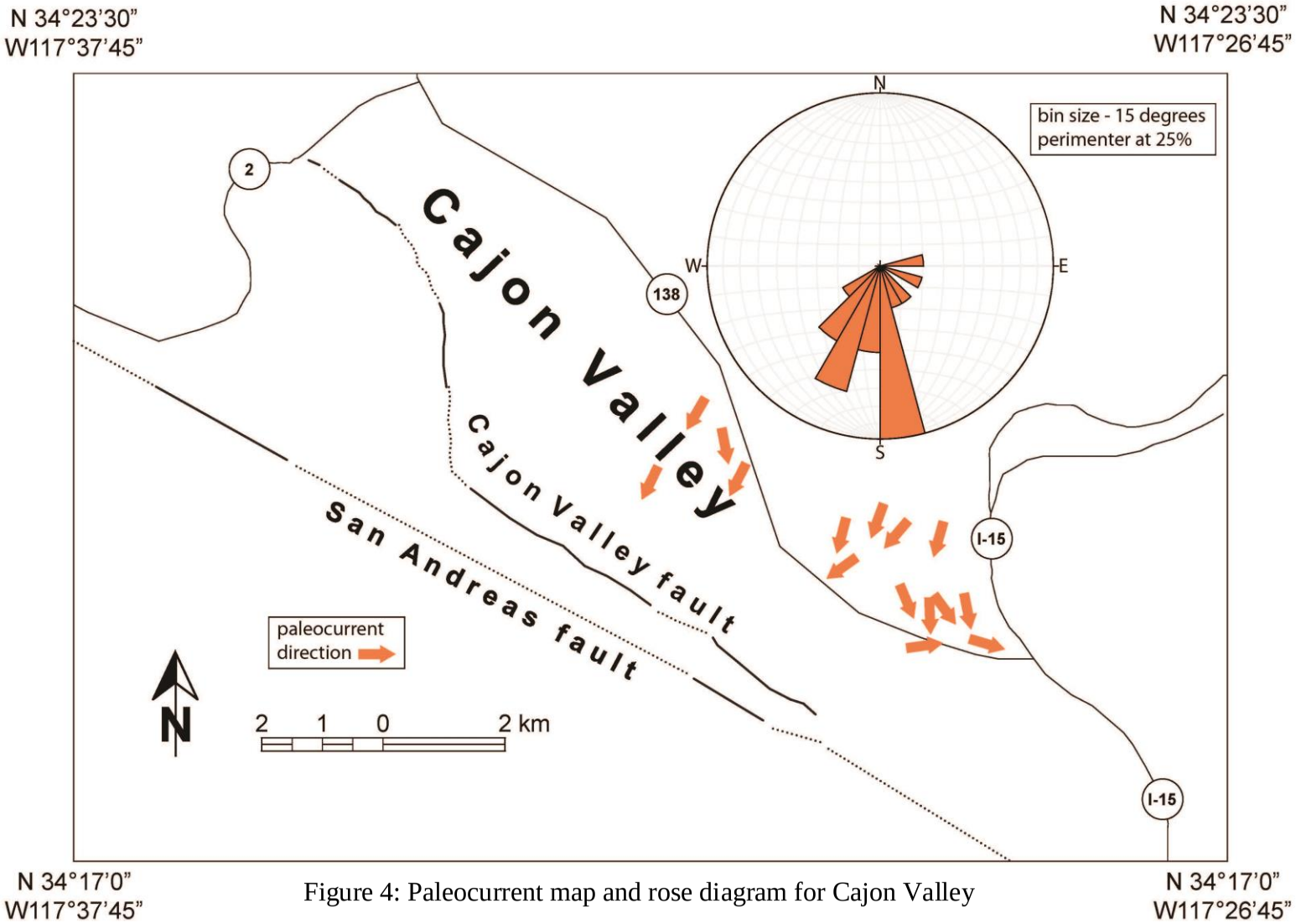

Figure 4: Paleocurrent map and rose diagram for Cajon Valley

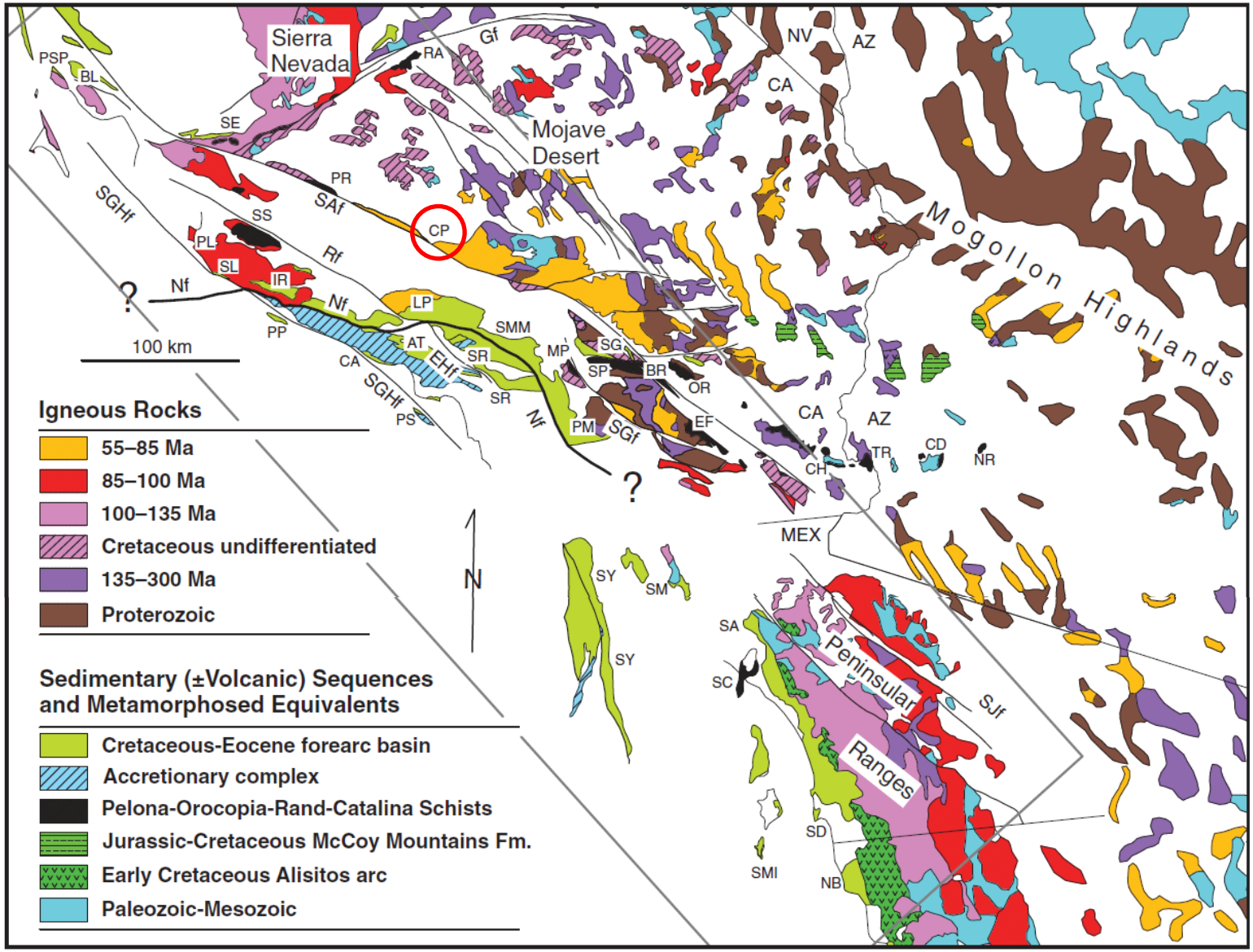

Figure 5: Plutonic and sedimentary rocks of southern California with ages determined by zircon dating, from Jacobson et al. (2011). Cajon Pass (CP) is circled in red.

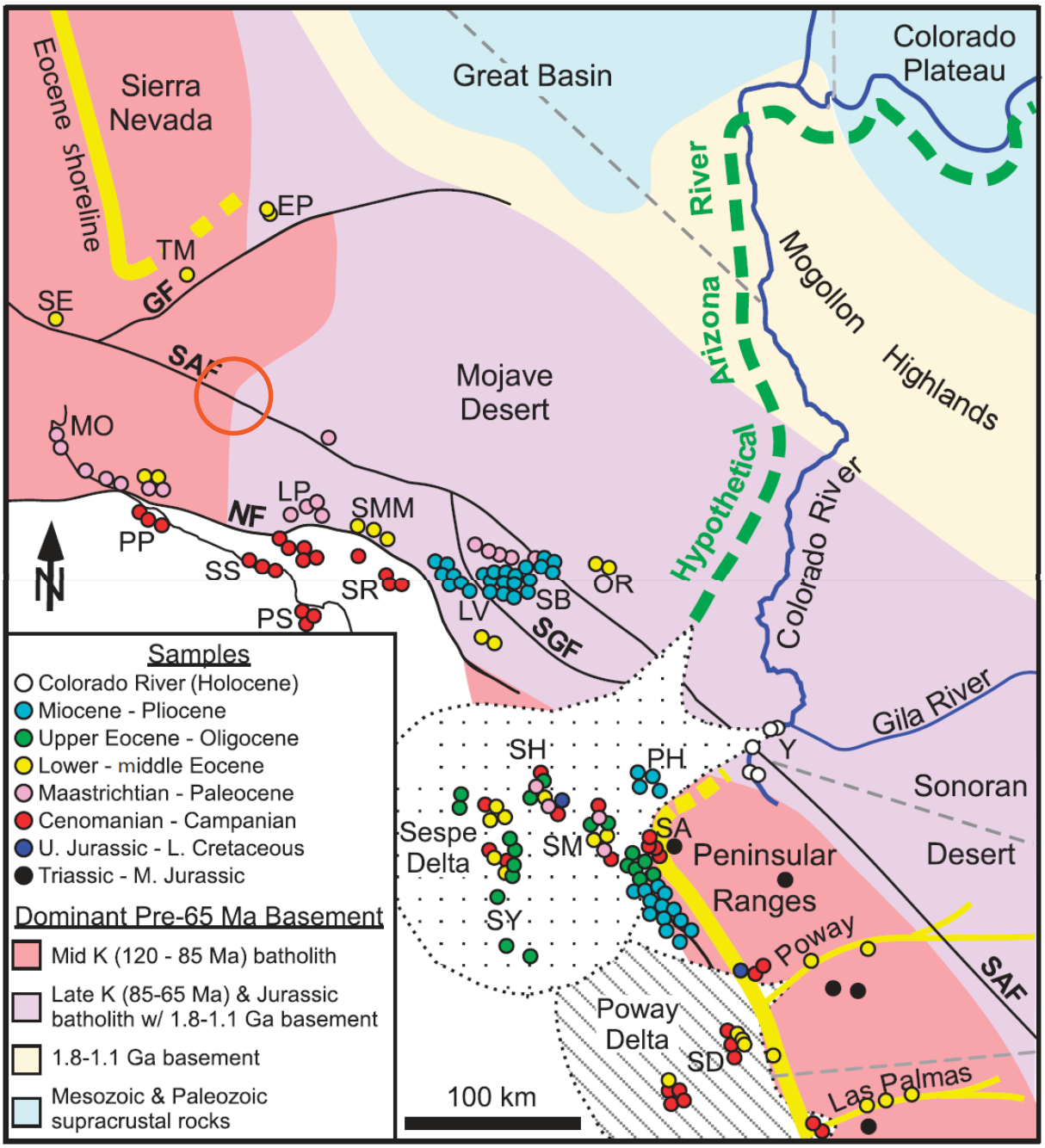

Figure 6: Southern California paleodrainage reconstruction of Ingersoll et al. (2013). Cajon Valley circled in red.

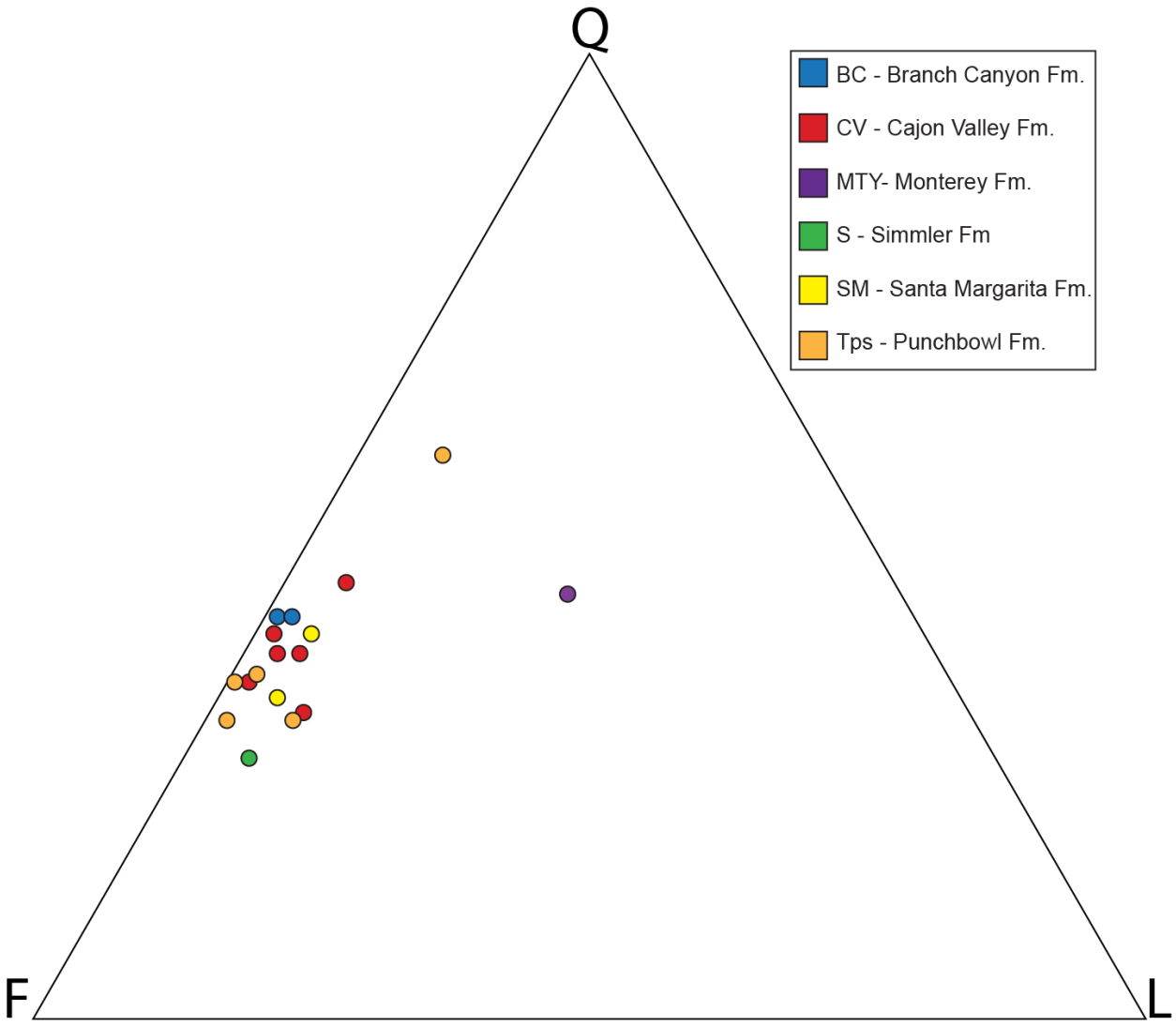

Figure 7: Sandstone point count QFL ternary diagram

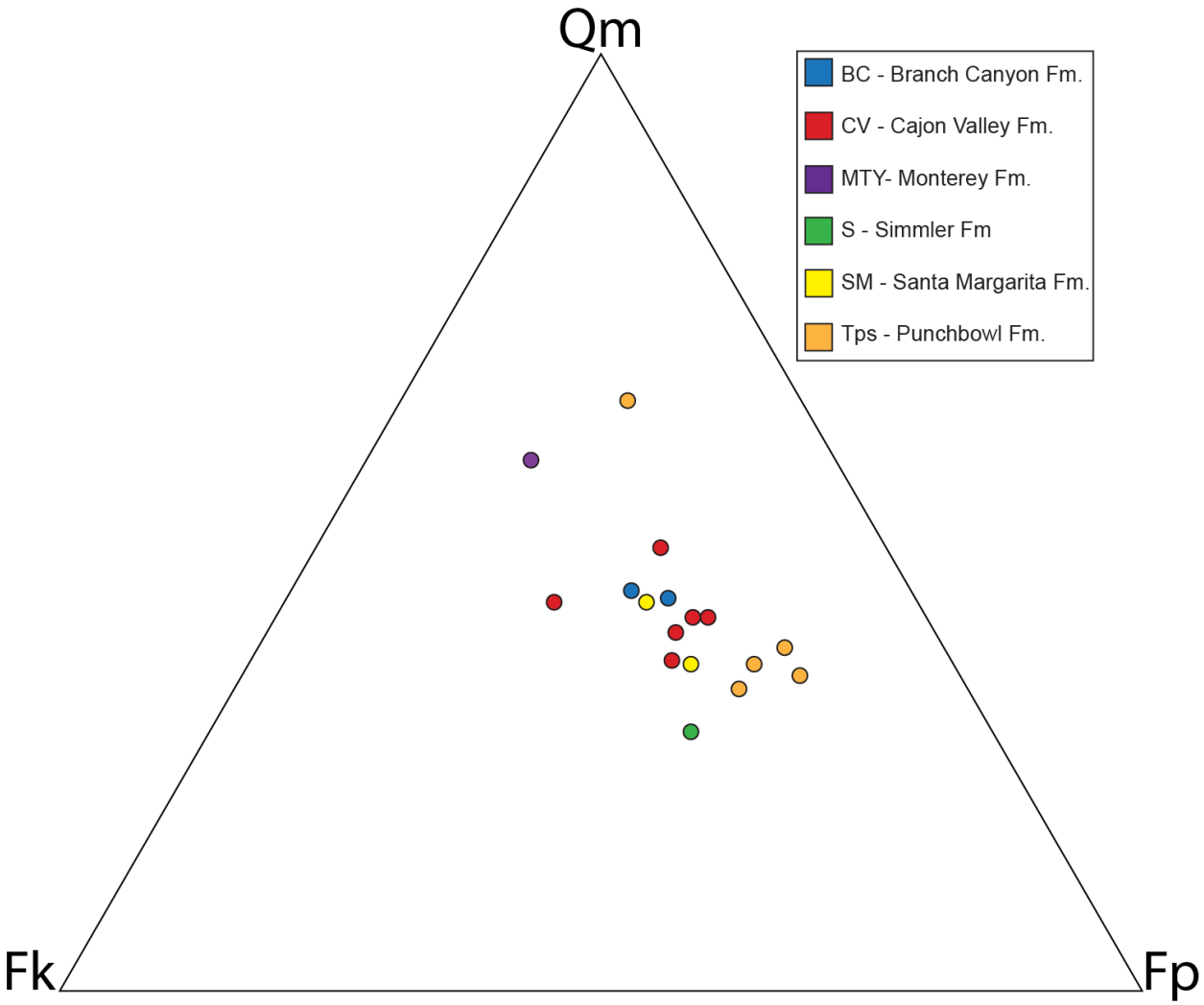

Figure 8: Sandstone point count QmFkFp ternary diagram

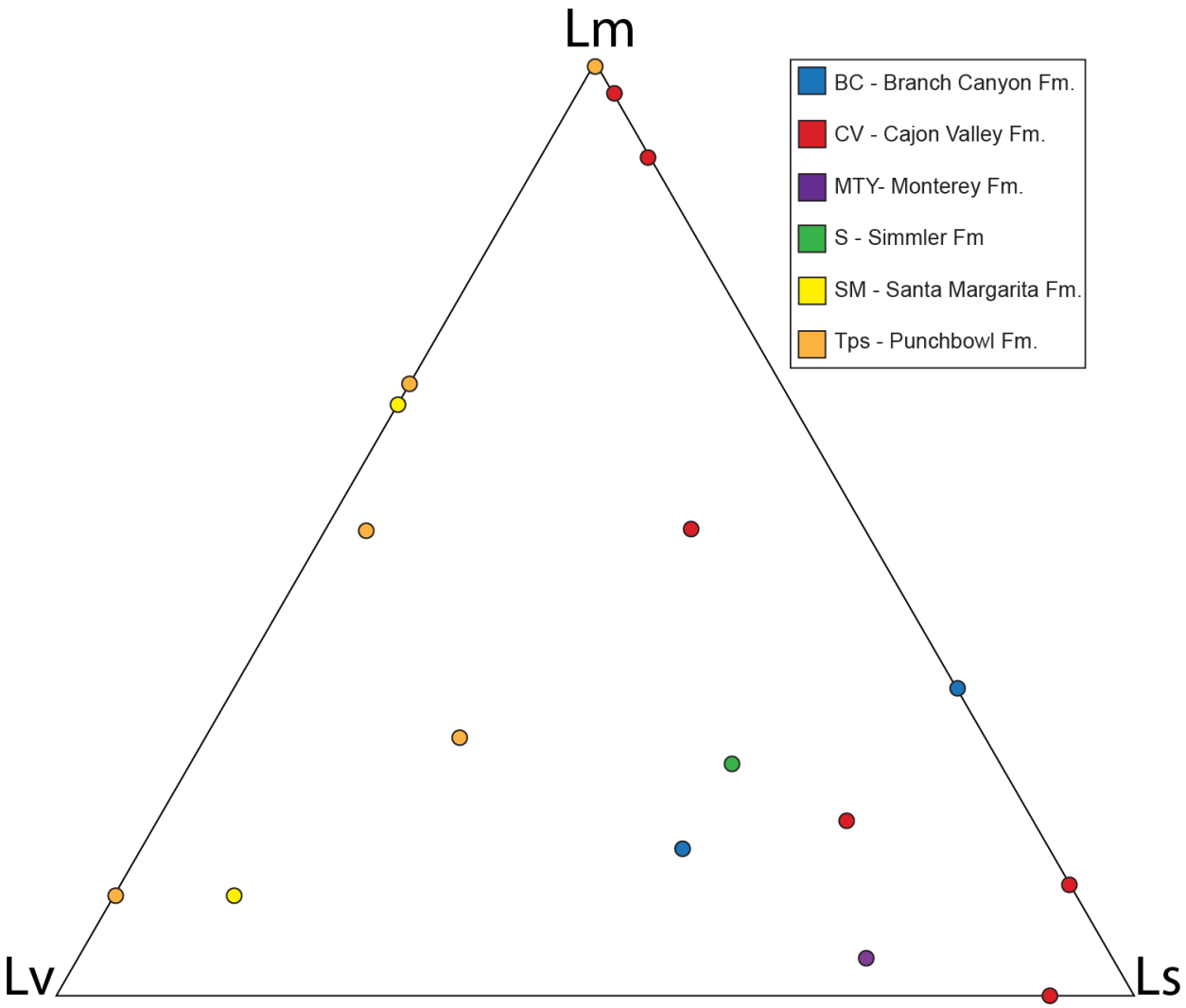

Figure 9: Sandstone point count LmLvLs ternary diagram

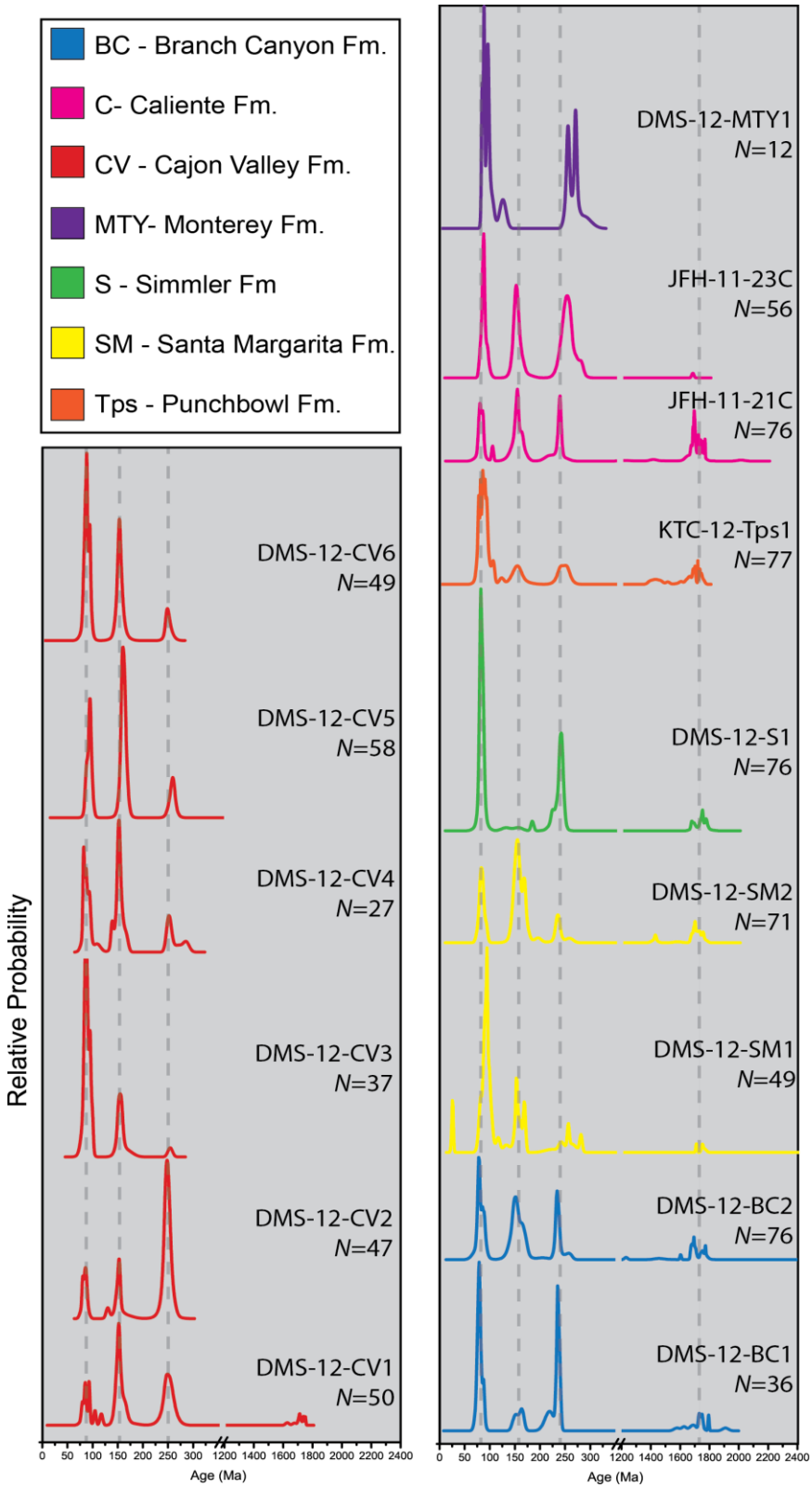

Figure 10: Detrital zircon probability density plots

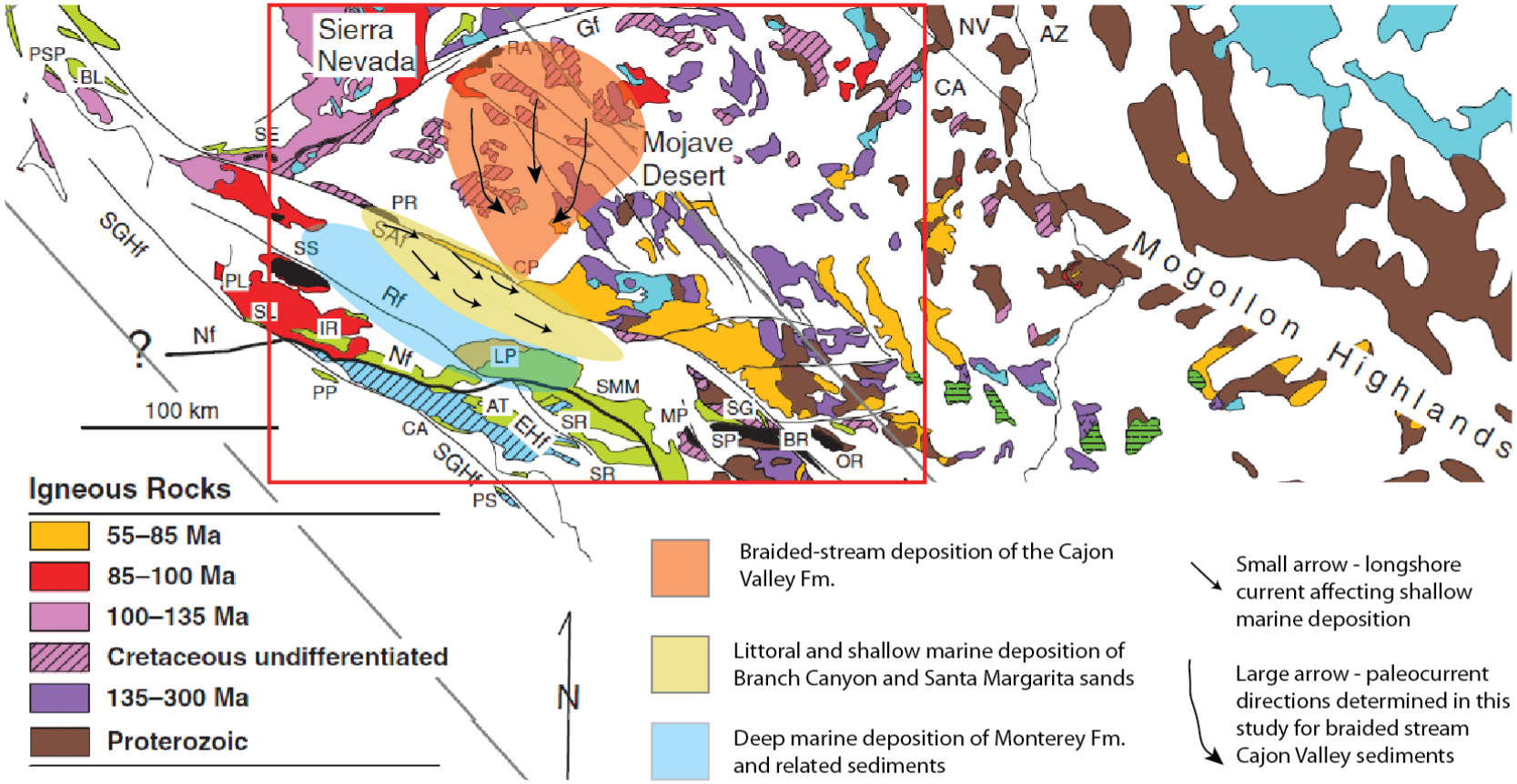

Figure 11: Plutonic source rocks of the Mojave Desert as shown in Fig. 5, palinspastically reconstructed with Miocene depositional styles overlain for the Cajon Valley area and offset equivalents

TABLES

Table 1: Sample List

Sample #	Latitude	Longitude	Formation	Zircon Analysis	Thin Section Analysis
DMS-12-CV1	N34.28679	W117.47552	Cajon Valley	Yes	Yes
DMS-12-CV2	N34.30057	W117.48272	Cajon Valley	Yes	Yes
DMS-12-CV3	N34.30590	W117.48538	Cajon Valley	Yes	Yes
DMS-12-CV4	N34.31405	W117.49677	Cajon Valley	Yes	Yes
DMS-12-CV5	N34.32245	W117.50633	Cajon Valley	Yes	Yes
DMS-12-CV6	N34.31903	W117.50489	Cajon Valley	Yes	Yes
DMS-12-BC1	N34.90154	W119.73817	Branch Canyon	Yes	Yes
DMS-12-BC2	N34.89192	W119.73122	Branch Canyon	Yes	Yes
DMS-12-MTY1	N35.45502	W120.39853	Monterey	Yes	Yes
DMS-12-S1	N35.45709	W120.41970	Simmler	Yes	Yes
DMS-12-SM1	N35.44756	W120.31415	Santa Margarita	Yes	Yes
DMS-12-SM2	N34.90143	W119.72958	Santa Margarita	Yes	Yes
JFH-11-21C	N34.84136	W119.33432	Caliente	Yes	No
JFH-11-23C	N34.88304	W119.43909	Caliente	Yes	No
JFH-11-25P	N34.41719	W117.85722	Punchbowl	No	Yes
JFH-11-26P	N34.41676	W117.85375	Punchbowl	No	Yes
JFH-11-27P	N34.44120	W117.89625	Punchbowl	No	Yes
JFH-11-28P	N34.40987	W117.83743	Punchbowl	No	Yes
KTC-12-Tpc1	N34.53054	W118.09026	Punchbowl	Yes	Yes

Table 2: Sandstone point count categories

	Abbreviation	Description
MINERAL GRAINS	Qm	Monocrystalline quartz
	Qp	Polycrystalline quartz
	Fp	Plagioclase feldspar
	Fk	Potassium feldspar
	M	Phyllosilicate minerals
	D	Dense minerals
LITHIC FRAGMENTS		
Volcanic & Hypabyssal	Lvv	Vitric Volcanic lithic; amorphous volcanic glass
	Lvfg	Felsitic-Granular Volcanic lithic; homogenous granular texture
	Lvfs	Felsitic-Seriate Volcanic lithic; contains phenocrysts of varying size
	Lvm	Microlitic Volcanic lithic; matrix of angular feldspar microlites, typically plagioclase, with no phenocrysts
	Lvl	Lathwork Volcanic lithic; fine-grained matrix with feldspar phenocryst laths
Metamorphic	Lmv	Metavolcanic lithic; metamorphosed volcanic lithic fragment with characteristic dense mineral replacement
	PxM	Polycrystalline Mica lithic; microgranular mica aggregate
	QMt	Tectonite lithic; preferred orientation of grains visible in aggregate
	QMFa	Aggregate Metamorphic lithic; microgranular aggregate of any combination of quartz, mica and feldspar
Sedimentary	Lss	Siliciclastic Sedimentary lithic; clay matrix with angular, silt-sized microclasts
	Lsc	Carbonate Sedimentary lithic; detrital carbonate grain or sedimentary lithic with a carbonate matrix
OTHER		
	Inter	Interstitial material
	Misc	Miscellaneous; not falling under any other category or unidentified grain

Table 3: Sandstone point counts

Sample	Qp	Qm	Fp	Fk	Lvv	Lvfg	Lvfs	Lvm	Lvl	Lmv	PxM	QMt	QMFa	Lss	Lsc	M	D	Inter	Misc	Total
DMS-12-CV1	7	157	175	114	2	0	0	0	0	0	0	2	0	7	0	12	4	16	4	500
DMS-12-CV2	0	196	120	164	0	1	0	0	0	0	0	1	2	2	0	1	2	9	2	500
DMS-12-CV3	2	163	164	96	0	0	0	0	0	0	0	0	1	8	0	24	3	36	3	500
DMS-12-CV4	4	111	143	67	0	0	0	0	0	2	1	0	28	1	0	16	7	17	3	400
DMS-12-CV5	1	138	132	79	0	0	0	0	0	4	2	0	11	2	0	7	4	20	0	400
DMS-12-CV6	6	204	130	90	0	2	0	0	0	0	0	0	0	23	0	14	5	23	3	500
DMS-12-BC1	0	148	109	89	0	0	0	0	0	0	0	0	1	2	0	5	0	45	1	400
DMS-12-BC2	6	159	133	88	0	2	0	0	0	0	0	0	1	3	0	2	0	6	0	400
DMS-12-MTY1	14	151	40	72	13	3	6	1	0	0	0	1	2	68	5	2	0	20	2	400
DMS-12-S1	3	100	157	95	2	2	1	0	0	0	1	0	4	3	7	5	5	13	2	400
DMS-12-SM1	7	127	145	94	1	4	2	0	0	0	0	4	8	0	0	5	0	0	3	400
DMS-12-SM2	5	153	124	90	5	7	2	0	0	0	0	0	2	2	0	2	6	2	0	400
JFH-11-25P	3	120	177	53	0	6	6	0	0	0	0	0	13	1	0	9	5	6	1	400
JFH-11-26P	2	117	166	77	0	0	0	0	0	0	0	2	6	0	0	14	5	11	0	400
JFH-11-27P	2	132	175	68	0	0	1	1	0	1	0	0	0	0	0	5	6	8	1	400
JFH-11-28P	2	220	75	56	2	3	7	0	2	6	1	0	1	7	0	3	2	13	0	400
KTC-12-Tps1	0	124	167	48	0	8	0	0	0	0	1	0	0	0	0	29	15	8	0	400

Table 4: Sandstone analysis recalculated parameters

Sandstone Categories	Q = Qm + Qp
	F = Fp + Fk
	Lv = Lvv + Lvfg + Lvfs + Lvm + Lvs
	Lm = Lmv + PxM + QMt + QMFa
	Ls = Lss + Lsc
	L= Lv + Lm + Ls
Sandstone recalculated parameters	QFL%Q = [Q/(Q + F + L)]*100
	QFL%F = [F/(Q + F + L)]*100
	QFL%L = [L/(Q + F + L)]*100
	QmFkFp%Qm = [Qm/(Qm + Fk + Fp)]*100
	QmFkFp%Fk = [Fk/(Qm + Fk + Fp)]*100
	QmFkFp%Fp = [Fp/(Qm + Fk + Fp)]*100
	LvLmLs%Lv = [Lv/(Lv + Lm + Ls)]*100
	LvLmLs%Lm = [Lm/(Lv + Lm + Ls)]*100
	LvLmLs%Ls = [Ls/(Lv + Lm + Ls)]*100

Table 5: Recalculated parameter percentages

Sample	Qp/Q	QFL %Q	QFL %F	QFL %L	Fp/F	LvLmLs %Lm	LvLmLs %Lv	LmLvLs %Ls	QmFkFp %Qm	QmFkFp %Fk	QmFkFp %Fp
DMS-12-CV1	0.04	35.3	62.3	2.4	0.61	18.2	18.2	63.6	35.2	25.6	39.2
DMS-12-CV2	0.00	40.3	58.4	1.2	0.42	50.0	16.7	33.3	40.8	34.2	25.0
DMS-12-CV3	0.01	38.0	59.9	2.1	0.63	11.1	0.0	88.9	38.5	22.7	38.8
DMS-12-CV4	0.03	32.2	58.8	9.0	0.68	96.9	0.0	3.1	34.6	20.9	44.5
DMS-12-CV5	0.01	37.7	57.2	5.1	0.63	89.5	0.0	10.5	39.5	22.6	37.8
DMS-12-CV6	0.03	46.2	48.4	5.5	0.59	0.0	8.0	92.0	48.1	21.2	30.7
DMS-12-BC1	0.00	42.4	56.7	0.9	0.55	33.3	0.0	66.7	42.8	25.7	31.5
DMS-12-BC2	0.04	42.1	56.4	1.5	0.60	16.7	33.3	50.0	41.8	23.2	35.0
DMS-12-MTY1	0.08	43.9	29.8	26.3	0.36	3.0	23.2	73.7	57.4	27.4	15.2
DMS-12-S1	0.03	27.5	67.2	5.3	0.62	25.0	25.0	50.0	28.4	27.0	44.6
DMS-12-SM1	0.05	34.2	61.0	4.8	0.61	63.2	36.8	0.0	34.7	25.7	39.6
DMS-12-SM2	0.03	40.5	54.9	4.6	0.58	11.1	77.8	11.1	41.7	24.5	33.8
JFH-11-25P	0.02	32.5	60.7	6.9	0.77	50.0	46.2	3.8	34.3	15.1	50.6
JFH-11-26P	0.02	32.2	65.7	2.2	0.68	100.0	0.0	0.0	32.5	21.4	46.1
JFH-11-27P	0.01	35.3	63.9	0.8	0.72	33.3	66.7	0.0	35.2	18.1	46.7
JFH-11-28P	0.01	58.1	34.3	7.6	0.57	27.6	48.3	24.1	62.7	16.0	21.4
KTC-12-Tps1	0.00	35.6	61.8	2.6	0.78	11.1	88.9	0.0	36.6	14.2	49.3

APPENDIX A

Imbrications - Set 1		Imbrications		Dip	Bedding	Bedding	Dip	Corrected
Lat	Lon	Strike	Dip	Direc'n	Strike	Dip	Direc'n	Paleoflow
N34 19.362'	W117 30.380'	285	50	NE	310	60	NE	97
N34 19.362'	W117 30.380'	280	50	NE	310	60	NE	100
N34 19.362'	W117 30.380'	290	55	NE	310	60	NE	108
N34 19.362'	W117 30.380'	305	35	NE	310	60	NE	47
N34 19.362'	W117 30.380'	260	50	NW	310	60	NE	102
N34 19.362'	W117 30.380'	310	50	NE	310	60	NE	40
N34 19.362'	W117 30.380'	300	45	NE	310	60	NE	65
N34 19.362'	W117 30.380'	295	50	NE	310	60	NE	87
N34 19.362'	W117 30.380'	300	60	NE	310	60	NE	127
N34 19.362'	W117 30.380'	300	50	NE	310	60	NE	77

Imbrications - Set 2		Imbrications		Dip	Bedding	Bedding	Dip	Corrected
Latitude	Longitude	Strike	Dip	Direc'n	Strike	Dip	Direc'n	Paleoflow
N34 18' 50''	W117 29' 28''	260	45	NW	311	55	NE	100
N34 18' 50''	W117 29' 28''	270	45	N	311	55	NE	101
N34 18' 50''	W117 29' 28''	275	49	NE	311	55	NE	108
N34 18' 50''	W117 29' 28''	255	75	NW	311	55	NE	138
N34 18' 50''	W117 29' 28''	275	37	NE	311	55	NE	84
N34 18' 50''	W117 29' 28''	270	32	N	311	55	NE	78
N34 18' 50''	W117 29' 28''	280	65	NE	311	55	NE	143
N34 18' 50''	W117 29' 28''	300	60	NE	311	55	NE	156
N34 18' 50''	W117 29' 28''	305	45	NE	311	55	NE	64
N34 18' 50''	W117 29' 28''	294	46	NE	311	55	NE	91

Imbrications - Set 3		Imbrications		Dip	Bedding	Bedding	Dip	Corrected
Latitude	Longitude	Strike	Dip	Direc'n	Strike	Dip	Direc'n	Paleoflow
N34 18' 56''	W117 29' 32''	270	55	N	310	47	NE	131
N34 18' 56''	W117 29' 32''	300	65	NE	310	47	NE	192
N34 18' 56''	W117 29' 32''	245	65	NW	310	47	NE	127
N34 18' 56''	W117 29' 32''	310	55	NE	310	47	NE	220
N34 18' 56''	W117 29' 32''	285	67	NE	310	47	NE	166
N34 18' 56''	W117 29' 32''	310	57	NE	310	47	NE	220
N34 18' 56''	W117 29' 32''	275	50	NE	310	47	NE	125
N34 18' 56''	W117 29' 32''	290	65	NE	310	47	NE	171
N34 18' 56''	W117 29' 32''	270	85	N	310	47	NE	165
N34 18' 56''	W117 29' 32''	280	63	NE	310	47	NE	154

Imbrications - Set 4		Imbrications		Dip	Bedding	Bedding	Dip	Corrected
Latitude	Longitude	Strike	Dip	Direc'n	Strike	Dip	Direc'n	Paleoflow
N34 18' 57''	W117 29' 37''	268	42	NW	275	45	NE	61
N34 18' 57''	W117 29' 37''	255	38	NW	275	45	NE	60
N34 18' 57''	W117 29' 37''	280	64	NE	275	45	NE	199

N34 18' 57"	W117 29' 37"	245	80	NW	275	45	NE	139
N34 18' 57"	W117 29' 37"	305	53	NE	275	45	NE	266
N34 18' 57"	W117 29' 37"	245	78	NW	275	45	NE	138
N34 18' 57"	W117 29' 37"	265	50	NW	275	45	NE	126
N34 18' 57"	W117 29' 37"	275	42	NE	275	45	NE	5
N34 18' 57"	W117 29' 37"	275	61	NE	275	45	NE	185
N34 18' 57"	W117 29' 37"	310	55	NE	275	45	NE	267

Imbrications - Set 5		Imbrications		Dip	Bedding	Bedding	Dip	Corrected
Latitude	Longitude	Strike	Dip	Direc'n	Strike	Dip	Direc'n	Paleoflow
N34 19' 10"	W117 29' 40"	280	59	NE	290	47	NE	163
N34 19' 10"	W117 29' 40"	270	60	N	290	47	NE	143
N34 19' 10"	W117 29' 40"	260	55	NW	290	47	NE	119
N34 19' 10"	W117 29' 40"	295	72	NE	290	47	NE	211
N34 19' 10"	W117 29' 40"	310	68	NE	290	47	NE	245
N34 19' 10"	W117 29' 40"	275	76	NE	290	47	NE	171
N34 19' 10"	W117 29' 40"	255	46	NW	290	47	NE	96
N34 19' 10"	W117 29' 40"	255	80	NW	290	47	NE	147
N34 19' 10"	W117 29' 40"	320	85	NE	290	47	NE	244
N34 19' 10"	W117 29' 40"	305	75	NE	290	47	NE	229

Imbrications - Set 6		Imbrications		Dip	Bedding	Bedding	Dip	Corrected
Latitude	Longitude	Strike	Dip	Direc'n	Strike	Dip	Direc'n	Paleoflow
N34 19' 44"	W117 28' 22"	300	55	NE	310	35	NE	197
N34 19' 44"	W117 28' 22"	310	43	NE	310	35	NE	220
N34 19' 44"	W117 28' 22"	310	48	NE	310	35	NE	220
N34 19' 44"	W117 28' 22"	290	42	NE	310	35	NE	151
N34 19' 44"	W117 28' 22"	310	50	NE	310	35	NE	220
N34 19' 44"	W117 28' 22"	290	25	NE	310	35	NE	77
N34 19' 44"	W117 28' 22"	300	30	NE	310	35	NE	83
N34 19' 44"	W117 28' 22"	290	40	NE	310	35	NE	144
N34 19' 44"	W117 28' 22"	310	60	NE	310	35	NE	220
N34 19' 44"	W117 28' 22"	310	40	NE	310	35	NE	220

Imbrications - Set 7		Imbrications		Dip	Bedding	Bedding	Dip	Corrected
Latitude	Longitude	Strike	Dip	Direc'n	Strike	Dip	Direc'n	Paleoflow
N34 19' 46"	W117 29' 33"	220	18	NW	310	45	NE	65
N34 19' 46"	W117 29' 33"	250	55	NW	310	45	NE	121
N34 19' 46"	W117 29' 33"	315	58	NE	310	45	NE	238
N34 19' 46"	W117 29' 33"	325	70	NE	310	45	NE	251
N34 19' 46"	W117 29' 33"	275	22	NE	310	45	NE	66
N34 19' 46"	W117 29' 33"	300	47	NE	310	45	NE	142
N34 19' 46"	W117 29' 33"	305	54	NE	310	45	NE	195
N34 19' 46"	W117 29' 33"	325	65	NE	310	45	NE	256
N34 19' 46"	W117 29' 33"	323	45	NE	310	45	NE	315
N34 19' 46"	W117 29' 33"	325	50	NE	310	45	NE	291

Imbrications - Set 8		Imbrications		Dip	Bedding	Bedding	Dip	Corrected
Latitude	Longitude	Strike	Dip	Direc'n	Strike	Dip	Direc'n	Paleoflow
N34 18' 55"	W117 29' 32"	295	37	NE	292	42	NE	2
N34 18' 55"	W117 29' 32"	308	40	NE	292	42	NE	309
N34 18' 55"	W117 29' 32"	307	63	NE	292	42	NE	236
N34 18' 55"	W117 29' 32"	315	50	NE	292	42	NE	275
N34 18' 55"	W117 29' 32"	305	58	NE	292	42	NE	238
N34 18' 55"	W117 29' 32"	305	46	NE	292	42	NE	273
N34 18' 55"	W117 29' 32"	297	72	NE	292	42	NE	211
N34 18' 55"	W117 29' 32"	315	46	NE	292	42	NE	286
N34 18' 55"	W117 29' 32"	285	54	NE	292	42	NE	176
N34 18' 55"	W117 29' 32"	290	62	NE	292	42	NE	197

Imbrications - Set 9		Imbrications		Dip	Bedding	Bedding	Dip	Corrected
Latitude	Longitude	Strike	Dip	Direc'n	Strike	Dip	Direc'n	Paleoflow
N34 19'56"	W117 28' 34"	312	57	NE	275	61	NE	292
N34 19'56"	W117 28' 34"	308	57	NE	275	61	NE	292
N34 19'56"	W117 28' 34"	300	78	NE	275	61	NE	154
N34 19'56"	W117 28' 34"	280	64	NE	275	61	NE	242
N34 19'56"	W117 28' 34"	320	70	NE	275	61	NE	273
N34 19'56"	W117 28' 34"	285	66	NE	275	61	NE	248
N34 19'56"	W117 28' 34"	310	82	NE	275	61	NE	249
N34 19'56"	W117 28' 34"	302	85	NE	275	61	NE	237
N34 19'56"	W117 28' 34"	275	55	NE	275	61	NE	5
N34 19'56"	W117 28' 34"	270	45	NE	275	61	NE	18

Imbrications - Set 10		Imbrications		Dip	Bedding	Bedding	Dip	Corrected
Latitude	Longitude	Strike	Dip	Direc'n	Strike	Dip	Direc'n	Paleoflow
N34 18' 56"	W117 29' 32"	315	85	NE	310	55	NE	230
N34 18' 56"	W117 29' 32"	320	65	NE	310	55	NE	264
N34 18' 56"	W117 29' 32"	327	55	NE	310	55	NE	315
N34 18' 56"	W117 29' 32"	320	35	NE	310	55	NE	24
N34 18' 56"	W117 29' 32"	295	48	NE	310	55	NE	95
N34 18' 56"	W117 29' 32"	270	48	N	310	55	NE	105
N34 18' 56"	W117 29' 32"	275	35	NE	310	55	NE	79
N34 18' 56"	W117 29' 32"	285	70	NE	310	55	NE	158
N34 18' 56"	W117 29' 32"	292	60	NE	310	55	NE	143
N34 18' 56"	W117 29' 32"	305	58	NE	310	55	NE	164

Imbrications - Set 11		Imbrications		Dip	Bedding	Bedding	Dip	Corrected
Latitude	Longitude	Strike	Dip	Direc'n	Strike	Dip	Direc'n	Paleoflow
N34 20' 32"	W117 31' 23"	285	34	NE	315	22	NE	161
N34 20' 32"	W117 31' 23"	285	48	NE	315	22	NE	178
N34 20' 32"	W117 31' 23"	282	43	NE	315	22	NE	170
N34 20' 32"	W117 31' 23"	320	48	NE	315	22	NE	233
N34 20' 32"	W117 31' 23"	305	61	NE	315	22	NE	211

N34 20' 32"	W117 31' 23"	315	40	NE	315	22	NE	225
N34 20' 32"	W117 31' 23"	310	45	NE	315	22	NE	216
N34 20' 32"	W117 31' 23"	310	55	NE	315	22	NE	217
N34 20' 32"	W117 31' 23"	320	53	NE	315	22	NE	233
N34 20' 32"	W117 31' 23"	300	44	NE	315	22	NE	198

Imbrications - Set 12		Imbrications		Dip	Bedding	Bedding	Dip	Corrected
Latitude	Longitude	Strike	Dip	Direc'n	Strike	Dip	Direc'n	Paleoflow
N34 20' 43"	W117 31' 46"	276	45	NE	285	35	NE	161
N34 20' 43"	W117 31' 46"	283	75	NE	285	35	NE	192
N34 20' 43"	W117 31' 46"	282	45	NE	285	35	NE	183
N34 20' 43"	W117 31' 46"	275	57	NE	285	35	NE	173
N34 20' 43"	W117 31' 46"	270	70	N	285	35	NE	171
N34 20' 43"	W117 31' 46"	270	54	N	285	35	NE	160
N34 20' 43"	W117 31' 46"	260	58	NW	285	35	NE	147
N34 20' 43"	W117 31' 46"	230	44	NW	285	35	NE	96
N34 20' 43"	W117 31' 46"	285	55	NE	285	35	NE	195
N34 20' 43"	W117 31' 46"	290	45	NE	285	35	NE	215

Imbrications - Set 13		Imbrications		Dip	Bedding	Bedding	Dip	Corrected
Latitude	Longitude	Strike	Dip	Direc'n	Strike	Dip	Direc'n	Paleoflow
N34 20' 55"	W117 32' 07"	295	54	NE	298	35	SW	206
N34 20' 55"	W117 32' 07"	265	54	NE	298	35	SW	324
N34 20' 55"	W117 32' 07"	280	63	NE	298	35	SW	192
N34 20' 55"	W117 32' 07"	285	72	NE	298	35	SW	195
N34 20' 55"	W117 32' 07"	290	60	NE	298	35	SW	201
N34 20' 55"	W117 32' 07"	290	80	NE	298	35	SW	199
N34 20' 55"	W117 32' 07"	275	60	NE	298	35	SW	188
N34 20' 55"	W117 32' 07"	300	80	NE	298	35	SW	210
N34 20' 55"	W117 32' 07"	290	65	NE	298	35	SW	201
N34 20' 55"	W117 32' 07"	275	68	NE	298	35	SW	186

Imbrications - Set 14		Imbrications		Dip	Bedding	Bedding	Dip	Corrected
Latitude	Longitude	Strike	Dip	Direc'n	Strike	Dip	Direc'n	Paleoflow
N34 20' 32"	W117 32' 27"	295	85	NE	285	50	NE	212
N34 20' 32"	W117 32' 27"	285	70	NE	285	50	NE	195
N34 20' 32"	W117 32' 27"	303	85	NE	285	50	NE	225
N34 20' 32"	W117 32' 27"	305	85	NE	285	50	NE	227
N34 20' 32"	W117 32' 27"	305	80	NE	285	50	NE	231
N34 20' 32"	W117 32' 27"	285	85	NE	285	50	NE	195
N34 20' 32"	W117 32' 27"	285	75	NE	285	50	NE	195
N34 20' 32"	W117 32' 27"	260	65	NW	285	50	NE	133
N34 20' 32"	W117 32' 27"	285	75	NE	285	50	NE	195
N34 20' 32"	W117 32' 27"	305	75	NE	285	50	NE	236

Imbrications - Set 15		Imbrications		Dip	Bedding	Bedding	Dip	Corrected
Latitude	Longitude	Strike	Dip	Direc'n	Strike	Dip	Direc'n	Paleoflow
N34 19' 40"	W117 30' 34"	0	50	E	320	45	NE	325
N34 19' 40"	W117 30' 34"	290	40	NE	320	45	NE	115
N34 19' 40"	W117 30' 34"	0	45	E	320	45	NE	334
N34 19' 40"	W117 30' 34"	280	70	NE	320	45	NE	164
N34 19' 40"	W117 30' 34"	295	35	NE	320	45	NE	99
N34 19' 40"	W117 30' 34"	315	55	NE	320	45	NE	207
N34 19' 40"	W117 30' 34"	320	60	NE	320	45	NE	230
N34 19' 40"	W117 30' 34"	310	35	NE	320	45	NE	79
N34 19' 40"	W117 30' 34"	325	65	NE	320	45	NE	243
N34 19' 40"	W117 30' 34"	295	45	NE	320	45	NE	131

Imbrications - Set 16		Imbrications		Dip	Bedding	Bedding	Dip	Corrected
Latitude	Longitude	Strike	Dip	Direc'n	Strike	Dip	Direc'n	Paleoflow
N34 20' 07"	W117 30' 29"	300	54	NE	297	30	NE	213
N34 20' 07"	W117 30' 29"	275	72	NE	297	30	NE	177
N34 20' 07"	W117 30' 29"	0	75	E	297	30	NE	281
N34 20' 07"	W117 30' 29"	340	62	NE	297	30	NE	269
N34 20' 07"	W117 30' 29"	320	70	NE	297	30	NE	239
N34 20' 07"	W117 30' 29"	320	55	NE	297	30	NE	248
N34 20' 07"	W117 30' 29"	340	68	NE	297	30	NE	265
N34 20' 07"	W117 30' 29"	308	43	NE	297	30	NE	238
N34 20' 07"	W117 30' 29"	290	70	NE	297	30	NE	197
N34 20' 07"	W117 30' 29"	295	50	NE	297	30	NE	203

APPENDIX B

DMS-12-BC1

U (ppm)	206Pb 204Pb	U/Th	206Pb* 207Pb*	± (%)	207Pb* 235U*	± (%)	206Pb* 238U	± (%)	error corr.	206Pb* 238U*	± (Ma)	207Pb* 235U	± (Ma)	206Pb* 207Pb*	± (Ma)	Best age (Ma)	± (Ma)
211	6483	1.01	24.4	22.9	0.07	23.7	0.01	6.2	0.26	75.5	4.6	65.5	15.0	-289	589.0	76	4.6
162	4235	0.99	27.2	38.4	0.06	38.9	0.01	6.2	0.16	75.7	4.6	59.0	22.3	-574	1070.9	76	4.6
339	19280	1.76	19.0	9.2	0.09	9.5	0.01	2.6	0.28	76.1	2.0	83.8	7.7	309	209.3	76	2.0
151	5249	0.82	23.4	23.3	0.07	23.6	0.01	3.8	0.16	76.9	2.9	69.3	15.8	-187	589.7	77	2.9
169	4695	114.37	21.2	20.1	0.08	20.5	0.01	4.2	0.20	78.1	3.2	77.4	15.3	56	483.2	78	3.2
360	16096	0.70	19.3	8.6	0.09	8.9	0.01	2.3	0.26	78.6	1.8	85.4	7.3	278	197.3	79	1.8
774	28898	1.09	21.6	6.6	0.08	6.8	0.01	1.8	0.27	79.5	1.4	77.5	5.1	17	157.7	79	1.4
361	22186	0.74	20.9	15.4	0.08	15.7	0.01	3.3	0.21	80.0	2.6	80.4	12.1	91	365.7	80	2.6
607	39311	1.00	21.2	4.1	0.08	4.8	0.01	2.4	0.51	82.7	2.0	81.7	3.7	54	97.4	83	2.0
143	12838	1.67	19.6	22.4	0.10	22.9	0.01	4.8	0.21	86.7	4.1	92.3	20.2	240	521.6	87	4.1
306	13320	1.43	21.4	11.9	0.09	12.1	0.01	2.0	0.16	87.8	1.7	86.1	10.0	39	286.7	88	1.7
171	10642	0.78	19.4	12.0	0.17	12.5	0.02	3.5	0.28	150.0	5.1	157.3	18.2	269	276.8	150	5.1
82	6241	0.83	20.3	28.9	0.17	29.2	0.02	4.2	0.14	158.7	6.6	158.9	42.9	162	687.5	159	6.6
115	12334	1.00	19.9	21.0	0.18	21.2	0.03	2.5	0.12	164.6	4.0	167.2	32.7	204	493.0	165	4.0
68	11876	1.15	20.7	24.4	0.23	24.8	0.03	4.5	0.18	217.4	9.6	209.1	46.9	117	582.5	217	9.6
76	13295	1.28	23.3	17.3	0.20	18.0	0.03	5.0	0.28	218.8	10.7	188.8	31.0	-172	433.7	219	10.7
90	20367	0.94	20.5	12.4	0.23	12.9	0.03	3.7	0.28	220.3	7.9	213.0	24.8	133	291.9	220	7.9
349	64796	1.81	19.7	3.2	0.26	3.4	0.04	1.1	0.32	233.5	2.4	232.8	7.0	225	73.9	233	2.4
569	152309	2.34	20.2	2.7	0.25	2.8	0.04	0.9	0.32	234.6	2.1	229.1	5.8	172	62.3	235	2.1
509	21362	0.90	19.7	3.7	0.26	3.9	0.04	1.2	0.31	234.8	2.7	234.6	8.1	233	85.2	235	2.7
549	73830	1.35	19.7	1.9	0.26	2.0	0.04	0.6	0.30	235.3	1.3	235.3	4.1	235	43.1	235	1.3
554	61716	2.08	19.1	2.5	0.27	2.7	0.04	1.1	0.39	237.6	2.5	243.1	5.8	297	56.8	238	2.5
879	715283	1.09	19.5	1.6	0.27	2.0	0.04	1.1	0.56	239.1	2.6	241.0	4.2	259	37.8	239	2.6
926	198639	1.05	19.3	2.0	0.27	2.2	0.04	0.9	0.40	239.3	2.0	242.5	4.7	274	45.7	239	2.0
218	125214	1.89	10.2	1.1	3.77	2.6	0.28	2.3	0.90	1593.2	32.8	1586.8	20.7	1578	21.0	1578	21.0
152	139878	1.05	10.0	0.8	3.84	3.5	0.28	3.4	0.97	1582.2	47.9	1601.7	28.3	1627	15.2	1627	15.2
141	155168	1.18	9.7	1.0	4.07	2.6	0.29	2.4	0.93	1627.4	34.1	1648.1	20.9	1675	18.0	1675	18.0

161	114258	1.75	9.6	0.9	4.38	2.2	0.31	2.0	0.92	1717.8	29.9	1708.4	17.8	1697	15.8	1697	15.8
490	386793	2.55	9.4	0.3	4.20	2.0	0.29	2.0	0.99	1631.0	28.7	1674.2	16.5	1729	5.3	1729	5.3
198	384334	1.49	9.4	0.5	4.78	2.4	0.33	2.3	0.98	1817.5	36.7	1781.7	19.8	1740	8.4	1740	8.4
122	67320	2.04	9.4	1.0	4.40	1.9	0.30	1.7	0.86	1684.3	24.5	1711.8	15.8	1746	17.7	1746	17.7
195	198195	1.54	9.3	0.3	4.58	3.1	0.31	3.0	0.99	1741.8	46.4	1745.9	25.5	1751	6.3	1751	6.3
196	30095	1.54	9.1	0.2	4.87	2.8	0.32	2.8	1.00	1800.9	44.3	1797.9	23.8	1794	3.9	1794	3.9
72	79941	0.46	8.6	1.2	5.48	2.5	0.34	2.2	0.89	1887.5	36.4	1897.8	21.5	1909	20.7	1909	20.7

DMS-12-BC2

U (ppm)	206Pb 204Pb	U/Th	206Pb* 207Pb*	± (%)	207Pb* 235U*	± (%)	206Pb* 238U	± (%)	error corr.	206Pb* 238U*	± (Ma)	207Pb* 235U	± (Ma)	206Pb* 207Pb*	± (Ma)	Best age (Ma)	± (Ma)
146	15184	0.69	29.3	23.2	0.05	25.5	0.01	10.5	0.41	71.6	7.5	52.0	12.9	-779	663.5	72	7.5
429	8169	0.97	18.4	30.2	0.08	32.3	0.01	11.4	0.35	71.8	8.1	81.8	25.4	386	691.9	72	8.1
307	8183	0.72	22.1	18.3	0.07	18.4	0.01	2.4	0.13	75.1	1.8	71.7	12.8	-41	447.1	75	1.8
112	5261	0.60	19.0	47.0	0.09	47.3	0.01	5.8	0.12	76.1	4.4	83.7	38.1	308	1128.4	76	4.4
255	12886	0.63	22.9	17.2	0.07	17.4	0.01	2.4	0.14	77.3	1.9	71.3	12.0	-127	428.0	77	1.9
415	18862	1.25	22.5	12.6	0.07	12.7	0.01	1.9	0.15	77.7	1.5	72.8	9.0	-85	309.4	78	1.5
306	10392	1.77	21.1	11.7	0.08	12.0	0.01	2.5	0.21	78.5	1.9	78.4	9.0	74	279.5	79	1.9
276	15040	1.05	23.2	5.5	0.07	6.0	0.01	2.2	0.37	78.8	1.7	71.6	4.1	-165	137.4	79	1.7
300	12090	1.35	22.6	12.3	0.08	12.4	0.01	2.1	0.17	79.2	1.6	73.9	8.9	-94	301.6	79	1.6
292	18933	0.97	22.7	15.9	0.08	16.1	0.01	2.9	0.18	79.3	2.3	73.7	11.5	-105	392.1	79	2.3
317	9864	1.35	20.3	10.8	0.09	11.1	0.01	2.8	0.25	81.6	2.3	84.2	9.0	159	252.3	82	2.3
176	17420	1.11	20.4	13.8	0.09	14.5	0.01	4.3	0.30	83.5	3.6	85.8	11.9	149	324.7	84	3.6
292	13262	4.51	22.1	15.6	0.08	16.1	0.01	3.8	0.24	83.8	3.2	79.6	12.3	-46	381.4	84	3.2
648	25463	2.01	20.8	7.0	0.09	7.2	0.01	1.7	0.23	85.4	1.4	86.1	5.9	106	164.5	85	1.4
36	2504	0.80	21.9	120.0	0.08	121.4	0.01	13.9	0.11	85.9	11.9	82.3	96.2	-21	1245.0	86	11.9
59	2881	1.52	23.3	63.6	0.08	64.0	0.01	7.1	0.11	86.2	6.1	78.0	48.0	-167	1755.0	86	6.1
1172	53135	1.38	21.0	4.4	0.09	7.7	0.01	6.3	0.82	86.9	5.5	86.7	6.4	79	104.8	87	5.5
532	24139	1.85	21.6	9.0	0.09	9.1	0.01	1.7	0.19	88.8	1.5	86.2	7.5	14	215.8	89	1.5
121	5857	2.41	28.2	58.4	0.07	58.6	0.01	5.1	0.09	89.9	4.5	67.4	38.2	-675	1745.5	90	4.5
250	6647	1.48	21.2	12.5	0.09	12.8	0.01	3.0	0.23	90.3	2.7	89.1	11.0	57	298.9	90	2.7
65	3659	0.61	19.6	42.4	0.16	42.6	0.02	3.9	0.09	143.0	5.5	148.8	59.0	242	1018.8	143	5.5
46	4292	1.17	31.9	69.7	0.10	70.2	0.02	8.7	0.12	143.7	12.4	94.3	63.4	-1028	2345.2	144	12.4
83	7609	1.77	20.8	20.5	0.15	21.2	0.02	5.3	0.25	144.5	7.5	142.4	28.1	108	488.3	144	7.5

118	5187	1.28	22.1	21.7	0.14	21.8	0.02	1.8	0.08	147.4	2.6	137.0	27.9	-39	532.5	147	2.6
37	16993	1.06	20.2	36.0	0.16	37.2	0.02	9.2	0.25	147.5	13.5	149.0	51.6	172	865.4	148	13.5
46	5018	0.65	11.3	220.3	0.28	220.4	0.02	5.7	0.03	147.7	8.3	252.2	537.3	1387	714.8	148	8.3
99	7656	0.84	19.2	15.8	0.17	16.8	0.02	5.7	0.34	147.8	8.4	156.8	24.4	294	362.2	148	8.4
169	13649	1.11	22.0	8.8	0.15	9.0	0.02	1.9	0.21	149.2	2.8	139.3	11.7	-27	213.1	149	2.8
115	7151	2.34	22.4	17.8	0.15	18.1	0.02	3.3	0.18	149.9	4.9	137.6	23.3	-71	437.6	150	4.9
64	5567	0.90	24.7	25.7	0.13	26.5	0.02	6.3	0.24	150.1	9.3	125.3	31.2	-325	670.5	150	9.3
34	4025	0.74	26.1	96.9	0.12	97.4	0.02	10.4	0.11	150.3	15.4	119.2	110.0	-464	1379.3	150	15.4
143	15259	1.09	20.6	22.6	0.16	22.9	0.02	3.7	0.16	150.5	5.5	148.9	31.7	123	538.6	151	5.5
116	7319	1.67	24.9	28.3	0.13	28.4	0.02	1.9	0.07	152.5	2.8	126.5	33.7	-338	741.2	152	2.8
215	28760	0.36	20.5	7.5	0.16	7.9	0.02	2.5	0.31	153.9	3.8	152.8	11.2	135	176.3	154	3.8
33	2597	0.53	15.6	203.9	0.21	204.1	0.02	8.4	0.04	154.1	12.8	197.2	383.0	750	1198.9	154	12.8
292	29066	0.34	20.9	8.9	0.16	9.1	0.02	1.7	0.19	154.9	2.6	151.2	12.7	93	211.1	155	2.6
166	805	1.06	13.5	38.2	0.26	38.6	0.03	5.3	0.14	160.9	8.4	233.8	80.7	1050	798.9	161	8.4
41	5698	1.39	7.5	265.9	0.47	266.0	0.03	7.6	0.03	161.6	12.2	387.8	1255.0	2136	303.5	162	12.2
91	10970	0.70	21.3	10.7	0.17	11.5	0.03	4.3	0.37	163.2	6.9	156.0	16.6	48	255.1	163	6.9
118	13068	0.68	22.2	12.2	0.16	12.5	0.03	2.8	0.23	163.6	4.6	150.2	17.5	-57	298.5	164	4.6
90	14475	0.35	25.4	33.6	0.14	33.8	0.03	3.7	0.11	164.0	6.0	132.8	42.0	-396	895.8	164	6.0
66	14639	0.35	21.4	28.9	0.17	29.4	0.03	5.4	0.18	164.4	8.8	156.4	42.6	36	704.0	164	8.8
109	17360	0.75	22.4	19.1	0.16	19.3	0.03	2.6	0.13	165.3	4.2	150.8	27.1	-71	471.1	165	4.2
41	8306	0.86	25.1	53.8	0.14	54.2	0.03	6.8	0.13	165.8	11.2	135.9	69.1	-359	1488.4	166	11.2
210	17013	0.73	20.3	7.5	0.18	7.8	0.03	2.1	0.27	171.9	3.6	171.2	12.2	160	175.1	172	3.6
41	4490	5.73	17.4	21.1	0.26	22.2	0.03	6.7	0.30	205.6	13.6	232.0	46.1	509	469.8	206	13.6
473	131937	2.10	19.6	1.6	0.26	2.4	0.04	1.7	0.72	230.3	3.9	231.6	4.9	245	37.6	230	3.9
267	36076	1.64	19.7	5.1	0.26	5.2	0.04	1.0	0.19	233.0	2.2	232.4	10.8	226	118.0	233	2.2
747	57207	4.89	19.5	2.1	0.26	2.3	0.04	0.7	0.32	233.2	1.7	234.8	4.7	250	49.3	233	1.7
162	29873	1.51	20.2	7.8	0.25	8.1	0.04	2.1	0.26	233.6	4.7	228.5	16.6	177	182.6	234	4.7
882	117327	7.47	19.6	1.0	0.26	1.7	0.04	1.4	0.82	233.6	3.2	233.9	3.5	237	22.6	234	3.2
225	31564	2.48	20.5	6.3	0.25	6.4	0.04	1.3	0.20	234.9	3.0	225.8	13.0	132	148.2	235	3.0
796	9895	1.14	19.3	2.5	0.27	3.0	0.04	1.6	0.53	235.5	3.7	239.5	6.4	280	58.3	235	3.7
385	55505	1.36	19.7	2.4	0.26	2.6	0.04	0.9	0.34	236.9	2.1	236.6	5.5	234	56.1	237	2.1
357	69038	1.22	19.8	4.0	0.26	4.2	0.04	1.2	0.28	237.7	2.7	235.4	8.8	213	93.3	238	2.7
426	24874	1.14	19.6	4.5	0.26	5.1	0.04	2.4	0.48	238.1	5.6	238.1	10.8	239	103.2	238	5.6
282	86672	1.72	19.1	2.7	0.28	3.9	0.04	2.8	0.72	249.2	6.9	253.9	8.8	298	61.9	249	6.9

70	8046	2.04	21.8	12.7	0.26	12.8	0.04	2.0	0.16	259.2	5.2	234.1	26.8	-10	307.1	259	5.2
241	213613	1.75	12.3	0.6	2.22	1.0	0.20	0.8	0.81	1165.2	8.2	1188.6	6.7	1231	11.0	1231	11.0
87	92030	1.08	10.9	1.6	3.18	1.7	0.25	0.7	0.39	1452.0	8.6	1452.7	13.0	1454	29.6	1454	29.6
30	11434	1.26	10.8	3.4	3.15	4.6	0.25	3.1	0.67	1424.2	39.1	1445.4	35.1	1477	64.1	1477	64.1
808	705819	6.17	10.1	0.3	3.56	1.6	0.26	1.6	0.99	1496.2	21.5	1541.2	12.9	1604	5.1	1604	5.1
235	194093	0.62	9.7	0.2	4.13	1.1	0.29	1.1	0.98	1652.5	15.9	1661.2	9.1	1672	4.1	1672	4.1
329	514011	6.22	9.7	0.3	4.18	0.5	0.29	0.4	0.75	1664.0	5.2	1670.9	3.9	1680	5.8	1680	5.8
907	49164	7.28	9.7	0.3	4.22	3.1	0.30	3.1	0.99	1674.7	45.6	1677.8	25.5	1682	6.1	1682	6.1
130	96278	1.04	9.7	0.7	3.94	3.3	0.28	3.2	0.98	1570.0	45.1	1621.7	26.7	1689	12.1	1689	12.1
112	174124	1.73	9.6	0.6	4.16	1.6	0.29	1.4	0.93	1648.8	21.0	1667.1	12.7	1690	10.4	1690	10.4
94	150838	0.70	9.6	0.6	4.23	2.7	0.30	2.7	0.97	1671.5	39.3	1680.2	22.5	1691	11.5	1691	11.5
191	133462	1.19	9.6	0.5	4.19	2.5	0.29	2.5	0.98	1658.2	36.5	1673.0	20.9	1692	9.0	1692	9.0
965	657807	9.09	9.6	0.1	4.36	0.7	0.30	0.7	0.98	1714.5	10.6	1705.4	5.9	1694	2.5	1694	2.5
154	139482	1.99	9.6	0.3	4.32	1.0	0.30	1.0	0.95	1692.7	14.2	1697.9	8.3	1704	5.9	1704	5.9
223	182972	1.16	9.6	0.5	3.51	0.9	0.24	0.8	0.86	1403.4	10.2	1529.4	7.4	1708	8.8	1708	8.8
102	112969	1.74	9.5	1.4	4.41	1.8	0.30	1.2	0.63	1704.2	17.4	1714.0	15.3	1726	26.5	1726	26.5
220	300437	1.78	9.4	0.3	4.67	1.6	0.32	1.6	0.98	1780.7	24.7	1761.7	13.5	1739	5.2	1739	5.2
447	423642	1.68	9.3	0.3	4.70	1.2	0.32	1.2	0.97	1781.4	18.4	1767.5	10.2	1751	5.4	1751	5.4
309	1312255	6.65	9.3	0.5	4.43	3.9	0.30	3.9	0.99	1684.7	58.0	1717.6	32.6	1758	8.6	1758	8.6
68	4433	2.07	9.3	2.6	4.51	9.1	0.30	8.7	0.96	1712.6	130.5	1733.6	75.4	1759	47.3	1759	47.3
487	459101	0.78	9.2	0.2	4.95	2.3	0.33	2.3	1.00	1844.9	36.4	1811.2	19.2	1773	2.8	1773	2.8
170	165359	1.62	9.2	0.6	4.59	2.3	0.31	2.2	0.97	1726.3	33.0	1748.0	18.8	1774	10.7	1774	10.7
82	95303	1.74	9.2	0.9	4.78	1.2	0.32	0.9	0.72	1781.8	13.8	1780.6	10.3	1779	15.6	1779	15.6
94	138870	1.79	5.9	0.3	11.30	0.8	0.48	0.8	0.92	2525.5	16.0	2547.8	7.8	2566	5.5	2566	5.5

DMS-12-CV1

U	206Pb	U/Th	206Pb*	±	207Pb*	±	206Pb*	±	error	206Pb*	±	207Pb*	±	206Pb*	±	Best age	±
(ppm)	204Pb		207Pb*	(%)	235U*	(%)	238U	(%)	corr.	238U*	(Ma)	235U	(Ma)	207Pb*	(Ma)	(Ma)	(Ma)
598	38561	3.24	22.1	7.2	0.08	7.7	0.01	2.5	0.33	77.0	1.9	73.5	5.4	-42	176.1	77	1.9
146	6868	1.68	32.6	32.6	0.05	33.7	0.01	8.4	0.25	79.5	6.6	52.0	17.1	NA	NA	79	6.6
267	14273	0.69	22.4	13.6	0.08	13.7	0.01	2.0	0.14	82.6	1.6	77.6	10.2	-75	333.1	83	1.6
182	13227	1.83	21.6	20.0	0.08	20.1	0.01	2.6	0.13	83.1	2.2	80.9	15.7	15	483.8	83	2.2
120	5490	0.83	26.5	41.5	0.07	42.3	0.01	8.3	0.20	84.8	7.0	67.6	27.7	-507	1147.6	85	7.0
731	42572	1.81	20.5	5.9	0.09	6.1	0.01	1.6	0.27	90.0	1.5	92.0	5.4	143	138.9	90	1.5

468	38446	0.85	20.6	7.1	0.10	7.3	0.01	1.7	0.23	91.0	1.5	92.4	6.5	129	167.5	91	1.5
230	14044	2.16	22.6	15.6	0.10	15.8	0.02	2.1	0.14	102.2	2.2	94.6	14.3	-91	385.9	102	2.2
258	16067	2.72	23.5	14.8	0.11	15.0	0.02	2.4	0.16	114.8	2.8	101.8	14.5	-193	371.2	115	2.8
75	5793	0.64	23.5	29.0	0.13	29.2	0.02	3.4	0.12	143.4	4.8	125.9	34.6	-193	739.5	143	4.8
87	7415	1.34	21.7	35.0	0.15	35.1	0.02	2.5	0.07	146.0	3.6	138.0	45.3	2	866.1	146	3.6
76	6532	1.66	25.7	23.4	0.12	24.0	0.02	5.1	0.21	147.5	7.4	118.9	26.9	-423	621.2	148	7.4
132	13162	1.29	19.2	15.7	0.17	15.9	0.02	2.6	0.17	148.3	3.9	157.0	23.1	290	359.7	148	3.9
71	7229	1.20	20.8	23.0	0.15	23.5	0.02	5.2	0.22	148.4	7.7	145.8	32.0	103	548.9	148	7.7
142	9941	1.30	21.4	14.2	0.15	14.5	0.02	3.1	0.21	148.6	4.5	142.2	19.3	37	340.9	149	4.5
114	17509	1.32	21.6	15.4	0.15	15.6	0.02	2.5	0.16	148.6	3.7	141.0	20.5	15	371.9	149	3.7
354	21618	1.24	21.5	6.1	0.15	6.4	0.02	1.7	0.27	149.6	2.6	142.7	8.5	29	146.8	150	2.6
355	36749	0.57	20.5	6.7	0.16	6.8	0.02	1.2	0.17	149.7	1.7	148.8	9.4	134	158.2	150	1.7
97	6346	0.78	22.3	28.3	0.15	28.5	0.02	3.7	0.13	150.4	5.4	138.2	36.9	-66	702.2	150	5.4
92	10593	0.81	21.0	13.6	0.15	14.4	0.02	4.6	0.32	150.4	6.8	146.3	19.6	80	325.2	150	6.8
489	61525	0.68	20.1	4.8	0.16	5.9	0.02	3.4	0.58	151.4	5.2	153.3	8.4	184	112.5	151	5.2
80	12389	1.37	25.5	37.5	0.13	37.7	0.02	3.9	0.10	152.0	5.9	123.2	43.7	-401	1007.2	152	5.9
113	13920	1.57	19.4	19.5	0.17	19.7	0.02	2.7	0.14	152.2	4.1	158.9	29.0	261	451.8	152	4.1
90	4029	1.28	20.0	27.3	0.17	27.8	0.02	5.1	0.18	153.1	7.8	155.5	40.1	192	646.0	153	7.8
246	15488	0.97	20.0	6.8	0.18	7.1	0.03	2.2	0.30	162.2	3.5	164.3	10.8	195	158.2	162	3.5
107	12792	0.82	21.3	14.8	0.17	15.2	0.03	3.2	0.21	164.5	5.3	157.2	22.1	48	356.2	165	5.3
69	1643	0.34	21.1	17.6	0.18	19.6	0.03	8.6	0.44	171.4	14.6	165.0	29.9	74	421.0	171	14.6
460	48121	2.38	20.1	5.9	0.26	8.6	0.04	6.2	0.72	239.6	14.7	234.6	18.1	185	138.4	240	14.7
102	15272	1.26	18.7	7.1	0.28	7.3	0.04	1.4	0.19	243.1	3.3	252.9	16.3	345	161.4	243	3.3
46	6309	1.82	18.3	14.6	0.29	15.5	0.04	5.3	0.34	243.6	12.6	258.4	35.4	396	328.6	244	12.6
72	15152	1.51	19.4	19.6	0.28	19.7	0.04	2.3	0.12	244.8	5.6	246.8	43.2	266	452.5	245	5.6
95	43218	1.20	20.0	18.7	0.27	19.2	0.04	4.5	0.23	244.9	10.7	240.4	41.2	197	438.3	245	10.7
107	12413	1.03	20.6	11.4	0.26	12.0	0.04	3.8	0.32	245.4	9.2	234.5	25.2	127	269.5	245	9.2
80	9460	1.46	19.3	16.4	0.28	16.9	0.04	4.1	0.24	247.6	10.0	250.0	37.6	273	379.1	248	10.0
86	9463	1.45	21.5	21.0	0.25	21.2	0.04	3.2	0.15	249.8	7.9	229.3	43.6	24	507.6	250	7.9
81	20394	1.18	20.4	16.1	0.27	16.3	0.04	2.8	0.17	250.5	6.9	241.2	35.0	151	378.3	251	6.9
74	10445	0.70	21.4	15.9	0.25	16.4	0.04	4.0	0.25	250.7	9.9	230.6	33.9	30	383.1	251	9.9
124	21670	1.36	19.6	11.9	0.28	12.3	0.04	3.2	0.26	250.9	7.8	249.6	27.3	238	275.3	251	7.8
102	17923	1.25	18.8	9.0	0.29	9.2	0.04	2.0	0.22	251.5	5.0	260.1	21.2	338	204.6	252	5.0
85	16039	1.22	20.5	12.9	0.27	13.4	0.04	3.8	0.28	252.0	9.4	241.2	28.9	137	304.0	252	9.4

58	9093	1.30	18.9	21.2	0.29	21.8	0.04	5.0	0.23	252.6	12.4	259.8	50.0	325	485.8	253	12.4
79	8038	1.00	18.1	13.0	0.31	14.5	0.04	6.6	0.45	252.7	16.3	270.6	34.5	428	290.0	253	16.3
96	9459	1.69	19.7	13.0	0.28	13.7	0.04	4.2	0.31	257.5	10.6	254.5	30.8	227	302.1	257	10.6
211	180267	1.01	10.0	0.7	3.56	3.6	0.26	3.5	0.98	1485.4	46.3	1541.3	28.2	1619	12.3	1619	12.3
138	147302	1.53	9.8	0.8	4.10	1.4	0.29	1.2	0.85	1642.3	17.3	1654.0	11.5	1669	13.9	1669	13.9
472	440872	12.13	9.6	0.3	4.16	2.0	0.29	2.0	0.99	1641.9	29.1	1665.8	16.6	1696	6.2	1696	6.2
635	712948	5.33	9.6	0.2	3.82	1.2	0.27	1.2	0.98	1517.2	16.2	1596.8	9.8	1704	4.3	1704	4.3
165	157954	1.79	9.5	0.4	4.47	1.7	0.31	1.7	0.97	1736.3	25.3	1726.3	14.2	1714	7.5	1714	7.5
277	223099	4.17	9.4	0.2	4.64	1.4	0.32	1.4	0.99	1779.2	21.5	1756.3	11.7	1729	3.8	1729	3.8
507	766155	5.63	9.4	0.2	4.13	1.9	0.28	1.9	0.99	1595.6	26.5	1659.7	15.4	1742	3.6	1742	3.6

DMS-12-CV2

U (ppm)	206Pb 204Pb	U/Th	206Pb* 207Pb*	± (%)	207Pb* 235U*	± (%)	206Pb* 238U	± (%)	error corr.	206Pb* 238U*	± (Ma)	207Pb* 235U	± (Ma)	206Pb* 207Pb*	± (Ma)	Best age (Ma)	± (Ma)
121	6352	4.38	21.9	40.7	0.07	41.0	0.01	4.9	0.12	75.5	3.7	72.5	28.7	-24	1024.0	75	3.7
457	23724	3.45	21.5	6.8	0.08	7.0	0.01	1.8	0.26	77.3	1.4	75.8	5.1	26	163.0	77	1.4
265	8728	1.28	24.4	23.4	0.07	23.5	0.01	2.6	0.11	80.4	2.1	69.7	15.9	-285	602.9	80	2.1
156	7853	1.48	23.3	30.7	0.08	30.9	0.01	3.9	0.13	82.6	3.2	74.5	22.2	-178	781.1	83	3.2
366	5416	1.35	21.2	9.6	0.09	9.9	0.01	2.5	0.25	83.9	2.0	83.1	7.9	61	230.1	84	2.0
188	14682	1.63	18.5	11.2	0.10	11.6	0.01	3.2	0.27	84.2	2.7	94.7	10.5	369	252.1	84	2.7
79	5123	1.02	22.7	47.4	0.08	47.6	0.01	4.7	0.10	86.9	4.1	80.5	36.8	-108	1227.9	87	4.1
242	12710	1.96	20.5	11.2	0.13	11.5	0.02	2.7	0.23	127.3	3.4	127.7	13.8	136	263.7	127	3.4
79	4951	1.45	23.7	23.5	0.13	23.8	0.02	3.5	0.15	147.0	5.1	128.0	28.6	-211	597.6	147	5.1
195	11549	1.17	21.3	11.4	0.15	11.6	0.02	2.3	0.20	147.2	3.3	141.5	15.3	46	272.2	147	3.3
87	8524	0.96	18.6	10.9	0.17	13.9	0.02	8.7	0.63	147.3	12.7	160.9	20.7	367	245.3	147	12.7
110	13417	0.97	18.7	16.7	0.17	16.9	0.02	2.6	0.15	147.6	3.8	160.3	25.1	352	380.1	148	3.8
258	23797	0.81	20.6	10.6	0.16	10.7	0.02	1.1	0.11	149.4	1.7	148.3	14.7	131	250.3	149	1.7
114	9996	1.11	21.1	31.0	0.15	31.5	0.02	5.6	0.18	149.9	8.4	145.1	42.6	67	753.2	150	8.4
236	14224	1.01	20.5	11.1	0.16	11.2	0.02	1.2	0.10	151.6	1.7	150.7	15.7	137	262.4	152	1.7
164	37028	1.97	24.1	19.9	0.15	21.5	0.03	8.0	0.37	166.9	13.3	142.0	28.4	-257	508.4	167	13.3
83	13071	1.44	19.2	8.6	0.27	8.9	0.04	2.5	0.28	240.3	6.0	245.1	19.5	291	196.3	240	6.0
61	8540	1.41	21.5	30.5	0.24	30.8	0.04	4.7	0.15	240.8	11.1	221.9	61.5	26	745.9	241	11.1
78	14062	1.39	19.2	12.3	0.27	13.0	0.04	4.1	0.32	241.7	9.8	246.1	28.4	288	282.8	242	9.8
75	13734	1.41	20.1	7.0	0.26	8.3	0.04	4.6	0.55	242.5	10.9	236.9	17.6	181	162.8	242	10.9

136	18372	1.79	21.4	6.8	0.25	6.9	0.04	1.5	0.22	242.5	3.6	224.1	14.0	35	162.3	243	3.6
366	38449	1.74	19.6	2.0	0.27	2.2	0.04	1.1	0.48	242.6	2.6	242.1	4.8	237	45.4	243	2.6
52	5792	1.59	24.5	16.9	0.22	18.5	0.04	7.6	0.41	242.8	18.1	198.4	33.4	-301	434.4	243	18.1
90	11314	1.31	20.9	16.2	0.25	16.3	0.04	1.9	0.12	243.2	4.5	229.7	33.5	94	385.2	243	4.5
166	39646	1.02	19.4	7.4	0.27	7.7	0.04	1.9	0.24	244.2	4.5	246.2	16.7	265	170.7	244	4.5
111	12384	1.36	20.8	7.8	0.26	8.3	0.04	2.8	0.33	244.4	6.7	231.5	17.2	103	185.4	244	6.7
116	11993	1.60	19.7	13.6	0.27	13.6	0.04	1.6	0.12	244.6	3.8	242.9	29.5	226	314.5	245	3.8
73	6758	2.02	18.3	12.1	0.29	12.6	0.04	3.4	0.27	244.9	8.3	259.6	28.8	394	271.9	245	8.3
151	25560	3.25	19.8	4.1	0.27	4.8	0.04	2.4	0.51	245.0	5.8	243.0	10.3	224	94.9	245	5.8
86	16268	1.46	21.8	29.8	0.25	30.0	0.04	2.8	0.09	245.2	6.8	222.7	60.0	-9	734.4	245	6.8
67	7011	1.26	19.9	19.9	0.27	20.0	0.04	2.3	0.12	245.2	5.5	242.0	43.1	211	464.4	245	5.5
91	16315	1.39	19.9	13.4	0.27	13.5	0.04	1.8	0.13	245.3	4.3	241.7	29.0	207	311.5	245	4.3
107	15023	1.69	22.4	11.8	0.24	12.0	0.04	2.3	0.19	245.5	5.5	217.2	23.5	-79	289.0	246	5.5
115	17895	1.83	21.4	9.2	0.25	9.3	0.04	1.3	0.14	246.2	3.2	227.2	19.0	35	221.2	246	3.2
88	12694	1.36	19.7	15.1	0.27	15.4	0.04	2.7	0.17	246.5	6.5	244.9	33.4	229	351.0	247	6.5
95	8118	1.59	19.0	14.8	0.28	14.9	0.04	2.2	0.15	246.7	5.4	253.2	33.5	314	337.4	247	5.4
89	18818	1.05	19.8	12.8	0.27	13.0	0.04	1.9	0.15	246.7	4.7	244.0	28.1	219	297.5	247	4.7
66	7729	1.72	20.5	13.3	0.26	13.7	0.04	3.2	0.23	246.8	7.8	236.3	28.9	133	314.8	247	7.8
64	12650	1.40	22.0	16.6	0.25	16.8	0.04	2.7	0.16	247.0	6.4	222.6	33.5	-28	403.6	247	6.4
68	13196	1.37	18.3	11.8	0.29	13.3	0.04	6.1	0.46	247.1	14.8	261.9	30.7	396	265.4	247	14.8
303	30645	1.77	19.9	2.6	0.27	2.9	0.04	1.2	0.43	247.5	3.0	243.6	6.2	206	59.8	248	3.0
98	16030	1.90	20.0	9.0	0.27	9.6	0.04	3.2	0.34	247.6	7.8	242.4	20.7	192	210.6	248	7.8
64	7122	1.42	19.1	20.0	0.28	20.3	0.04	3.8	0.19	249.5	9.3	254.0	45.7	296	460.1	250	9.3
238	32151	1.90	20.2	2.6	0.27	3.5	0.04	2.3	0.67	250.2	5.7	242.3	7.5	166	60.1	250	5.7
123	15695	1.17	19.6	10.2	0.28	10.5	0.04	2.2	0.21	250.4	5.4	249.2	23.1	238	236.1	250	5.4
701	107140	2.25	19.6	1.4	0.28	1.9	0.04	1.3	0.67	250.6	3.2	250.1	4.3	245	32.8	251	3.2
130	28220	2.00	19.9	5.7	0.28	6.0	0.04	2.0	0.33	258.6	5.0	253.4	13.4	205	131.2	259	5.0

DMS-12-CV3

U	206Pb	U/Th	206Pb*	±	207Pb*	±	206Pb*	±	error	206Pb*	±	207Pb*	±	206Pb*	±	Best age	±
(ppm)	204Pb		207Pb*	(%)	235U*	(%)	238U	(%)	corr.	238U*	(Ma)	235U	(Ma)	207Pb*	(Ma)	(Ma)	(Ma)
65	4953	1.51	24.7	65.9	0.14	66.3	0.02	7.3	0.11	154.8	11.1	129.0	80.5	-325	1894.1	155	11.1
335	31469	1.56	20.7	6.9	0.16	7.1	0.02	1.8	0.25	151.9	2.7	149.8	9.9	117	162.4	152	2.7
67	7107	1.22	23.4	31.1	0.14	31.7	0.02	6.1	0.19	149.1	9.0	130.9	38.9	-188	793.4	149	9.0

276	13615	0.89	23.4	22.6	0.08	22.7	0.01	2.2	0.10	81.5	1.8	73.5	16.1	-179	571.0	81	1.8
436	23620	0.90	20.0	14.8	0.09	15.1	0.01	3.0	0.20	80.8	2.4	84.8	12.3	198	345.9	81	2.4
441	16932	1.56	22.2	12.1	0.08	12.3	0.01	2.1	0.17	78.1	1.7	74.2	8.8	-48	296.4	78	1.7
95	6388	0.75	21.8	53.2	0.08	53.8	0.01	8.2	0.15	82.8	6.7	79.8	41.3	-9	1375.7	83	6.7
180	10907	0.79	21.8	34.8	0.08	35.0	0.01	3.4	0.10	85.5	2.9	82.2	27.6	-12	863.2	85	2.9
612	39595	1.39	21.4	3.9	0.09	4.8	0.01	2.7	0.56	90.9	2.4	88.9	4.1	36	94.4	91	2.4
462	23971	0.82	20.6	6.5	0.09	6.7	0.01	1.6	0.24	83.7	1.3	85.0	5.4	122	152.6	84	1.3
234	53363	1.37	21.4	11.2	0.15	11.3	0.02	2.0	0.18	153.0	3.1	146.3	15.5	38	267.6	153	3.1
149	13102	0.58	18.1	21.5	0.09	22.5	0.01	6.7	0.30	76.1	5.0	88.0	19.0	425	484.6	76	5.0
391	32564	1.47	22.4	14.3	0.08	14.5	0.01	2.7	0.19	80.7	2.2	75.8	10.6	-78	351.1	81	2.2
550	22121	1.09	21.1	5.8	0.10	6.1	0.01	1.8	0.30	95.2	1.7	94.1	5.5	66	138.7	95	1.7
178	14834	1.15	21.8	14.9	0.17	16.3	0.03	6.6	0.40	167.8	10.9	156.8	23.6	-7	360.6	168	10.9
313	17218	1.21	22.2	11.1	0.08	11.4	0.01	2.4	0.21	83.0	2.0	78.8	8.6	-48	271.9	83	2.0
457	17772	1.18	22.1	5.8	0.08	6.4	0.01	2.8	0.43	80.7	2.2	76.9	4.8	-39	141.1	81	2.2
271	26139	0.99	20.4	8.9	0.09	9.3	0.01	2.7	0.29	82.4	2.2	84.8	7.6	153	209.8	82	2.2
260	19413	1.02	19.8	4.3	0.16	4.5	0.02	1.6	0.34	147.1	2.3	151.3	6.4	218	98.8	147	2.3
116	7133	0.78	22.1	31.3	0.08	32.1	0.01	7.2	0.22	86.0	6.1	81.8	25.2	-39	776.3	86	6.1
100	5718	0.68	18.4	25.7	0.10	26.7	0.01	7.2	0.27	84.8	6.1	96.2	24.5	388	585.1	85	6.1
129	27100	0.89	22.1	10.7	0.15	11.1	0.02	2.7	0.24	148.9	3.9	138.2	14.3	-42	261.3	149	3.9
659	11817	0.57	21.0	6.1	0.08	6.7	0.01	2.7	0.41	80.6	2.2	80.5	5.2	78	144.8	81	2.2
258	58552	1.13	21.5	15.1	0.09	15.2	0.01	1.9	0.12	90.3	1.7	88.1	12.8	29	363.1	90	1.7
65	4446	0.64	24.8	42.5	0.13	42.6	0.02	3.5	0.08	146.2	5.1	122.1	49.1	-325	1135.9	146	5.1
173	7436	1.18	22.9	33.8	0.09	34.0	0.01	3.7	0.11	90.7	3.4	83.1	27.1	-129	856.1	91	3.4
106	5500	0.95	23.4	40.3	0.07	40.9	0.01	7.2	0.18	80.7	5.8	72.6	28.7	-185	1043.1	81	5.8
492	26098	2.11	18.9	8.5	0.10	8.7	0.01	1.7	0.20	90.2	1.6	99.2	8.2	322	194.1	90	1.6
154	21872	1.18	19.6	11.8	0.17	12.4	0.02	3.5	0.28	151.5	5.2	157.0	18.0	240	274.0	152	5.2
291	10448	1.35	21.4	14.1	0.09	14.5	0.01	3.3	0.23	90.6	3.0	88.6	12.3	37	338.4	91	3.0
185	8080	0.72	20.8	19.2	0.08	20.0	0.01	5.8	0.29	77.1	4.4	78.0	15.0	105	457.1	77	4.4
449	33082	0.93	21.4	9.7	0.09	9.8	0.01	1.5	0.15	85.6	1.3	83.7	7.9	32	232.8	86	1.3
100	8251	1.42	24.3	21.9	0.07	24.4	0.01	10.7	0.44	77.9	8.3	67.7	16.0	-282	564.5	78	8.3
82	11070	1.41	21.0	7.7	0.26	7.9	0.04	1.9	0.24	249.7	4.7	234.1	16.6	81	183.1	250	4.7
165	5461	0.93	23.3	27.2	0.08	27.4	0.01	3.4	0.13	81.7	2.8	74.0	19.6	-169	687.2	82	2.8
211	7919	0.73	22.0	17.8	0.08	18.1	0.01	3.2	0.18	85.1	2.7	81.3	14.1	-31	434.9	85	2.7
111	8287	1.22	24.1	53.0	0.08	53.3	0.01	5.2	0.10	84.9	4.4	74.4	38.2	-252	1434.2	85	4.4

DMS-12-CV4

U (ppm)	206Pb 204Pb	U/Th	206Pb* 207Pb*	± (%)	207Pb* 235U*	± (%)	206Pb* 238U	± (%)	error corr.	206Pb* 238U*	± (Ma)	207Pb* 235U	± (Ma)	206Pb* 207Pb*	± (Ma)	Best age (Ma)	± (Ma)
309	34170	3.03	20.7	8.3	0.08	10.7	0.01	6.7	0.63	80.5	5.4	81.5	8.3	111	195.9	80	5.4
47	5428	1.25	17.4	42.5	0.19	42.7	0.02	4.5	0.11	149.1	6.7	172.7	68.0	509	976.4	149	6.7
412	152891	0.43	20.9	4.9	0.16	5.1	0.02	1.2	0.24	150.4	1.8	146.7	6.9	88	117.0	150	1.8
65	4259	1.03	15.9	44.9	0.11	45.7	0.01	8.3	0.18	82.4	6.8	107.3	46.5	703	1006.3	82	6.8
151	7005	3.11	25.3	17.9	0.07	18.6	0.01	4.9	0.26	86.7	4.2	72.2	12.9	-385	469.4	87	4.2
81	21394	1.14	20.3	12.7	0.31	12.9	0.04	2.2	0.17	283.1	6.1	270.7	30.7	166	298.4	283	6.1
375	18317	1.27	20.8	7.3	0.08	7.5	0.01	1.9	0.25	79.4	1.5	80.0	5.8	99	172.2	79	1.5
191	10480	1.33	22.4	29.0	0.08	29.3	0.01	3.7	0.13	84.9	3.1	79.6	22.4	-76	723.4	85	3.1
232	9519	1.66	23.3	23.3	0.08	23.4	0.01	2.0	0.09	83.4	1.7	75.4	17.0	-169	587.8	83	1.7
364	15953	1.54	19.8	9.0	0.09	9.1	0.01	1.7	0.19	78.6	1.4	83.3	7.3	221	208.0	79	1.4
236	13583	1.25	19.9	7.0	0.16	7.1	0.02	1.2	0.17	147.7	1.8	151.6	9.9	212	161.3	148	1.8
74	7734	1.39	21.4	27.4	0.15	27.6	0.02	3.2	0.12	148.2	4.6	142.0	36.6	40	666.4	148	4.6
424	28974	1.46	20.5	4.7	0.10	6.5	0.01	4.5	0.69	90.8	4.1	92.7	5.8	143	110.6	91	4.1
581	11654	1.33	21.8	9.1	0.10	11.3	0.02	6.8	0.60	105.6	7.1	101.0	10.9	-8	219.3	106	7.1
75	3681	0.87	24.5	20.5	0.13	21.0	0.02	4.7	0.22	150.4	7.0	126.5	25.0	-301	529.0	150	7.0
118	2522	0.72	19.3	17.6	0.17	18.0	0.02	3.5	0.20	150.2	5.2	157.9	26.3	275	406.4	150	5.2
152	8256	0.78	19.7	7.9	0.30	8.6	0.04	3.3	0.39	266.4	8.7	263.1	19.8	234	182.3	266	8.7
175	5971	1.11	21.8	16.8	0.09	17.0	0.01	2.5	0.15	91.0	2.2	87.2	14.2	-14	407.7	91	2.2
104	14215	1.39	21.0	8.9	0.26	9.1	0.04	2.1	0.23	250.3	5.1	235.0	19.1	85	210.4	250	5.1
64	5385	1.47	21.2	18.0	0.15	19.0	0.02	6.2	0.33	144.0	8.8	139.2	24.7	59	431.5	144	8.8
150	13108	1.07	21.5	8.9	0.15	9.1	0.02	2.2	0.24	148.3	3.2	141.0	12.0	20	212.9	148	3.2
419	25701	0.94	19.7	5.1	0.15	5.4	0.02	1.8	0.34	135.6	2.4	141.0	7.1	232	117.4	136	2.4
75	6336	0.67	22.2	20.6	0.16	20.7	0.03	2.5	0.12	163.7	4.0	150.6	29.0	-51	505.3	164	4.0
79	7590	1.51	20.1	17.0	0.27	17.1	0.04	1.8	0.11	247.4	4.4	241.6	36.7	186	397.5	247	4.4
126	18238	1.15	19.5	8.7	0.28	8.9	0.04	2.0	0.22	248.8	4.9	248.9	19.7	250	200.5	249	4.9
135	8843	1.18	22.0	15.4	0.15	15.8	0.02	3.4	0.22	153.1	5.2	142.3	21.0	-34	376.4	153	5.2
163	8613	0.94	20.1	8.9	0.16	9.5	0.02	3.4	0.36	151.4	5.1	153.0	13.5	178	207.7	151	5.1

DMS-12-CV5

U	206Pb	U/Th	206Pb*	±	207Pb*	±	206Pb*	±	error	206Pb*	±	207Pb*	±	206Pb*	±	Best age	±

(ppm)	204Pb		207Pb*	(%)	235U*	(%)	238U	(%)	corr.	238U*	(Ma)	235U	(Ma)	207Pb*	(Ma)	(Ma)	(Ma)
261	16287	0.62	19.0	11.2	0.09	11.5	0.01	2.8	0.24	76.4	2.1	84.2	9.3	312	255.2	76	2.1
154	4627	1.21	21.4	18.5	0.08	18.8	0.01	3.6	0.19	76.8	2.7	75.6	13.7	39	445.6	77	2.7
207	12030	0.74	22.6	13.4	0.07	13.9	0.01	3.4	0.25	77.5	2.6	72.4	9.7	-92	330.7	78	2.6
147	7733	0.85	25.2	37.7	0.07	38.2	0.01	5.7	0.15	78.7	4.4	66.1	24.4	-373	1009.2	79	4.4
162	12998	1.45	21.2	44.8	0.08	45.5	0.01	7.8	0.17	78.8	6.1	78.2	34.2	60	1118.6	79	6.1
181	9671	2.99	23.2	17.3	0.07	17.9	0.01	4.5	0.25	79.6	3.6	72.3	12.5	-163	433.9	80	3.6
194	15600	0.93	26.3	25.5	0.07	25.7	0.01	2.7	0.11	81.6	2.2	65.5	16.3	-488	686.8	82	2.2
190	8648	0.82	20.0	13.0	0.09	13.5	0.01	3.8	0.28	82.9	3.1	86.9	11.3	198	303.1	83	3.1
318	33078	1.34	21.3	9.8	0.08	10.0	0.01	1.9	0.19	83.4	1.6	82.0	7.9	42	234.9	83	1.6
204	8519	1.34	21.2	20.4	0.08	20.6	0.01	2.6	0.13	83.7	2.1	82.6	16.3	53	491.9	84	2.1
243	35763	1.34	23.3	14.2	0.08	14.3	0.01	2.2	0.16	83.8	1.9	75.6	10.4	-176	354.4	84	1.9
207	13793	2.11	18.1	19.3	0.10	20.8	0.01	7.7	0.37	84.1	6.4	96.8	19.2	422	433.7	84	6.4
303	11927	1.49	21.9	18.4	0.08	18.6	0.01	2.9	0.16	84.7	2.4	81.3	14.5	-17	448.0	85	2.4
179	7992	0.95	24.7	22.4	0.07	22.6	0.01	3.7	0.16	84.9	3.1	72.6	15.9	-318	579.3	85	3.1
203	6526	1.28	20.9	17.3	0.09	17.6	0.01	3.4	0.19	85.0	2.9	85.1	14.4	89	412.5	85	2.9
332	15643	0.93	20.5	8.0	0.09	8.5	0.01	2.7	0.32	85.3	2.3	87.2	7.1	139	188.3	85	2.3
157	9963	0.98	19.0	21.2	0.10	21.7	0.01	4.9	0.22	86.4	4.2	94.8	19.7	310	486.9	86	4.2
287	13019	2.36	21.2	15.0	0.09	15.4	0.01	3.2	0.21	88.7	2.8	87.5	12.9	56	359.9	89	2.8
181	13452	1.12	20.1	13.3	0.16	13.5	0.02	2.6	0.19	146.6	3.8	148.7	18.7	182	310.2	147	3.8
236	27482	1.35	20.9	9.9	0.15	10.1	0.02	1.9	0.19	146.6	2.8	143.8	13.6	96	235.6	147	2.8
420	27566	0.68	20.0	4.6	0.16	5.4	0.02	3.0	0.54	146.7	4.3	149.7	7.6	196	105.8	147	4.3
218	32457	0.93	21.0	6.2	0.15	6.3	0.02	1.0	0.16	147.0	1.4	143.0	8.4	77	147.1	147	1.4
104	11634	1.59	23.4	36.3	0.14	36.5	0.02	3.4	0.09	147.2	5.0	129.5	44.4	-185	933.4	147	5.0
104	9653	1.30	20.4	18.5	0.16	18.9	0.02	3.8	0.20	147.7	5.5	147.5	25.9	144	437.5	148	5.5
104	13621	0.94	21.4	24.1	0.15	25.1	0.02	7.2	0.29	147.8	10.5	141.1	33.1	30	583.9	148	10.5
285	17023	0.85	21.6	7.8	0.15	7.9	0.02	1.3	0.17	148.1	1.9	140.7	10.4	17	187.2	148	1.9
148	18764	1.62	21.4	9.0	0.15	9.3	0.02	2.6	0.28	148.4	3.8	141.7	12.3	31	215.3	148	3.8
169	30501	1.20	20.2	14.1	0.16	14.2	0.02	1.4	0.10	148.5	2.1	149.8	19.8	171	331.6	148	2.1
170	7812	0.63	19.6	13.3	0.16	13.7	0.02	3.3	0.24	148.8	4.9	154.2	19.7	238	309.0	149	4.9
70	4686	0.94	24.4	47.2	0.13	47.4	0.02	4.5	0.09	148.8	6.6	126.0	56.2	-286	1264.5	149	6.6
88	10570	1.46	21.9	27.3	0.15	27.7	0.02	4.6	0.17	148.8	6.8	139.5	36.0	-17	670.0	149	6.8
109	8409	1.09	25.8	27.7	0.13	28.0	0.02	3.9	0.14	149.6	5.7	120.0	31.7	-433	740.1	150	5.7
211	17734	0.66	20.4	13.8	0.16	13.9	0.02	2.0	0.15	149.6	3.0	149.7	19.4	150	323.6	150	3.0

136	9256	0.94	23.5	21.1	0.14	22.1	0.02	6.6	0.30	149.7	9.7	130.9	27.1	-197	532.1	150	9.7
329	40212	0.71	20.9	10.3	0.15	10.5	0.02	2.1	0.20	149.8	3.1	146.1	14.3	86	245.3	150	3.1
103	7099	0.53	22.5	25.5	0.14	25.5	0.02	1.4	0.05	150.0	2.1	137.0	32.7	-83	633.0	150	2.1
66	2128	1.11	16.2	20.7	0.20	21.2	0.02	4.7	0.22	150.1	6.9	185.6	36.0	665	447.3	150	6.9
139	8127	0.73	21.4	16.4	0.15	16.5	0.02	1.7	0.11	150.6	2.6	143.9	22.1	34	394.0	151	2.6
130	11401	0.94	20.2	11.8	0.16	12.1	0.02	2.3	0.19	150.9	3.4	152.4	17.1	175	277.0	151	3.4
192	19828	1.45	19.0	11.4	0.17	11.8	0.02	3.0	0.25	151.4	4.4	161.2	17.6	308	260.6	151	4.4
164	16109	0.91	21.0	12.3	0.16	12.5	0.02	2.3	0.18	152.3	3.5	148.2	17.2	85	292.0	152	3.5
360	48054	0.64	20.5	6.0	0.16	6.1	0.02	1.1	0.17	152.9	1.6	151.6	8.6	132	140.8	153	1.6
201	25592	1.14	19.4	8.1	0.17	8.4	0.02	2.3	0.27	153.0	3.4	160.1	12.5	267	186.9	153	3.4
139	19957	0.64	24.5	33.5	0.14	33.5	0.02	1.9	0.06	153.0	2.9	128.7	40.6	-299	876.7	153	2.9
209	30634	1.00	21.1	11.6	0.16	11.9	0.02	2.6	0.22	153.2	3.9	148.6	16.4	74	276.7	153	3.9
86	15812	1.39	18.6	15.7	0.18	16.1	0.02	3.4	0.21	153.5	5.2	167.3	24.8	367	356.6	154	5.2
258	36878	0.77	20.3	5.1	0.17	5.5	0.02	2.1	0.38	156.3	3.2	156.4	8.0	159	119.2	156	3.2
117	12851	1.13	18.8	11.8	0.18	12.1	0.02	2.8	0.23	156.4	4.3	168.0	18.7	336	267.2	156	4.3
53	4866	0.78	24.0	74.8	0.14	74.9	0.02	3.3	0.04	156.5	5.1	134.2	94.4	-245	2222.4	157	5.1
85	10546	1.33	19.8	9.7	0.27	9.9	0.04	2.1	0.21	243.9	5.0	241.1	21.3	213	225.4	244	5.0
221	28025	1.87	19.6	5.6	0.27	6.5	0.04	3.3	0.51	245.2	8.0	244.6	14.2	238	129.8	245	8.0
394	52895	1.92	19.8	2.1	0.27	3.0	0.04	2.2	0.72	245.8	5.3	242.7	6.6	213	48.5	246	5.3
179	44729	1.73	19.9	6.5	0.27	6.7	0.04	1.3	0.19	248.2	3.1	244.1	14.5	205	151.8	248	3.1
98	10091	1.07	20.6	13.2	0.26	13.7	0.04	3.8	0.28	248.7	9.2	236.9	29.0	122	311.5	249	9.2
179	54508	0.91	19.1	3.7	0.28	4.4	0.04	2.5	0.55	249.2	6.0	254.0	10.0	298	84.6	249	6.0
257	47857	1.11	19.4	3.7	0.28	4.0	0.04	1.3	0.33	249.7	3.2	251.4	8.8	267	85.6	250	3.2
192	21886	1.59	19.4	5.4	0.28	5.8	0.04	2.1	0.36	250.1	5.2	251.2	12.9	261	124.5	250	5.2
128	61944	1.40	13.3	1.0	1.79	2.3	0.17	2.1	0.90	1024.2	19.6	1041.6	15.0	1078	20.2	1078	20.2

DMS-12-CV6

U (ppm)	206Pb 204Pb	U/Th	206Pb* 207Pb*	± (%)	207Pb* 235U*	± (%)	206Pb* 238U	± (%)	error corr.	206Pb* 238U*	± (Ma)	207Pb* 235U	± (Ma)	206Pb* 207Pb*	± (Ma)	Best age (Ma)	± (Ma)
73	2413	1.43	31.2	76.6	0.05	76.9	0.01	7.5	0.10	74.2	5.6	50.7	38.1	-958	2635.3	74	5.6
132	12080	1.82	21.7	21.3	0.08	21.8	0.01	4.5	0.21	78.1	3.5	75.8	15.9	6	517.4	78	3.5
384	23383	3.69	19.9	10.8	0.09	11.0	0.01	2.2	0.20	78.6	1.8	82.9	8.8	208	251.5	79	1.8
420	27305	0.78	21.4	5.7	0.08	6.6	0.01	3.2	0.49	80.0	2.6	78.5	5.0	31	136.8	80	2.6
381	14459	0.79	21.9	10.9	0.08	11.3	0.01	2.6	0.24	80.1	2.1	76.8	8.3	-25	265.7	80	2.1

337	30479	1.07	23.8	13.0	0.07	13.9	0.01	4.8	0.35	81.9	3.9	72.5	9.7	-228	328.7	82	3.9
355	14859	1.03	20.1	10.2	0.09	10.3	0.01	1.6	0.15	82.2	1.3	85.9	8.5	189	237.3	82	1.3
112	3536	0.75	24.2	30.0	0.07	30.3	0.01	3.8	0.13	82.7	3.2	71.9	21.0	-273	778.2	83	3.2
487	22057	0.97	21.7	11.6	0.08	11.7	0.01	2.1	0.18	83.0	1.7	80.5	9.1	7	278.9	83	1.7
401	24261	1.25	21.2	9.6	0.08	9.9	0.01	2.5	0.25	83.2	2.1	82.2	7.9	55	230.3	83	2.1
146	34742	2.52	24.1	35.7	0.07	36.0	0.01	4.5	0.13	83.2	3.7	72.7	25.3	-262	931.6	83	3.7
144	9728	1.44	22.0	17.3	0.08	17.7	0.01	3.9	0.22	84.0	3.2	80.2	13.6	-32	421.2	84	3.2
277	9565	1.30	20.6	7.5	0.09	7.9	0.01	2.5	0.31	84.3	2.1	85.6	6.5	124	176.2	84	2.1
383	22038	1.07	21.0	8.1	0.09	8.2	0.01	1.1	0.13	84.5	0.9	84.2	6.6	76	192.7	85	0.9
134	6941	1.14	20.4	14.7	0.09	15.4	0.01	4.5	0.29	84.7	3.8	87.1	12.9	153	346.8	85	3.8
284	28958	1.17	18.9	13.5	0.10	13.6	0.01	1.3	0.09	85.1	1.1	93.8	12.2	321	308.8	85	1.1
395	17575	1.08	20.4	7.4	0.09	8.2	0.01	3.4	0.41	85.9	2.9	88.1	6.9	149	174.5	86	2.9
132	6978	1.52	20.1	35.5	0.09	35.9	0.01	5.1	0.14	86.5	4.4	90.0	30.9	184	851.1	87	4.4
385	38583	0.66	21.2	6.7	0.09	7.3	0.01	2.8	0.38	88.5	2.5	87.5	6.1	61	160.6	89	2.5
84	8860	1.41	21.8	97.6	0.09	97.7	0.01	4.9	0.05	89.6	4.3	86.2	81.0	-5	175.4	90	4.3
314	10548	1.35	21.7	10.2	0.09	10.7	0.01	3.2	0.30	90.1	2.8	86.9	8.9	-2	246.9	90	2.8
1375	88972	1.63	20.7	2.2	0.09	2.7	0.01	1.5	0.55	90.6	1.3	91.5	2.3	114	52.7	91	1.3
568	24659	1.17	20.3	5.0	0.10	6.3	0.01	3.8	0.60	90.8	3.4	93.2	5.6	156	117.0	91	3.4
525	31210	1.30	21.1	4.9	0.09	5.1	0.01	1.5	0.28	90.8	1.3	89.9	4.4	66	116.8	91	1.3
259	21411	1.47	20.8	11.8	0.10	12.1	0.01	2.9	0.24	92.1	2.6	92.7	10.7	109	278.6	92	2.6
143	6285	0.91	24.5	24.2	0.08	25.0	0.01	6.1	0.24	92.4	5.6	79.2	19.0	-303	626.5	92	5.6
174	10166	0.89	19.9	9.4	0.16	9.7	0.02	2.5	0.25	142.6	3.5	146.3	13.2	207	217.3	143	3.5
261	27010	1.04	20.0	8.5	0.16	8.7	0.02	1.8	0.21	147.2	2.6	149.9	12.1	192	198.1	147	2.6
240	16437	0.72	20.1	9.0	0.16	9.1	0.02	1.7	0.18	148.4	2.4	150.3	12.7	180	209.4	148	2.4
93	11012	1.33	20.1	19.9	0.16	20.4	0.02	4.6	0.23	148.4	6.8	150.5	28.6	185	467.0	148	6.8
151	11432	1.01	20.9	13.1	0.15	13.3	0.02	2.3	0.17	148.6	3.4	145.5	18.1	96	312.1	149	3.4
108	7981	1.05	23.0	24.9	0.14	26.0	0.02	7.6	0.29	148.9	11.1	133.2	32.5	-138	624.0	149	11.1
95	7594	1.46	20.9	16.1	0.15	16.3	0.02	2.7	0.17	149.1	4.0	145.6	22.2	90	384.2	149	4.0
123	9718	1.52	23.2	11.7	0.14	11.8	0.02	1.1	0.09	149.7	1.6	132.6	14.6	-163	292.4	150	1.6
95	9419	1.31	23.0	27.3	0.14	28.6	0.02	8.5	0.30	149.8	12.6	133.8	35.9	-142	687.0	150	12.6
86	6811	0.89	19.5	13.9	0.17	14.4	0.02	3.9	0.27	150.2	5.8	156.2	20.9	249	321.4	150	5.8
116	34566	0.86	20.8	15.3	0.16	15.7	0.02	3.5	0.22	150.2	5.2	147.7	21.6	109	363.3	150	5.2
188	10411	0.92	20.2	8.4	0.16	8.7	0.02	2.1	0.25	150.2	3.2	151.3	12.2	169	196.5	150	3.2
83	7528	1.31	20.9	14.4	0.16	14.6	0.02	2.5	0.17	150.7	3.8	147.0	20.0	88	342.6	151	3.8

131	14816	1.40	20.0	18.7	0.16	18.9	0.02	2.5	0.13	151.8	3.8	154.2	27.0	192	439.0	152	3.8
132	8448	1.10	22.5	18.1	0.15	18.3	0.02	2.3	0.13	152.1	3.5	138.5	23.7	-89	447.8	152	3.5
115	7984	1.06	24.7	15.9	0.13	16.6	0.02	4.7	0.29	154.0	7.2	128.4	20.0	-323	411.2	154	7.2
133	12954	1.28	21.4	14.8	0.16	15.1	0.02	2.9	0.19	156.0	4.5	148.8	20.9	35	355.5	156	4.5
91	9333	1.23	21.4	41.6	0.16	42.2	0.02	7.1	0.17	156.3	11.0	149.2	58.6	38	1035.5	156	11.0
202	19483	1.04	19.6	4.6	0.27	4.7	0.04	1.1	0.24	243.8	2.7	243.4	10.3	240	106.3	244	2.7
72	45833	1.36	20.0	19.0	0.27	19.2	0.04	2.9	0.15	246.2	7.1	240.9	41.2	190	444.3	246	7.1
127	31591	1.06	18.8	9.7	0.29	9.8	0.04	1.5	0.15	246.4	3.5	254.9	22.0	334	219.4	246	3.5
157	32115	1.64	19.4	5.4	0.28	5.9	0.04	2.3	0.38	247.6	5.5	249.6	13.0	268	124.9	248	5.5
77	16862	2.25	18.2	5.9	0.30	6.8	0.04	3.3	0.49	251.3	8.2	267.7	16.0	413	132.6	251	8.2

DMS-12-MTY1

U	206Pb	U/Th	206Pb*	±	207Pb*	±	206Pb*	±	error	206Pb*	±	207Pb*	±	206Pb*	±	Best age	±
(ppm)	204Pb		207Pb*	(%)	235U*	(%)	238U	(%)	corr.	238U*	(Ma)	235U	(Ma)	207Pb*	(Ma)	(Ma)	(Ma)
360	16671	1.04	19.7	9.4	0.09	9.6	0.01	1.9	0.20	79.4	1.5	84.5	7.8	230	217.6	79	1.5
564	27388	0.98	21.6	6.0	0.08	6.2	0.01	1.3	0.21	83.0	1.1	80.6	4.8	9	145.3	83	1.1
200	2302	1.42	17.3	20.4	0.10	20.9	0.01	4.3	0.20	83.6	3.5	100.5	20.0	522	452.5	84	3.5
682	18430	2.97	21.2	7.3	0.09	7.6	0.01	2.0	0.27	90.1	1.8	89.1	6.5	63	174.9	90	1.8
414	30048	1.89	19.2	10.2	0.10	10.5	0.01	2.8	0.26	91.4	2.5	98.8	9.9	284	232.8	91	2.5
127	9221	1.99	28.9	46.1	0.07	46.4	0.02	5.3	0.11	96.8	5.1	70.9	31.8	-737	1350.9	97	5.1
153	11083	4.15	21.3	20.3	0.12	20.9	0.02	5.2	0.25	119.6	6.1	116.4	23.0	51	488.3	120	6.1
125	15250	1.52	19.7	10.3	0.27	10.5	0.04	2.3	0.21	245.5	5.4	244.0	22.8	230	237.6	245	5.4
164	15811	1.07	20.3	10.0	0.26	10.1	0.04	1.1	0.11	246.2	2.6	238.1	21.4	159	234.8	246	2.6
86	12635	1.61	21.4	20.6	0.26	20.7	0.04	2.2	0.11	259.9	5.6	238.2	43.9	30	497.4	260	5.6
600	91029	1.70	19.5	1.8	0.29	2.0	0.04	0.9	0.43	261.0	2.2	260.3	4.6	254	41.7	261	2.2
199	13354	2.27	19.3	4.2	0.31	6.7	0.04	5.3	0.78	276.1	14.2	276.2	16.3	278	96.2	276	14.2

DMS-12-S1

U	206Pb	U/Th	206Pb*	±	207Pb*	±	206Pb*	±	error	206Pb*	±	207Pb*	±	206Pb*	±	Best age	±
(ppm)	204Pb		207Pb*	(%)	235U*	(%)	238U	(%)	corr.	238U*	(Ma)	235U	(Ma)	207Pb*	(Ma)	(Ma)	(Ma)
185	11802	0.69	24.2	27.9	0.07	28.1	0.01	3.7	0.13	83.5	3.1	72.7	19.8	-269	720.2	84	3.1
148	6937	0.81	26.5	39.4	0.06	39.9	0.01	6.4	0.16	79.8	5.1	63.6	24.6	-508	1085.6	80	5.1
681	124842	2.62	19.6	1.6	0.26	2.0	0.04	1.1	0.57	237.2	2.6	237.5	4.2	240	37.6	237	2.6
87	15878	0.56	24.4	28.5	0.07	30.3	0.01	10.3	0.34	84.9	8.7	73.3	21.4	-291	738.8	85	8.7

463	55084	4.88	20.9	5.1	0.09	5.5	0.01	2.2	0.39	83.8	1.8	84.1	4.5	92	120.5	84	1.8
305	9389	1.59	19.9	10.8	0.08	11.0	0.01	2.1	0.19	76.9	1.6	81.2	8.6	210	252.1	77	1.6
358	79455	4.23	19.1	3.4	0.27	3.8	0.04	1.8	0.47	239.1	4.2	245.0	8.3	302	76.6	239	4.2
278	9170	1.20	23.0	23.1	0.08	23.3	0.01	3.2	0.14	81.4	2.6	74.5	16.7	-142	577.4	81	2.6
327	44621	3.29	20.1	4.1	0.17	7.0	0.02	5.7	0.81	153.6	8.6	155.2	10.1	180	96.7	154	8.6
455	49990	2.65	19.1	3.0	0.25	3.3	0.03	1.3	0.39	221.6	2.8	228.8	6.7	304	68.2	222	2.8
152	8738	1.60	25.4	20.7	0.07	21.2	0.01	4.3	0.21	80.8	3.5	67.2	13.8	-394	544.3	81	3.5
522	77669	2.41	19.5	1.2	0.27	1.7	0.04	1.1	0.68	241.4	2.7	242.6	3.7	253	28.6	241	2.7
147	4566	1.22	20.7	21.6	0.08	22.2	0.01	4.9	0.22	77.9	3.8	79.1	16.9	116	515.3	78	3.8
501	62085	24.31	21.1	7.9	0.08	8.2	0.01	2.4	0.29	75.9	1.8	75.6	6.0	67	187.7	76	1.8
812	64229	1.42	19.7	1.5	0.24	3.7	0.03	3.4	0.91	221.4	7.3	222.4	7.4	233	34.6	221	7.3
251	10327	1.57	20.6	10.5	0.08	10.9	0.01	2.9	0.26	79.1	2.3	80.5	8.4	122	247.1	79	2.3
179	8131	1.17	21.5	12.5	0.08	12.8	0.01	3.0	0.23	81.7	2.4	80.0	9.8	29	299.4	82	2.4
856	96573	0.51	21.3	2.5	0.08	2.9	0.01	1.6	0.55	78.8	1.3	77.9	2.2	48	58.8	79	1.3
103	4555	1.82	20.6	31.2	0.08	33.6	0.01	12.4	0.37	80.6	9.9	82.3	26.6	131	750.8	81	9.9
194	13285	0.90	21.2	19.7	0.08	20.1	0.01	4.0	0.20	82.6	3.3	81.6	15.8	52	473.6	83	3.3
592	256858	2.12	11.8	2.3	0.90	4.2	0.08	3.5	0.84	479.1	16.4	651.9	20.4	1307	45.0	479	16.4
126	194160	1.51	9.3	0.4	4.35	1.7	0.29	1.7	0.97	1656.6	24.7	1702.1	14.4	1759	8.2	1759	8.2
229	42700	2.75	16.6	7.3	0.30	9.2	0.04	5.6	0.61	226.8	12.5	263.9	21.4	607	157.7	227	12.5
203	9253	1.08	21.8	9.2	0.08	10.2	0.01	4.4	0.43	84.1	3.6	80.9	7.9	-12	223.3	84	3.6
426	52343	2.64	19.4	2.2	0.26	2.5	0.04	1.2	0.48	235.9	2.8	238.6	5.4	266	51.4	236	2.8
182	8159	1.50	19.7	27.2	0.09	27.7	0.01	5.1	0.18	78.5	4.0	83.4	22.2	226	638.7	79	4.0
495	295868	3.43	9.4	0.3	4.18	1.0	0.28	1.0	0.96	1614.5	14.2	1670.9	8.5	1742	5.0	1742	5.0
407	32776	3.09	19.5	5.4	0.20	5.7	0.03	1.6	0.28	181.4	2.8	186.3	9.6	249	125.0	181	2.8
310	31886	1.96	19.6	4.0	0.26	4.5	0.04	2.0	0.44	230.4	4.4	231.1	9.2	238	92.4	230	4.4
512	163844	2.02	19.4	2.2	0.27	2.3	0.04	0.9	0.39	236.5	2.1	239.5	5.0	269	49.5	236	2.1
134	5057	0.69	28.8	54.1	0.06	54.3	0.01	5.0	0.09	81.6	4.1	60.0	31.7	-733	1614.6	82	4.1
786	789	0.62	16.4	31.1	0.10	32.9	0.01	10.9	0.33	73.1	8.0	92.9	29.2	636	684.0	73	8.0
282	15647	1.15	22.8	21.1	0.08	21.2	0.01	2.4	0.11	85.6	2.0	79.1	16.2	-114	525.2	86	2.0
495	39120	1.17	21.3	13.7	0.08	14.1	0.01	3.1	0.22	81.6	2.5	80.4	10.9	45	329.4	82	2.5
152	150957	1.22	9.7	0.5	4.06	3.5	0.29	3.4	0.99	1616.8	49.0	1646.0	28.2	1683	9.6	1683	9.6
263	7171	1.24	24.6	17.7	0.07	18.0	0.01	2.8	0.16	77.5	2.2	66.5	11.6	-314	457.8	78	2.2
218	171550	0.87	9.7	0.4	3.85	1.6	0.27	1.5	0.96	1546.4	20.8	1602.9	12.7	1678	8.1	1678	8.1
220	298445	1.27	9.3	0.3	4.66	1.4	0.31	1.4	0.97	1756.8	21.1	1760.9	11.8	1766	6.2	1766	6.2

295	12408	1.58	22.4	15.5	0.08	15.8	0.01	2.8	0.18	80.2	2.2	75.4	11.5	-75	382.1	80	2.2
361	164989	1.01	22.5	8.9	0.08	9.2	0.01	2.2	0.24	79.4	1.7	74.3	6.6	-87	218.7	79	1.7
497	72439	2.55	19.4	2.0	0.27	2.7	0.04	1.9	0.68	240.8	4.4	242.7	5.9	261	46.3	241	4.4
198	132267	2.92	9.6	0.6	3.75	5.9	0.26	5.9	0.99	1497.6	78.5	1581.3	47.4	1695	11.6	1695	11.6
319	37106	3.25	19.6	4.0	0.27	4.6	0.04	2.3	0.50	238.3	5.4	239.1	9.8	247	91.7	238	5.4
270	8788	1.19	24.1	14.6	0.07	14.7	0.01	1.9	0.13	77.2	1.5	67.8	9.7	-253	371.0	77	1.5
411	566156	2.61	9.8	0.3	3.75	0.8	0.27	0.8	0.95	1520.1	10.8	1582.5	6.7	1667	4.6	1667	4.6
355	318234	2.21	9.2	0.6	4.41	3.5	0.30	3.5	0.98	1668.2	51.2	1714.5	29.3	1772	11.4	1772	11.4
323	27153	1.38	22.5	13.6	0.08	13.9	0.01	2.8	0.20	78.6	2.1	73.5	9.9	-87	335.5	79	2.1
288	302064	8.96	9.4	0.2	4.17	1.4	0.28	1.4	0.99	1610.0	19.3	1667.7	11.3	1741	4.0	1741	4.0
115	213449	1.52	9.2	0.6	4.46	1.5	0.30	1.4	0.90	1686.5	20.2	1723.4	12.5	1769	11.7	1769	11.7
169	5531	2.36	29.9	40.5	0.06	41.1	0.01	6.6	0.16	81.5	5.4	57.9	23.1	-837	1198.7	81	5.4
534	64672	2.76	19.6	1.8	0.27	2.3	0.04	1.4	0.61	242.3	3.4	242.2	5.0	241	42.4	242	3.4
116	104211	2.11	9.8	0.9	3.50	2.7	0.25	2.6	0.94	1431.2	33.2	1528.1	21.7	1665	16.9	1665	16.9
327	39826	4.22	21.1	9.5	0.13	11.8	0.02	7.0	0.60	129.0	9.0	126.2	14.0	74	225.3	129	9.0
368	4970	1.17	17.8	16.4	0.10	16.6	0.01	2.6	0.16	81.2	2.1	94.9	15.1	455	366.5	81	2.1
137	51685	1.47	9.1	1.5	4.83	4.0	0.32	3.6	0.92	1789.6	56.9	1789.9	33.2	1790	28.1	1790	28.1
338	44437	2.72	20.2	4.1	0.26	4.2	0.04	0.9	0.22	237.0	2.2	231.0	8.7	170	96.2	237	2.2
405	152667	5.16	19.6	4.9	0.25	5.8	0.04	3.1	0.53	228.9	6.9	230.4	12.0	245	114.0	229	6.9
729	27306	3.37	20.8	5.4	0.08	5.6	0.01	1.2	0.22	79.0	1.0	79.7	4.3	101	128.6	79	1.0
87	85436	1.63	9.5	0.9	4.24	2.7	0.29	2.6	0.94	1645.3	37.1	1682.2	22.3	1729	17.1	1729	17.1
318	54235	2.23	19.5	3.9	0.27	5.0	0.04	3.0	0.61	240.6	7.2	241.6	10.7	252	90.5	241	7.2
389	69499	3.16	19.7	1.8	0.26	2.3	0.04	1.5	0.63	231.2	3.3	231.6	4.8	235	41.8	231	3.3
125	148555	1.53	9.5	1.0	4.06	3.5	0.28	3.3	0.96	1584.5	46.7	1646.2	28.2	1726	17.8	1726	17.8
542	378590	3.31	9.5	0.5	4.20	2.1	0.29	2.0	0.97	1631.6	29.1	1674.0	17.1	1728	9.2	1728	9.2
183	7199	1.60	22.5	22.9	0.08	23.5	0.01	5.1	0.22	79.5	4.0	74.4	16.8	-87	567.2	79	4.0
207	11565	3.91	21.6	22.9	0.08	23.5	0.01	5.5	0.23	77.7	4.2	75.8	17.2	15	556.4	78	4.2
500	24214	1.44	21.5	5.9	0.08	6.2	0.01	2.1	0.33	82.7	1.7	80.9	4.8	28	140.5	83	1.7
384	87516	13.60	19.5	2.1	0.27	2.5	0.04	1.4	0.57	240.8	3.4	242.4	5.5	258	47.9	241	3.4
265	38835	2.18	19.4	4.8	0.27	5.0	0.04	1.4	0.28	242.7	3.3	244.3	10.9	259	110.2	243	3.3
768	619151	30.04	9.4	0.5	4.29	1.5	0.29	1.4	0.94	1654.1	20.5	1690.8	12.2	1736	9.1	1736	9.1
325	69867	3.08	20.2	3.7	0.26	3.9	0.04	1.2	0.30	237.6	2.8	231.3	8.1	169	86.9	238	2.8
157	10417	0.73	22.9	23.5	0.07	23.9	0.01	4.6	0.19	78.9	3.6	72.8	16.8	-124	586.4	79	3.6
199	18680	4.31	19.8	5.8	0.09	10.6	0.01	8.8	0.83	84.6	7.4	89.4	9.0	220	135.2	85	7.4

679	53411	3.47	19.7	1.8	0.27	1.9	0.04	0.6	0.32	240.5	1.4	239.3	4.1	227	42.4	240	1.4
388	311208	2.72	9.4	0.4	4.53	1.5	0.31	1.5	0.96	1739.5	22.1	1736.3	12.6	1732	8.3	1732	8.3
454	129052	2.21	19.8	2.7	0.25	5.5	0.04	4.8	0.87	227.0	10.8	226.1	11.2	216	62.6	227	10.8
215	12991	1.40	24.1	18.0	0.07	18.6	0.01	4.9	0.26	77.4	3.8	67.8	12.2	-259	458.3	77	3.8

DMS-12-SM1

U	206Pb	U/Th	206Pb*	±	207Pb*	±	206Pb*	±	error	206Pb*	±	207Pb*	±	206Pb*	±	Best age	±
(ppm)	204Pb		207Pb*	(%)	235U*	(%)	238U	(%)	corr.	238U*	(Ma)	235U	(Ma)	207Pb*	(Ma)	(Ma)	(Ma)
385	692	2.20	12.9	19.4	0.04	21.0	0.00	8.1	0.39	22.0	1.8	36.3	7.5	1130	388.9	22	1.8
258	838	2.91	18.5	34.6	0.03	35.1	0.00	5.7	0.16	22.8	1.3	26.4	9.1	371	801.0	23	1.3
197	6226	0.81	22.5	19.5	0.07	19.8	0.01	3.7	0.19	76.9	2.8	72.2	13.8	-81	479.9	77	2.8
130	4937	1.03	19.4	17.4	0.09	18.7	0.01	6.6	0.35	77.9	5.1	84.2	15.1	267	403.0	78	5.1
242	13379	1.40	24.0	10.8	0.07	12.1	0.01	5.3	0.44	78.1	4.1	68.7	8.0	-245	274.5	78	4.1
258	12123	1.08	22.7	14.2	0.08	14.5	0.01	2.8	0.19	79.2	2.2	73.6	10.3	-106	350.4	79	2.2
734	19899	0.97	21.0	3.9	0.09	4.4	0.01	2.0	0.44	84.0	1.6	84.0	3.5	82	93.5	84	1.6
113	5257	1.17	25.4	60.1	0.07	60.4	0.01	6.0	0.10	85.0	5.0	70.7	41.2	-391	1706.7	85	5.0
486	22345	1.75	21.2	10.3	0.09	10.5	0.01	2.2	0.21	86.7	1.9	85.6	8.7	54	246.6	87	1.9
225	30234	2.76	22.7	21.0	0.08	21.2	0.01	2.8	0.13	87.7	2.4	81.4	16.6	-102	522.1	88	2.4
275	8851	1.53	20.9	16.6	0.09	17.3	0.01	4.7	0.27	87.9	4.1	87.8	14.6	87	397.0	88	4.1
233	8164	1.21	19.6	12.4	0.10	13.3	0.01	4.7	0.36	88.1	4.2	93.8	11.9	241	287.0	88	4.2
166	10801	1.70	24.5	27.4	0.08	27.7	0.01	4.0	0.14	88.4	3.5	75.9	20.3	-300	712.2	88	3.5
190	15869	3.17	22.0	20.9	0.09	21.5	0.01	5.0	0.23	88.5	4.4	84.3	17.4	-34	512.0	89	4.4
232	6933	0.84	21.5	23.2	0.09	23.3	0.01	2.1	0.09	88.6	1.8	86.4	19.3	27	562.7	89	1.8
116	5100	1.54	20.0	20.3	0.10	21.1	0.01	5.4	0.26	89.7	4.8	93.7	18.8	197	476.9	90	4.8
106	3273	0.86	24.7	58.2	0.08	58.3	0.01	3.7	0.06	89.9	3.3	76.6	43.1	-319	1621.0	90	3.3
222	10697	2.18	21.0	9.0	0.09	9.9	0.01	4.1	0.41	90.6	3.7	90.4	8.5	86	213.3	91	3.7
611	30559	5.05	21.6	6.7	0.09	6.8	0.01	0.9	0.13	90.8	0.8	88.0	5.7	11	162.1	91	0.8
676	32884	1.89	21.3	5.6	0.09	5.9	0.01	1.8	0.31	91.2	1.6	89.4	5.1	44	134.9	91	1.6
513	26406	9.36	21.5	7.6	0.09	7.7	0.01	1.2	0.15	91.8	1.1	89.3	6.6	21	183.8	92	1.1
160	8943	3.06	24.7	28.4	0.08	28.8	0.01	5.0	0.17	93.2	4.6	79.3	22.0	-323	740.4	93	4.6
515	24721	1.95	21.9	8.6	0.09	8.7	0.01	1.6	0.18	94.6	1.5	90.2	7.5	-25	207.7	95	1.5
281	8808	2.84	22.9	17.1	0.09	17.1	0.02	1.6	0.09	96.6	1.5	88.3	14.5	-132	424.4	97	1.5
281	1551	1.66	18.0	10.3	0.12	10.6	0.02	2.6	0.24	99.1	2.5	113.9	11.4	436	229.0	99	2.5
303	27260	2.35	19.8	17.4	0.11	17.6	0.02	2.8	0.16	100.5	2.8	105.4	17.6	217	405.2	100	2.8

125	6393	0.86	21.4	31.3	0.11	31.8	0.02	6.0	0.19	105.0	6.2	102.3	31.0	40	764.7	105	6.2
111	8076	2.45	24.6	20.4	0.10	20.6	0.02	3.0	0.15	114.2	3.4	97.0	19.1	-308	527.3	114	3.4
295	14515	2.03	20.7	5.0	0.13	6.7	0.02	4.5	0.66	129.1	5.7	128.2	8.1	110	118.5	129	5.7
68	4763	0.98	23.6	18.4	0.13	18.9	0.02	4.2	0.22	145.4	6.0	126.8	22.5	-209	464.6	145	6.0
156	13663	0.97	18.8	13.6	0.17	13.8	0.02	2.2	0.16	149.0	3.2	160.5	20.5	334	310.2	149	3.2
1293	148814	5.61	20.3	1.1	0.16	1.4	0.02	0.9	0.64	150.0	1.3	150.8	1.9	163	24.7	150	1.3
187	16390	1.36	21.1	6.6	0.16	6.9	0.02	2.1	0.30	151.5	3.1	146.3	9.4	64	156.2	151	3.1
124	11224	0.90	19.4	14.0	0.17	14.3	0.02	2.8	0.20	151.5	4.3	158.9	21.1	270	323.5	152	4.3
118	6075	1.04	26.3	25.5	0.13	25.7	0.02	3.2	0.13	153.9	4.9	121.0	29.4	-487	687.2	154	4.9
222	14643	0.84	21.2	7.5	0.16	7.6	0.02	1.6	0.21	158.0	2.5	152.2	10.8	62	178.3	158	2.5
248	29934	0.88	20.4	5.7	0.17	6.0	0.03	1.7	0.29	163.8	2.8	163.0	9.0	151	133.7	164	2.8
443	96659	0.92	19.7	5.0	0.18	5.1	0.03	1.1	0.22	165.4	1.9	169.8	8.0	232	115.0	165	1.9
290	31240	0.77	20.3	5.2	0.18	5.3	0.03	1.4	0.26	167.0	2.2	166.6	8.2	161	121.0	167	2.2
231	27273	2.02	19.9	7.9	0.24	10.2	0.03	6.4	0.63	220.0	13.8	219.1	20.0	209	183.6	220	13.8
174	26081	1.14	20.9	3.2	0.25	3.8	0.04	2.1	0.56	238.8	5.0	225.6	7.7	91	74.7	239	5.0
310	59231	1.60	19.2	3.5	0.29	3.6	0.04	0.8	0.22	253.1	1.9	256.5	8.1	288	79.3	253	1.9
203	35423	1.76	18.8	4.9	0.30	6.0	0.04	3.5	0.58	254.9	8.7	262.7	13.8	333	110.2	255	8.7
163	29001	1.88	20.0	6.2	0.29	7.1	0.04	3.5	0.49	263.5	9.0	256.7	16.0	196	143.2	263	9.0
273	40035	5.02	19.8	3.5	0.31	3.6	0.04	0.9	0.26	278.2	2.5	271.5	8.6	213	80.4	278	2.5
472	533789	6.62	9.6	0.3	3.70	2.1	0.26	2.1	0.99	1478.3	28.2	1572.0	17.2	1700	4.8	1700	4.8
342	758411	1.35	9.4	0.3	4.51	1.9	0.31	1.9	0.98	1728.0	28.1	1733.3	15.7	1740	6.3	1740	6.3
201	152288	2.61	9.3	0.7	4.52	2.0	0.31	1.9	0.94	1716.8	28.2	1734.3	16.6	1756	12.4	1756	12.4
201	139724	1.94	5.9	0.3	10.24	7.6	0.44	7.6	1.00	2356.6	150.6	2457.1	70.7	2541	4.4	2541	4.4

DMS-12-SM2

U (ppm)	206Pb 204Pb	U/Th	206Pb* 207Pb*	± (%)	207Pb* 235U*	± (%)	206Pb* 238U	± (%)	error corr.	206Pb* 238U*	± (Ma)	207Pb* 235U	± (Ma)	206Pb* 207Pb*	± (Ma)	Best age (Ma)	± (Ma)
114	4894	0.53	16.1	81.4	0.10	81.5	0.01	5.0	0.06	77.1	3.8	99.8	77.6	683	2200.8	77	3.8
106	7624	0.80	19.5	13.9	0.17	14.2	0.02	2.9	0.20	150.0	4.3	156.6	20.6	258	320.5	150	4.3
292	21823	0.92	21.7	5.1	0.15	6.1	0.02	3.4	0.56	148.2	5.0	139.8	8.0	0	122.5	148	5.0
83	28087	0.38	21.6	22.0	0.16	23.0	0.03	6.8	0.29	163.4	10.9	154.0	32.8	11	533.6	163	10.9
168	22758	1.10	21.2	18.0	0.15	18.5	0.02	4.4	0.24	150.8	6.6	145.3	25.1	57	432.2	151	6.6
596	40000	5.69	9.4	0.6	4.62	1.3	0.31	1.2	0.90	1763.2	18.6	1752.5	11.1	1740	10.5	1740	10.5
111	14319	0.64	24.1	31.5	0.13	31.9	0.02	4.9	0.15	148.6	7.2	127.1	38.1	-258	816.4	149	7.2

117	127665	1.45	9.4	0.7	4.51	1.1	0.31	0.8	0.75	1730.5	12.4	1732.8	9.1	1735	13.3	1735	13.3
380	58762	1.54	19.1	2.7	0.29	3.9	0.04	2.9	0.73	255.8	7.2	259.7	9.0	295	61.7	256	7.2
94	8539	0.69	19.2	25.7	0.18	25.9	0.03	2.8	0.11	163.8	4.5	171.9	40.9	286	596.8	164	4.5
478	1921	0.37	16.6	29.6	0.10	30.2	0.01	6.1	0.20	76.2	4.6	95.4	27.5	608	653.3	76	4.6
170	7554	2.05	20.3	12.5	0.08	14.8	0.01	7.9	0.53	78.2	6.1	80.8	11.5	159	293.5	78	6.1
127	6588	0.82	19.3	18.8	0.09	19.9	0.01	6.7	0.33	79.6	5.3	86.4	16.5	280	433.4	80	5.3
396	22048	1.43	20.8	9.6	0.08	9.9	0.01	2.6	0.26	81.9	2.1	82.5	7.9	101	227.5	82	2.1
336	4481	1.17	20.0	7.9	0.09	9.2	0.01	4.7	0.51	82.0	3.8	85.8	7.5	192	183.5	82	3.8
733	45706	1.66	20.8	2.3	0.16	3.7	0.02	2.9	0.78	154.8	4.5	151.4	5.2	99	54.5	155	4.5
272	8438	1.83	19.5	4.3	0.26	4.5	0.04	1.4	0.31	233.0	3.2	234.7	9.5	252	99.2	233	3.2
113	18183	0.84	22.2	19.9	0.15	21.3	0.02	7.8	0.36	149.6	11.5	138.4	27.6	-49	487.6	150	11.5
94	5018	1.16	27.0	31.1	0.12	31.3	0.02	3.9	0.12	150.7	5.7	115.9	34.3	-551	853.3	151	5.7
409	95099	0.86	20.0	5.0	0.17	5.7	0.02	2.6	0.46	152.7	3.9	155.2	8.1	195	116.9	153	3.9
460	574929	40.47	10.3	1.6	3.43	2.7	0.26	2.2	0.80	1467.4	28.7	1510.7	21.4	1572	30.2	1572	30.2
94	8692	0.57	21.3	13.5	0.17	13.8	0.03	2.6	0.19	163.6	4.3	156.5	20.0	50	323.8	164	4.3
110	9955	1.44	22.4	23.9	0.14	24.2	0.02	3.4	0.14	144.5	4.8	132.7	30.1	-73	592.4	144	4.8
242	7077	0.76	22.8	15.3	0.08	15.7	0.01	3.1	0.20	84.6	2.6	77.9	11.7	-123	380.4	85	2.6
54	5592	1.31	22.5	27.9	0.15	28.9	0.02	7.5	0.26	151.8	11.3	138.5	37.4	-84	694.3	152	11.3
36	2295	0.80	18.7	44.7	0.17	45.7	0.02	9.9	0.22	150.9	14.7	163.6	69.2	351	1059.1	151	14.7
188	5924	0.98	19.3	8.1	0.17	8.6	0.02	2.7	0.32	152.8	4.2	160.8	12.8	281	186.6	153	4.2
817	116775	4.44	9.5	1.2	4.49	3.9	0.31	3.7	0.95	1740.8	57.0	1729.3	32.6	1715	22.1	1715	22.1
100	8936	1.11	22.3	25.1	0.15	25.4	0.02	3.7	0.15	149.9	5.5	137.9	32.8	-65	621.5	150	5.5
541	315269	1.24	11.1	0.3	2.85	1.7	0.23	1.7	0.98	1334.3	20.6	1367.8	13.1	1421	5.9	1421	5.9
252	169406	0.99	9.8	0.4	4.06	1.9	0.29	1.8	0.97	1631.2	26.5	1647.0	15.4	1667	8.0	1667	8.0
54	5013	0.76	28.1	48.6	0.11	48.7	0.02	4.0	0.08	147.7	5.9	109.5	50.6	-658	1406.9	148	5.9
62	8662	0.61	25.4	45.2	0.14	45.5	0.03	5.7	0.12	159.3	8.9	129.1	55.2	-397	1231.3	159	8.9
113	204944	4.06	9.5	0.9	3.82	5.0	0.26	4.9	0.98	1509.3	65.6	1596.8	40.0	1714	17.4	1714	17.4
197	9192	0.59	20.2	12.8	0.09	13.1	0.01	2.7	0.21	82.3	2.2	85.5	10.7	174	299.1	82	2.2
516	2348876	7.74	9.5	0.3	4.44	1.2	0.31	1.2	0.97	1718.0	17.9	1719.7	10.1	1722	5.6	1722	5.6
300	8556	1.55	21.5	15.0	0.08	15.3	0.01	2.7	0.18	78.2	2.1	76.6	11.3	28	362.1	78	2.1
191	29849	0.67	9.7	0.7	4.18	1.3	0.29	1.1	0.86	1658.1	16.4	1669.2	10.7	1683	12.3	1683	12.3
253	246236	1.78	9.7	0.2	4.13	1.0	0.29	1.0	0.98	1643.3	14.1	1661.1	8.1	1684	4.0	1684	4.0
575	4348	1.05	18.2	10.4	0.28	12.4	0.04	6.7	0.55	231.2	15.3	248.6	27.3	416	232.0	231	15.3
328	20422	2.80	9.3	0.7	4.42	6.1	0.30	6.1	0.99	1676.9	89.4	1716.7	50.5	1766	12.9	1766	12.9

368	19674	2.06	21.4	8.1	0.09	10.3	0.01	6.4	0.62	85.6	5.4	83.9	8.3	37	194.9	86	5.4
187	26874	0.34	20.3	6.0	0.18	6.2	0.03	1.5	0.24	164.1	2.4	164.2	9.4	165	140.6	164	2.4
525	40513	0.99	19.9	4.8	0.18	4.9	0.03	1.2	0.25	166.4	2.0	169.1	7.7	207	111.0	166	2.0
336	21195	0.99	20.6	11.5	0.09	11.8	0.01	2.7	0.23	89.9	2.4	91.2	10.3	124	271.1	90	2.4
91	8681	0.64	25.2	33.4	0.13	33.7	0.02	4.1	0.12	150.7	6.1	123.4	39.1	-374	887.5	151	6.1
319	28844	1.93	19.4	3.9	0.26	4.4	0.04	2.0	0.46	235.1	4.6	237.5	9.3	261	89.4	235	4.6
340	389203	1.82	9.6	0.4	4.31	1.6	0.30	1.5	0.96	1695.4	22.2	1695.8	12.8	1696	8.1	1696	8.1
65	134928	1.24	9.6	0.7	4.19	2.6	0.29	2.5	0.96	1652.1	36.2	1672.5	21.2	1698	13.1	1698	13.1
135	16653	0.55	9.7	1.0	4.40	1.9	0.31	1.6	0.86	1731.7	24.6	1711.9	15.6	1688	17.7	1688	17.7
249	183472	3.41	9.4	0.3	4.70	2.8	0.32	2.7	0.99	1786.8	42.9	1768.1	23.2	1746	5.7	1746	5.7
390	31540	3.21	19.8	5.3	0.26	5.6	0.04	1.9	0.34	232.6	4.3	231.4	11.6	220	122.1	233	4.3
145	281495	1.56	9.8	0.5	4.15	2.7	0.29	2.7	0.98	1658.5	39.1	1663.5	22.2	1670	9.0	1670	9.0
212	369673	1.69	11.2	1.0	3.08	2.0	0.25	1.7	0.87	1434.9	21.9	1426.9	15.0	1415	18.7	1415	18.7
552	38650	14.89	19.2	1.9	0.26	2.5	0.04	1.6	0.65	228.9	3.6	234.2	5.2	287	43.6	229	3.6
1088	2752228	15.49	9.6	0.2	4.29	1.1	0.30	1.1	0.99	1691.3	16.0	1691.2	8.9	1691	3.0	1691	3.0
94	6931	0.65	23.0	31.5	0.15	31.8	0.02	4.4	0.14	156.1	6.9	139.3	41.4	-138	796.1	156	6.9
116	10105	1.28	24.4	29.1	0.13	29.3	0.02	3.0	0.10	151.7	4.5	128.0	35.2	-294	756.8	152	4.5
93	3312	0.58	17.8	20.9	0.20	21.6	0.03	5.4	0.25	168.1	9.0	188.9	37.2	458	467.5	168	9.0
163	176528	0.60	11.2	1.1	3.05	1.7	0.25	1.3	0.77	1426.6	16.6	1421.4	12.9	1413	20.5	1413	20.5
187	9333	6.89	19.1	8.0	0.22	8.7	0.03	3.2	0.37	193.1	6.2	201.4	15.8	300	183.4	193	6.2
253	31440	0.98	20.4	9.5	0.18	9.7	0.03	1.7	0.17	166.5	2.8	165.2	14.8	148	224.1	166	2.8
97	5536	0.94	23.6	20.1	0.14	20.8	0.02	5.2	0.25	151.3	7.8	131.7	25.7	-209	509.4	151	7.8
307	24911	0.53	20.0	6.1	0.18	6.5	0.03	2.4	0.36	170.8	4.0	172.3	10.4	193	141.8	171	4.0
239	8491	0.68	19.6	14.3	0.08	15.5	0.01	5.9	0.38	76.7	4.5	82.3	12.2	246	331.1	77	4.5
317	8954	0.97	20.2	18.2	0.08	18.4	0.01	2.7	0.15	78.6	2.1	81.6	14.4	169	427.3	79	2.1
192	24748	0.86	23.6	13.6	0.14	13.7	0.02	2.1	0.15	154.1	3.2	134.1	17.2	-207	341.7	154	3.2
328	74375	3.74	9.5	0.4	3.86	2.0	0.27	2.0	0.98	1525.9	27.0	1604.8	16.3	1710	7.0	1710	7.0
85	4724	1.22	17.9	32.2	0.18	32.6	0.02	5.2	0.16	147.5	7.6	166.8	50.2	451	733.2	147	7.6
140	12457	1.06	23.5	14.3	0.14	14.9	0.02	4.2	0.28	152.3	6.3	133.1	18.6	-196	360.2	152	6.3
98	18232	0.71	20.0	15.9	0.16	16.2	0.02	3.0	0.18	147.2	4.3	150.2	22.6	197	371.2	147	4.3

JFH-11-21C

U (ppm)	206Pb 204Pb	U/Th	206Pb* 207Pb*	± (%)	207Pb* 235U*	± (%)	206Pb* 238U	± (%)	error corr.	206Pb* 238U*	± (Ma)	207Pb* 235U	± (Ma)	206Pb* 207Pb*	± (Ma)	Best age (Ma)	± (Ma)

160	23211	1.98	10.0	0.8	3.86	2.0	0.28	1.8	0.92	1586.6	25.7	1604.7	16.0	1629	14.7	1629	14.7
562	34262	0.97	20.2	4.7	0.11	5.0	0.02	1.9	0.37	102.2	1.9	105.1	5.0	171	109.2	102	1.9
959	917545	10.28	9.7	0.1	4.21	0.8	0.30	0.8	0.99	1674.5	12.1	1675.2	6.8	1676	2.0	1676	2.0
1059	1632197	16.00	9.6	0.6	3.97	3.5	0.28	3.5	0.99	1569.6	48.8	1628.4	28.8	1705	10.4	1705	10.4
294	289188	2.95	9.7	0.4	3.94	0.8	0.28	0.6	0.85	1576.9	9.0	1621.6	6.1	1680	7.5	1680	7.5
154	8149	0.68	20.9	13.1	0.17	13.7	0.03	4.0	0.29	165.2	6.5	160.7	20.3	96	311.0	165	6.5
82	92235	0.77	11.2	1.1	2.97	1.6	0.24	1.1	0.69	1395.1	13.5	1399.0	11.9	1405	21.7	1405	21.7
778	966216	3.14	9.5	0.2	4.20	1.3	0.29	1.3	0.99	1642.3	19.0	1673.3	10.8	1712	2.9	1712	2.9
286	16371	0.79	18.4	9.4	0.10	9.6	0.01	1.9	0.19	83.1	1.5	94.2	8.6	384	211.9	83	1.5
829	216888	1.69	19.5	1.5	0.27	1.9	0.04	1.2	0.62	237.9	2.8	238.8	4.0	248	34.1	238	2.8
303	63468	1.33	19.4	3.1	0.26	4.0	0.04	2.5	0.63	231.5	5.7	235.0	8.3	270	70.7	231	5.7
497	208223	5.40	9.4	0.3	4.63	0.9	0.32	0.9	0.95	1768.0	13.6	1755.0	7.7	1740	5.0	1740	5.0
271	259612	0.74	9.6	0.3	4.30	1.2	0.30	1.1	0.97	1694.1	17.0	1693.5	9.7	1693	5.1	1693	5.1
301	419884	2.06	9.8	0.2	4.10	0.5	0.29	0.5	0.90	1648.6	6.8	1655.1	4.2	1663	4.2	1663	4.2
200	38579	0.71	21.1	5.8	0.16	5.9	0.02	1.1	0.18	152.3	1.6	147.7	8.1	74	137.5	152	1.6
41	53841	0.36	11.1	3.8	2.96	4.2	0.24	1.7	0.41	1381.1	21.3	1398.5	31.7	1425	72.8	1425	72.8
156	7829	0.86	23.0	13.5	0.07	14.2	0.01	4.1	0.29	80.0	3.3	73.2	10.0	-142	336.9	80	3.3
298	479353	2.06	9.7	0.3	4.21	1.1	0.30	1.0	0.96	1668.1	14.9	1676.3	8.7	1687	5.8	1687	5.8
39	3248	0.72	18.9	30.5	0.16	32.0	0.02	9.7	0.30	142.1	13.6	152.7	45.4	320	707.4	142	13.6
79	5625	0.71	22.4	48.2	0.07	49.3	0.01	10.3	0.21	73.8	7.6	69.6	33.2	-70	1244.4	74	7.6
351	145933	2.68	9.5	0.5	4.03	6.3	0.28	6.3	1.00	1573.4	87.7	1640.1	51.3	1727	9.4	1727	9.4
222	7608	0.76	21.7	12.3	0.08	13.0	0.01	4.3	0.33	80.5	3.4	77.9	9.7	0	296.2	80	3.4
58	19393	1.45	9.9	1.5	3.95	2.4	0.28	1.8	0.76	1603.5	25.4	1624.5	19.1	1652	28.5	1652	28.5
46	4077	3.10	18.4	39.0	0.17	39.4	0.02	5.7	0.14	145.4	8.1	160.3	58.5	386	907.6	145	8.1
977	713355	17.95	9.7	0.2	3.61	4.0	0.25	4.0	1.00	1455.5	52.1	1552.1	31.9	1686	4.6	1686	4.6
49	3343	0.72	22.9	59.4	0.14	59.7	0.02	6.5	0.11	151.1	9.7	135.3	75.8	-133	1602.5	151	9.7
90	5311	0.85	17.7	22.1	0.18	22.7	0.02	5.1	0.23	149.4	7.5	170.0	35.5	467	494.5	149	7.5
219	21915	0.87	20.9	10.6	0.16	10.7	0.02	1.8	0.17	150.0	2.7	146.6	14.7	91	251.4	150	2.7
1546	1806045	1.90	9.3	0.2	4.56	1.0	0.31	1.0	0.98	1731.5	14.7	1741.4	8.2	1753	3.1	1753	3.1
108	13548	0.72	21.0	16.9	0.17	17.0	0.03	1.7	0.10	161.0	2.7	156.2	24.6	83	403.1	161	2.7
18	28436	0.56	9.7	3.3	3.90	4.9	0.28	3.6	0.74	1567.5	50.2	1613.2	39.3	1673	60.4	1673	60.4
204	352434	2.32	9.7	0.5	4.16	0.9	0.29	0.7	0.81	1660.5	10.8	1666.3	7.4	1674	9.9	1674	9.9
242	63307	1.60	19.4	5.6	0.27	5.9	0.04	1.8	0.31	236.2	4.2	238.7	12.5	263	127.9	236	4.2
54	28073	0.94	12.4	2.0	2.25	3.4	0.20	2.7	0.81	1189.8	29.6	1196.9	23.7	1210	39.4	1210	39.4

79	104423	1.08	9.7	1.0	4.28	1.3	0.30	0.8	0.61	1698.6	11.9	1689.0	10.7	1677	19.0	1677	19.0
96	13468	1.55	18.6	6.3	0.25	7.9	0.03	4.7	0.59	212.8	9.8	225.2	15.9	357	142.7	213	9.8
142	442124	2.17	8.1	1.5	6.07	2.5	0.36	2.0	0.79	1967.5	34.0	1985.4	22.0	2004	27.3	2004	27.3
118	9872	1.10	21.2	14.8	0.16	15.1	0.02	2.7	0.18	152.2	4.1	146.6	20.6	56	355.6	152	4.1
83	94507	1.25	9.9	0.6	4.12	1.7	0.30	1.5	0.92	1666.7	22.6	1657.5	13.6	1646	11.8	1646	11.8
193	21449	0.71	19.4	7.2	0.17	7.4	0.02	1.8	0.24	150.6	2.7	157.5	10.8	262	165.4	151	2.7
296	23037	1.40	19.6	13.0	0.08	13.5	0.01	3.5	0.26	76.2	2.6	81.8	10.6	246	300.7	76	2.6
140	8728	0.62	22.4	8.4	0.14	11.2	0.02	7.4	0.66	149.8	10.9	137.1	14.4	-76	206.2	150	10.9
89	8682	0.62	23.6	14.2	0.14	14.5	0.02	2.6	0.18	150.3	3.9	131.3	17.8	-202	357.8	150	3.9
1026	1330920	58.86	9.5	0.1	4.39	0.9	0.30	0.9	0.99	1706.2	14.1	1710.2	7.8	1715	2.4	1715	2.4
112	124897	3.51	9.3	0.8	4.83	6.1	0.33	6.1	0.99	1824.1	96.3	1789.7	51.4	1750	14.0	1750	14.0
51	3467	1.59	9.6	4.4	4.14	4.6	0.29	1.3	0.29	1628.2	18.9	1662.8	37.4	1707	80.6	1707	80.6
336	42298	1.64	19.4	2.8	0.26	2.9	0.04	0.9	0.30	235.5	2.0	238.4	6.2	266	64.3	236	2.0
151	8227	0.89	22.8	19.2	0.08	19.7	0.01	4.5	0.23	82.1	3.6	75.9	14.4	-116	475.7	82	3.6
321	127912	1.18	12.1	2.7	0.73	7.0	0.06	6.4	0.92	396.9	24.8	554.0	29.9	1266	53.4	397	24.8
266	20718	0.80	19.5	4.6	0.27	5.9	0.04	3.7	0.62	245.5	8.8	246.0	12.8	251	105.9	245	8.8
1087	1564466	2.14	9.3	0.1	4.86	1.8	0.33	1.8	1.00	1825.6	28.1	1794.5	14.9	1758	1.7	1758	1.7
56	4505	1.09	23.2	57.5	0.15	57.7	0.02	5.3	0.09	156.4	8.1	138.4	74.8	-161	1549.8	156	8.1
34	5432	0.79	17.7	45.8	0.19	46.7	0.02	9.1	0.19	151.3	13.5	172.7	74.2	476	1065.6	151	13.5
207	246474	2.02	9.5	0.5	4.46	1.2	0.31	1.0	0.91	1731.2	15.9	1723.6	9.5	1714	8.7	1714	8.7
36	2069	1.01	17.7	65.9	0.10	67.1	0.01	12.5	0.19	81.6	10.1	96.2	61.7	477	1648.2	82	10.1
90	190966	1.29	9.7	0.5	4.33	0.8	0.30	0.6	0.71	1708.9	8.4	1698.8	6.5	1686	10.1	1686	10.1
51	5199	1.33	21.8	16.0	0.22	16.5	0.03	4.1	0.25	219.2	8.7	200.7	30.1	-11	388.7	219	8.7
427	73714	1.81	19.6	2.4	0.26	2.5	0.04	0.8	0.33	236.9	1.9	237.7	5.3	246	54.6	237	1.9
76	70310	1.65	9.7	0.8	4.29	1.1	0.30	0.8	0.73	1699.2	12.5	1691.6	9.4	1682	14.4	1682	14.4
311	488940	2.03	9.7	0.3	4.25	0.8	0.30	0.7	0.93	1681.9	10.5	1682.8	6.3	1684	5.4	1684	5.4
170	5447	1.12	21.4	14.9	0.08	15.3	0.01	3.2	0.21	75.3	2.4	74.0	10.9	32	359.1	75	2.4
142	29066	2.53	9.3	1.0	4.64	1.6	0.31	1.3	0.78	1761.3	19.6	1756.3	13.6	1750	18.7	1750	18.7
65	11000	0.50	17.6	16.9	0.19	18.1	0.02	6.4	0.36	153.1	9.7	175.2	29.1	485	375.0	153	9.7
235	261095	1.85	9.7	0.5	4.32	0.9	0.30	0.8	0.84	1708.7	11.6	1696.9	7.6	1682	9.2	1682	9.2
349	56915	2.34	19.8	3.7	0.26	3.9	0.04	1.1	0.29	233.4	2.6	232.0	8.0	218	85.9	233	2.6
526	405483	17.18	9.7	0.2	4.31	0.9	0.30	0.9	0.98	1701.2	12.9	1695.5	7.2	1688	3.1	1688	3.1
41	4596	0.62	31.5	46.1	0.10	46.7	0.02	7.4	0.16	150.4	11.1	99.7	44.4	-992	1427.5	150	11.1
1201	87266	2.22	9.7	0.1	4.31	0.7	0.30	0.7	0.99	1704.9	10.7	1695.5	5.9	1684	2.0	1684	2.0

889	24993	0.64	21.3	6.1	0.08	6.5	0.01	2.5	0.38	77.1	1.9	76.1	4.8	45	145.0	77	1.9
595	937062	2.60	9.4	0.2	4.52	0.9	0.31	0.9	0.98	1730.5	13.2	1735.1	7.3	1741	2.9	1741	2.9
1029	1575238	14.74	9.4	0.1	4.54	1.6	0.31	1.6	1.00	1746.6	23.9	1738.4	13.0	1729	1.8	1729	1.8
214	10596	1.49	21.9	18.1	0.08	18.7	0.01	4.4	0.23	81.0	3.5	77.7	14.0	-24	442.5	81	3.5
1606	1518555	17.16	9.8	0.7	4.13	1.1	0.29	0.9	0.81	1651.8	13.2	1660.3	9.2	1671	12.1	1671	12.1
364	81262	1.24	19.4	3.8	0.27	3.9	0.04	1.0	0.25	236.7	2.3	239.0	8.4	261	87.7	237	2.3

JFH-11-23C

U (ppm)	206Pb 204Pb	U/Th	206Pb* 207Pb*	± (%)	207Pb* 235U*	± (%)	206Pb* 238U	± (%)	error corr.	206Pb* 238U*	± (Ma)	207Pb* 235U	± (Ma)	206Pb* 207Pb*	± (Ma)	Best age (Ma)	± (Ma)
253	12984	5.42	22.0	17.9	0.08	18.2	0.01	3.0	0.17	77.2	2.3	73.7	12.9	-36	438.1	77	2.3
323	11156	0.98	21.7	4.3	0.08	5.4	0.01	3.2	0.59	80.6	2.6	78.2	4.1	5	104.7	81	2.6
363	20784	1.04	21.5	8.7	0.08	8.9	0.01	1.9	0.22	82.4	1.6	80.6	6.9	28	209.7	82	1.6
279	18952	1.26	22.1	8.8	0.08	9.1	0.01	2.4	0.27	83.1	2.0	78.9	6.9	-47	213.5	83	2.0
153	7557	1.00	19.8	33.3	0.09	33.7	0.01	5.5	0.16	83.9	4.6	88.9	28.7	224	788.8	84	4.6
299	16737	1.41	23.3	18.1	0.08	18.4	0.01	3.4	0.18	84.0	2.8	75.8	13.4	-177	453.6	84	2.8
495	29309	1.21	19.8	10.3	0.09	10.4	0.01	1.7	0.16	84.6	1.4	89.2	8.9	214	238.5	85	1.4
295	7512	1.35	20.4	12.4	0.09	12.6	0.01	2.2	0.18	84.7	1.9	86.9	10.5	148	290.5	85	1.9
291	12166	0.48	25.1	10.1	0.07	10.2	0.01	1.8	0.18	85.3	1.6	71.6	7.1	-365	261.1	85	1.6
127	5323	1.69	24.0	38.1	0.08	38.6	0.01	6.1	0.16	86.0	5.2	75.6	28.1	-244	994.2	86	5.2
137	6162	1.29	21.8	36.6	0.09	37.2	0.01	6.5	0.17	86.2	5.6	82.9	29.6	-9	911.3	86	5.6
326	10307	1.06	22.2	13.8	0.08	14.0	0.01	2.3	0.16	86.2	1.9	81.4	11.0	-58	338.4	86	1.9
334	28321	8.52	20.4	11.0	0.10	11.3	0.01	2.6	0.23	91.9	2.4	94.0	10.2	149	258.5	92	2.4
110	3838	1.02	21.8	14.5	0.09	15.4	0.01	5.2	0.34	93.9	4.9	90.0	13.3	-14	352.9	94	4.9
129	15936	1.05	20.0	14.8	0.16	15.3	0.02	3.7	0.24	146.2	5.4	148.9	21.1	193	345.6	146	5.4
73	11946	0.60	18.8	22.7	0.17	23.1	0.02	4.3	0.19	147.7	6.3	159.3	34.1	335	521.5	148	6.3
72	4730	1.15	26.6	43.1	0.12	43.3	0.02	4.3	0.10	148.7	6.3	116.0	47.5	-512	1197.6	149	6.3
47	5837	0.58	20.7	40.9	0.16	41.5	0.02	7.2	0.17	148.7	10.6	146.7	56.8	115	1001.6	149	10.6
133	9769	0.83	22.1	22.0	0.15	22.1	0.02	2.3	0.10	148.9	3.4	138.5	28.6	-37	538.9	149	3.4
123	7621	1.19	24.6	26.1	0.13	26.2	0.02	2.7	0.10	149.1	3.9	124.9	30.8	-314	678.5	149	3.9
167	16884	0.94	21.8	11.2	0.15	11.6	0.02	3.0	0.26	149.2	4.4	140.5	15.2	-4	270.1	149	4.4
93	8162	0.85	20.1	23.6	0.16	24.2	0.02	5.4	0.22	149.4	8.0	151.3	34.1	182	556.9	149	8.0
229	23991	4.44	20.3	6.9	0.16	7.5	0.02	2.9	0.39	149.6	4.3	149.9	10.4	155	161.7	150	4.3
80	6079	0.55	17.7	18.4	0.18	18.7	0.02	3.6	0.19	149.7	5.4	170.5	29.4	470	409.7	150	5.4

197	25975	1.07	20.6	8.2	0.16	8.8	0.02	3.1	0.35	150.8	4.6	149.2	12.2	124	194.3	151	4.6
58	11449	0.70	18.8	29.1	0.17	29.9	0.02	6.5	0.22	151.3	9.8	163.1	45.0	338	672.9	151	9.8
130	2448	0.63	19.6	23.9	0.17	24.1	0.02	3.5	0.14	151.6	5.2	157.5	35.2	247	556.2	152	5.2
77	8658	0.96	19.8	16.5	0.17	16.9	0.02	3.9	0.23	154.0	6.0	158.1	24.8	220	383.3	154	6.0
182	15531	0.78	19.5	14.0	0.18	14.3	0.03	2.9	0.20	162.0	4.6	168.0	22.1	253	323.1	162	4.6
152	722	0.70	15.9	30.8	0.23	31.6	0.03	7.1	0.23	170.6	12.0	212.7	60.7	710	669.1	171	12.0
67	7576	1.09	17.4	10.5	0.30	11.0	0.04	3.4	0.31	237.3	7.9	264.7	25.7	515	230.8	237	7.9
130	26325	3.45	20.8	10.7	0.25	10.9	0.04	2.4	0.22	240.3	5.7	227.8	22.3	101	253.1	240	5.7
76	16591	1.34	20.5	11.9	0.26	12.5	0.04	3.8	0.30	244.1	9.0	234.8	26.2	143	280.5	244	9.0
89	10218	0.96	21.3	15.0	0.25	15.3	0.04	2.8	0.18	244.5	6.6	227.0	31.1	49	360.4	244	6.6
47	11299	1.29	20.4	33.0	0.26	33.4	0.04	4.6	0.14	244.6	11.1	236.2	70.4	153	793.1	245	11.1
58	27419	1.08	19.5	21.1	0.27	21.6	0.04	4.3	0.20	244.8	10.4	245.9	47.2	256	491.0	245	10.4
41	8161	1.26	19.2	22.8	0.28	23.5	0.04	6.0	0.25	245.1	14.4	249.8	52.2	294	525.8	245	14.4
53	11783	0.99	26.1	41.7	0.21	42.0	0.04	5.4	0.13	246.4	13.1	189.7	72.9	-468	1144.6	246	13.1
95	12224	1.00	21.0	19.3	0.26	19.4	0.04	2.1	0.11	247.2	5.0	232.4	40.4	85	461.9	247	5.0
49	5782	1.08	18.5	19.9	0.29	20.3	0.04	4.0	0.20	247.4	9.8	259.4	46.5	369	451.9	247	9.8
486	68037	1.15	19.3	3.9	0.28	4.8	0.04	2.7	0.56	247.8	6.5	250.6	10.6	277	90.2	248	6.5
219	36790	4.80	19.4	7.1	0.28	7.4	0.04	2.1	0.29	248.5	5.2	250.2	16.5	267	163.8	248	5.2
68	21393	1.77	19.3	9.5	0.28	9.9	0.04	2.9	0.29	249.9	7.0	252.3	22.1	274	217.3	250	7.0
404	45119	1.95	19.7	6.1	0.28	6.3	0.04	1.8	0.28	250.4	4.3	248.6	13.9	231	140.4	250	4.3
140	26001	1.38	20.2	7.7	0.27	8.1	0.04	2.7	0.33	250.9	6.5	243.1	17.6	168	179.6	251	6.5
65	10380	1.77	24.3	28.3	0.23	28.6	0.04	3.8	0.13	251.9	9.4	207.1	53.5	-277	732.4	252	9.4
265	37347	6.58	19.3	3.9	0.29	4.2	0.04	1.5	0.36	253.2	3.7	255.8	9.4	280	88.9	253	3.7
95	11836	1.39	21.9	13.0	0.25	13.3	0.04	2.9	0.22	253.6	7.3	228.4	27.2	-23	315.2	254	7.3
326	95236	1.33	19.7	4.1	0.29	4.3	0.04	1.3	0.30	257.1	3.2	254.8	9.6	234	94.4	257	3.2
151	71207	2.22	20.1	9.4	0.28	9.5	0.04	1.4	0.15	258.0	3.5	251.2	21.3	188	220.3	258	3.5
48	7802	1.59	19.2	27.2	0.30	27.6	0.04	4.7	0.17	265.9	12.1	267.7	65.0	284	632.1	266	12.1
414	62635	2.24	19.4	2.9	0.30	3.5	0.04	2.0	0.57	267.6	5.3	267.3	8.3	265	66.2	268	5.3
81	10927	1.73	20.2	12.4	0.29	12.8	0.04	3.1	0.24	268.5	8.0	258.5	29.2	169	290.5	269	8.0
103	10754	1.52	19.1	9.9	0.31	10.7	0.04	4.1	0.38	271.6	10.9	274.5	25.8	299	226.3	272	10.9
718	81400	1.37	19.2	1.6	0.32	2.1	0.04	1.5	0.68	279.3	4.0	280.0	5.3	286	36.0	279	4.0
257	55354	2.71	9.7	0.4	3.49	1.8	0.25	1.8	0.97	1419.1	22.7	1525.0	14.5	1675	7.8	1675	7.8

KTC-12-Tps1

U (ppm)	206Pb 204Pb	U/Th	206Pb* 207Pb*	± (%)	207Pb* 235U*	± (%)	206Pb* 238U	± (%)	error corr.	206Pb* 238U*	± (Ma)	207Pb* 235U	± (Ma)	206Pb* 207Pb*	± (Ma)	Best age (Ma)	± (Ma)
122	5514	8.71	20.2	12.1	0.08	15.2	0.01	9.2	0.60	72.0	6.6	74.9	11.0	168	284.1	72	6.6
297	21415	3.58	22.1	14.0	0.07	14.5	0.01	4.0	0.27	72.7	2.9	69.4	9.7	-43	341.0	73	2.9
203	7114	1.24	20.0	25.4	0.08	25.9	0.01	4.8	0.18	72.9	3.5	76.6	19.1	192	599.9	73	3.5
1123	2632	1.10	20.3	7.2	0.08	8.0	0.01	3.4	0.42	74.4	2.5	77.1	5.9	162	169.0	74	2.5
364	40891	3.27	21.4	13.9	0.08	14.0	0.01	1.9	0.14	74.7	1.4	73.5	9.9	35	333.1	75	1.4
391	17054	0.79	21.7	8.7	0.07	8.8	0.01	1.5	0.17	75.1	1.1	72.9	6.2	2	209.2	75	1.1
427	21707	4.35	21.8	8.8	0.07	9.3	0.01	2.8	0.30	75.7	2.1	73.1	6.5	-9	213.8	76	2.1
1348	72992	8.55	21.1	2.7	0.08	2.8	0.01	0.6	0.23	78.0	0.5	77.9	2.1	73	64.3	78	0.5
163	6714	1.86	25.3	19.5	0.07	19.8	0.01	3.3	0.16	78.6	2.5	65.7	12.6	-383	510.5	79	2.5
681	42494	4.84	20.6	4.1	0.08	4.3	0.01	1.4	0.32	79.2	1.1	80.6	3.3	125	96.1	79	1.1
177	7682	1.78	19.3	19.6	0.09	20.6	0.01	6.3	0.30	80.9	5.0	87.6	17.3	274	452.8	81	5.0
217	17170	2.20	20.8	13.0	0.08	13.2	0.01	2.1	0.16	81.8	1.7	82.5	10.5	103	309.0	82	1.7
390	19183	7.37	20.3	6.2	0.09	6.4	0.01	1.6	0.25	82.0	1.3	84.6	5.2	159	146.1	82	1.3
445	17522	1.41	21.9	7.2	0.08	7.4	0.01	1.9	0.25	82.2	1.5	78.9	5.6	-21	173.3	82	1.5
749	42383	2.83	21.4	5.8	0.08	5.9	0.01	1.1	0.19	83.2	0.9	81.6	4.6	35	138.2	83	0.9
146	13978	1.48	24.0	59.1	0.08	59.3	0.01	4.6	0.08	84.5	3.9	74.1	42.4	-249	1629.7	85	3.9
445	16741	3.19	21.0	10.0	0.09	10.2	0.01	1.8	0.18	84.7	1.5	84.7	8.3	86	238.7	85	1.5
498	25917	2.20	22.0	11.3	0.08	11.4	0.01	1.5	0.13	86.0	1.3	82.2	9.0	-27	274.8	86	1.3
85	3618	10.45	27.5	33.4	0.07	34.2	0.01	7.8	0.23	86.0	6.6	66.1	21.9	-605	928.7	86	6.6
584	24286	3.43	21.4	5.7	0.09	5.8	0.01	1.2	0.20	87.1	1.0	85.2	4.7	34	135.7	87	1.0
222	12314	0.94	21.1	16.1	0.09	16.6	0.01	3.8	0.23	87.6	3.3	86.8	13.8	66	386.6	88	3.3
181	9245	1.33	23.7	17.7	0.08	18.2	0.01	4.3	0.24	87.8	3.8	77.9	13.6	-217	446.7	88	3.8
158	6452	0.59	31.5	41.2	0.06	41.4	0.01	4.5	0.11	88.5	3.9	59.6	24.0	-987	1260.2	88	3.9
470	51917	6.17	21.1	3.9	0.09	4.4	0.01	2.0	0.46	89.0	1.8	88.2	3.7	66	93.4	89	1.8
787	73376	0.53	20.6	5.2	0.09	6.0	0.01	3.0	0.50	90.0	2.7	91.2	5.2	122	121.4	90	2.7
115	7383	2.32	28.8	31.1	0.07	31.6	0.01	5.7	0.18	90.4	5.1	66.4	20.3	-731	886.0	90	5.1
203	8799	2.08	18.9	9.9	0.10	10.0	0.01	1.4	0.14	91.0	1.3	100.2	9.5	326	224.9	91	1.3
88	5739	0.82	24.6	44.4	0.08	44.6	0.01	3.9	0.09	91.8	3.5	78.5	33.7	-310	1189.1	92	3.5
206	6974	0.95	20.1	13.0	0.10	13.5	0.01	3.7	0.27	92.8	3.4	96.2	12.4	181	304.5	93	3.4
167	10228	2.50	25.8	32.1	0.08	33.3	0.01	8.9	0.27	95.7	8.4	78.1	25.1	-431	861.6	96	8.4
157	8804	0.79	22.7	20.4	0.09	21.0	0.02	5.1	0.24	96.9	4.9	89.1	17.9	-113	506.5	97	4.9

170	19487	0.89	20.0	12.5	0.11	12.7	0.02	2.7	0.21	102.2	2.7	106.3	12.9	200	290.1	102	2.7
238	34491	0.63	20.6	13.8	0.11	14.0	0.02	2.2	0.16	104.7	2.3	105.6	14.0	125	326.5	105	2.3
205	24591	0.78	18.8	10.7	0.14	11.4	0.02	3.7	0.33	120.1	4.4	131.3	14.0	338	243.6	120	4.4
50	4818	1.96	16.3	39.4	0.20	40.1	0.02	7.4	0.19	148.8	10.9	183.1	67.2	652	878.1	149	10.9
51	5831	0.59	30.0	59.7	0.11	60.1	0.02	6.8	0.11	149.1	10.0	103.8	59.4	-844	1857.1	149	10.0
30	1537	0.65	23.8	39.6	0.14	40.0	0.02	5.4	0.13	149.3	8.0	129.1	48.5	-229	1033.3	149	8.0
37	3308	0.93	19.7	39.2	0.17	39.7	0.02	6.0	0.15	151.7	9.0	156.7	57.7	232	938.5	152	9.0
116	6243	1.88	23.6	25.1	0.14	25.4	0.02	4.1	0.16	153.3	6.2	133.4	31.8	-208	638.7	153	6.2
64	11222	0.82	23.4	15.0	0.15	17.5	0.03	9.1	0.52	165.8	14.9	144.9	23.7	-184	375.6	166	14.9
330	55647	5.30	12.2	2.5	0.42	3.2	0.04	2.0	0.63	236.8	4.6	357.5	9.6	1241	48.9	237	4.6
56	7660	1.00	18.7	10.6	0.28	11.7	0.04	5.0	0.43	237.6	11.7	248.1	25.7	349	239.3	238	11.7
59	12191	0.77	20.3	23.8	0.26	24.2	0.04	3.9	0.16	241.6	9.2	234.5	50.6	164	564.4	242	9.2
57	7217	0.83	19.8	29.0	0.27	29.3	0.04	4.5	0.15	242.2	10.6	239.7	62.7	215	684.0	242	10.6
48	11390	1.01	18.3	15.5	0.29	16.0	0.04	4.0	0.25	245.9	9.7	261.2	36.8	401	348.6	246	9.7
49	7456	1.04	20.5	19.2	0.26	19.8	0.04	4.8	0.24	246.3	11.7	235.9	41.7	133	455.4	246	11.7
51	12518	0.86	17.3	16.3	0.31	16.8	0.04	3.8	0.22	249.8	9.2	277.7	40.8	520	360.8	250	9.2
124	33320	1.25	19.5	11.6	0.28	11.8	0.04	2.0	0.17	250.6	4.9	250.6	26.2	251	268.2	251	4.9
139	93480	53.34	11.4	0.7	2.63	1.9	0.22	1.8	0.92	1267.6	20.5	1310.1	14.2	1380	14.4	1380	14.4
102	96720	0.62	11.2	1.2	2.95	2.5	0.24	2.2	0.88	1388.1	27.6	1395.8	19.1	1408	23.1	1408	23.1
72	146559	0.87	11.2	1.2	2.72	3.3	0.22	3.1	0.94	1284.8	36.2	1333.2	24.7	1412	22.4	1412	22.4
82	86815	0.69	11.2	1.1	3.07	1.6	0.25	1.1	0.69	1432.3	14.2	1425.0	12.2	1414	21.9	1414	21.9
119	170389	0.54	11.1	0.9	2.96	1.2	0.24	0.7	0.60	1375.2	8.8	1398.0	9.0	1433	18.1	1433	18.1
76	14817	1.56	10.9	1.9	2.60	2.8	0.21	2.1	0.76	1207.9	23.7	1299.8	20.8	1455	35.2	1455	35.2
131	74568	8.60	10.9	0.7	3.02	4.3	0.24	4.3	0.99	1382.8	53.3	1412.9	33.1	1459	13.9	1459	13.9
646	330237	6.02	10.7	0.7	3.02	1.4	0.23	1.3	0.88	1354.0	15.4	1413.8	10.9	1505	12.6	1505	12.6
63	44777	1.68	10.2	1.6	3.43	2.5	0.26	2.0	0.78	1464.4	25.9	1512.3	19.9	1580	29.7	1580	29.7
270	200558	3.89	10.2	0.7	3.49	3.3	0.26	3.2	0.98	1475.9	42.4	1526.0	25.9	1596	12.8	1596	12.8
721	344291	4.81	10.0	0.5	3.63	2.0	0.26	1.9	0.96	1501.6	26.1	1555.1	16.1	1629	9.9	1629	9.9
213	221528	2.47	9.9	0.6	3.91	4.9	0.28	4.9	0.99	1595.2	69.3	1615.5	39.9	1642	10.6	1642	10.6
231	283030	5.24	9.8	0.5	3.61	2.9	0.26	2.9	0.98	1477.4	38.4	1550.9	23.5	1652	9.5	1652	9.5
242	307788	1.64	9.8	0.6	3.68	1.2	0.26	1.1	0.90	1499.3	14.9	1566.0	10.0	1657	10.3	1657	10.3
117	123683	0.99	9.7	0.9	4.24	2.4	0.30	2.3	0.93	1686.3	33.5	1681.2	19.9	1675	16.0	1675	16.0
314	381743	0.68	9.7	0.2	4.14	0.8	0.29	0.8	0.96	1651.7	11.6	1663.1	6.8	1678	4.5	1678	4.5
152	200218	1.13	9.7	0.8	3.34	4.6	0.24	4.5	0.99	1361.2	55.6	1490.6	35.9	1680	14.4	1680	14.4

397	631687	6.51	9.7	0.4	4.20	2.1	0.30	2.1	0.99	1669.7	30.7	1674.7	17.4	1681	6.6	1681	6.6
150	163112	1.69	9.7	0.8	4.05	3.4	0.28	3.3	0.97	1610.3	46.4	1644.0	27.3	1687	14.8	1687	14.8
396	598536	2.90	9.7	0.2	4.34	1.1	0.30	1.1	0.97	1712.3	16.0	1701.8	9.0	1689	4.5	1689	4.5
844	877993	7.47	9.6	0.2	4.32	0.8	0.30	0.8	0.97	1702.0	11.3	1697.7	6.4	1692	3.4	1692	3.4
1320	3498705	14.76	9.6	0.1	4.39	0.5	0.30	0.5	0.99	1712.7	7.4	1711.1	4.1	1709	1.2	1709	1.2
461	1042752	1.49	9.5	0.3	3.72	1.5	0.26	1.5	0.99	1471.8	19.9	1575.9	12.3	1718	4.7	1718	4.7
382	682518	2.65	9.5	0.2	4.30	1.6	0.30	1.6	0.99	1670.6	22.9	1693.3	12.9	1722	3.4	1722	3.4
378	344006	1.37	9.4	0.3	4.41	1.5	0.30	1.5	0.98	1699.8	21.8	1713.7	12.3	1731	5.7	1731	5.7
1412	243056	2.85	9.4	0.4	4.14	1.6	0.28	1.6	0.97	1605.6	22.7	1661.4	13.4	1733	6.7	1733	6.7
96	95259	1.63	9.4	0.7	4.60	3.0	0.31	2.9	0.97	1757.3	44.6	1750.1	24.9	1742	12.7	1742	12.7
157	192393	2.06	9.4	0.6	3.84	3.8	0.26	3.7	0.99	1492.5	49.8	1601.1	30.4	1747	10.3	1747	10.3

REFERENCES CITED

Allmendinger, R. W., Cardozo, N., and Fisher, D., 2012, Structural geology algorithms: Vectors and tensors in structural geology: Cambridge University Press, Cambridge, 302 p.

Barth, A.P., and Wooden, J.L., 2006, Timing of magmatism following initial convergence at a passive margin, southwestern U.S. Cordillera, and ages of lower crustal magma sources: Geology, v. 114, p. 231-245.

Barth, A.P., Tosdal, R.M., Wooden, J.L., and Howard, K.A., 1997, Triassic Plutonism in southern California: southward younging of arc initiation along a truncated continental margin: Tectonics, v. 16, p. 290-304.

Barth, A.P., Wooden, J.L., Howard, K.A., and Richards, J.L., 2008, Late Jurassic plutonism in the southwest U.S. Cordillera: Geological Society of America Special Paper 438, p. 379-396.

Beckerman, G.M., Robinson, J.P., and Anderson, J.L., 1982, The Teutonia batholith: A large intrusive complex of Jurassic and Cretaceous age in the eastern Mojave Desert, California, *in* Frost, E.G., and Martin, D.L., eds., Mesozoic-Cenozoic tectonic evolution of the Colorado River region, California, Arizona, and Nevada: San Diego, Cordilleran Publishers, p. 205-221.

Burchfiel, B.C., and Davis, G.A., 1981, Mojave Desert and Environs: *In* Ernst, W.G., ed., The geotectonic development of California: Englewood Cliffs, NJ, Prentice Hall, p. 217-252.

Dibblee, T.W., Jr., 1967, Areal geology of the Western Mojave Desert California: Grological Society of America Professional Paper 522, 153 p.

Dibblee, T.W., Jr., 2003a, Geologic map of the Cajon Valley quadrangle, San Bernardino County, California: Dibblee Geological Foundation Map DF-104, scale 1:24,000.

Dibblee, T.W., Jr., 2003b, Geologic map of the Telegraph Peak and Phelan quadrangles, San Bernardino County, California: Dibblee Geological Foundation Map DF-107, scale 1:24,000.

Dibblee, T.W., Jr., 2005a, Geologic map of the Cuyama quadrangle, San Luis Obispo and Santa Barbara Counties, California: Dibblee Geological Foundation Map DF-176, scale 1:24,000.

Dibblee, T.W., Jr., 2005b, Geologic map of the New Cuyama quadrangle, San Luis Obispo and Santa Barbara Counties, California: Dibblee Geological Foundation Map DF-179, scale 1:24,000.

Dickinson, W.R., 1970, Interpreting detrital modes of greywacke and arkose: Journal of Sedimentary Petrology, v. 40, p. 695-707.

Gazzi, P., 1966, Le arenarie del flysch sopracretaceo dell'Appenmino modenese: correlazioni con il flysch di Monghidoro: Mineralogica e Petrografia Acta, v. 12, p. 69-97.

Gehrels, G.E., Valencia, V.A., and Ruiz, J., 2008, Enhanced precision, accuracy, efficiency, and spatial resolution of U-Pb ages by laser ablation-multicollector-inductively coupled plasma-mass spectrometry: Geochemistry, Geophysics, Geosystems, v. 9, p. 1-13.

Graham, S.A., Stanley, R.G., Bent, J.V., and Carter, J.B., 1989, Oligocene and Miocene paleogeography of central California and displacement along the San Andreas fault: Geological Society of America Bulletin, v. 101, p. 711-730.

Hendrix, E.D., and Ingersoll, R.V., 1987, Tectonics and alluvial sedimentation of the upper Oligocene/lower Miocene Vasquez Formation, Soledad basin, southern California: Geological Society of America Bulletin, v. 98, p. 647-663.

Hill, M.L., Carlson, S.A., and Dibblee, T.W., Jr., 1958, Stratigraphy of Cuyama Valley – Caliente Range area, California: American Association of Petroleum Geologists Bulletin, v. 42, p. 2973-3000.

Hoyt, J.F., 2012, Provenance and detrital-zircon studies of the Mint Canyon Formation and its correlation to the Caliente Formation, southern California [M.S. thesis]: University of California, Los Angeles, 78 p.

Ingersoll, R. V., 2008, Reconstructing southern California, in Spencer, J. E., and Titley, S. R., eds., Ores and orogenesis: Circum-Pacific tectonics, geologic evolution, and ore deposits: Arizona Geological Society Digest 22, p. 409-417.

Ingersoll, R. V., 2009, Diligencia basin (southern California) revisited: sedimentation in half graben bounded on the northeast by normal fault: Geological Society of America Abstracts with Programs, v. 41, n. 7, p. 569.

Ingersoll, R.V., and Cavazza, W., 1991, Reconstruction of Oligo-Miocene volcaniclastic dispersal patterns in north-central New Mexico using sandstone petrofacies, *in* Fisher, R.V., and Smith, G.A., eds., Sedimentation in volcanic settings: SEPM (Society for Sedimentary Geology) Special Publication 45, p. 227-236.

Ingersoll, R.V., and Eastmond, D.J., 2007, Composition of modern sand from the Sierra Nevada, California, U.S.A.: implications for actualistic petrofacies of continental-margin magmatic arcs: Journal of Sedimentary Research, v. 77, p. 784-796.

Ingersoll, R.V., and Rumelhart, P.E., 1999, Three-stage evolution of the Los Angeles basin, southern California: Geology, v. 27, p. 593-596.

Ingersoll, R.V., Bullard, T.F., Ford, R.L., Grimm, J.P., Pickle, J.D., and Sares, S.W., 1984, The effect of grain size on detrital modes: a test of the Gazzi-Dickinson point-counting method: Journal of Sedimentary Research, v. 54, p. 103-116.

Ingersoll, R.V., Kretchmer, A.G., and Valles, P.K., 1993, The effect of sampling scale on actualistic sandstone petrofacies: Sedimentology, v. 40, p. 937-953.

Ingersoll, R.V., Grove, M., Jacobson, C.E., Kimbrough, D.L., and Hoyt, J.F., 2013, Detrital zircons indicate no link between southern California rivers and the Colorado Plateau from mid-Cretaceous through Pliocene: Geology, v. 41, p. 311-314.

Jacobson, C.E., Grove, M., Pedrick, J.N., Barth, A.P., Marsaglia, K.M., Gehrels, G.E., and Nourse, J.A., 2011, Late Cretaceous-early Cenozoic tectonic evolution of the southern California margin inferred from provenance of trench and forearc sediments: Geological Society of America Bulletin, v. 123, p. 485-506.

Liu, W., Kirschvink, J.L. and Weldon, R.J., 1988, Paleomagnetism of sedimentary rocks from near the DOSECC Cajon Pass Well, southern California: Geophysical Research Letters, v. 15, p. 1065-1068.

Miller, J.S., Glazner, A.F., and Crowe, D.E., 1996, Muscovite-garnet granites in the Cretaceous arc: Relation to crustal structures of the Mojave Desert: Geology, v. 24, p. 335-338.

Noble, L.F., 1954, The San Andreas fault zone from Soledad Pass to Cajon Pass, California, *in* Jahns, R.H., ed., Geology of southern California, [pt. 5]: California Division of Mines Bulletin 170, p. 37-48.

Reynolds, R. E., 1984, Miocene faunas in the Lower Crowder Formation, Cajon Pass, California: A preliminary discussion, *in* Hester, R. L. and D. E. Hallinger, eds., San Andreas fault -

Cajon Pass to Wrightwood: Pacific Section, American Association of Petroleum Geologists, Volume and Guidebook 55, p. 17-21.

Schermer, E.R., Stephens, V.A., and Walker, J.D., 2001, Continental margin tectonic evolution, Tiefort Mountains, northern Mojave Desert, California: Geological Society of America Bulletin, v. 113, p. 920-938.

Tedford, R.H., and Downs, T., 1965, Age of the Punchbowl Formation, Los Angeles and San Bernardino counties, California: Geological Society of America Special Paper 87, p. 234.

Walker, J.D., Martin, M.W., and Glazner, A.F., 2002, Late Paleozoic to Mesozoic development of the Mojave Desert and environs, California: in Glazner, A.F., Walker, J.D., and Bartley, J.M., eds., Geologic evolution of the Mojave Desert and southwestern Basin and Range: Geological Society of America Memoir 195, p. 1-18.

Weldon, R.J., II, 1986, The late Cenozoic geology of Cajon Pass: implications for tectonics and sedimentation along the San Andreas fault [PhD thesis]: California Institute of Technology, Pasadena, 400p.

Weldon, R.J., II, Meisling, K.E., and Alexander, J., 1993, A speculative history of the San Andreas fault in the central Transverse Ranges, California: in Powell, R.E., Weldon, R.J., II, and Matti, J.C., eds., The San Andreas fault system: Displacement, palinspastic reconstruction, and geologic evolution: Geological Society of America Memoir 178, p. 161-198.

Woodburne, M.O., 1975, Cenozoic stratigraphy of the Transverse Ranges and adjacent areas, southern California: Geological Society of America Special Paper 162, 91p.

Woodburne, M.O., and Golz, D.J., 1972, Stratigraphy of the Punchbowl Formation Cajon Valley, southern California: University of California Publications in Geological Sciences, v. 92, 73p.

Wright, J.E., Howard, K.A., and Anderson, J.L., 1987, Isotopic systematics of zircons from late Cretaceous intrusive rocks, southeastern California: Implications for a vertically stratified crustal column: Geological Society of America Abstracts with Programs, v. 19, p. 898.